2015

DEPARTAMENTO DE CIÊNCIAS DA VIDA

FACULDADE DE CIÊNCIAS E TECNOLOGIA
UNIVERSIDADE DE COIMBRA

Characterizing Iron transporters in *Plasmodium* species

Aparajita Lahree

2015

Characterizing Iron transporters in *Plasmodium* species

Aparajita Lahree

DEPARTAMENTO DE CIÊNCIAS DA VIDA

FACULDADE DE CIÊNCIAS E TECNOLOGIA
UNIVERSIDADE DE COIMBRA

Characterizing Iron transporters in *Plasmodium* species.

Dissertação apresentada à Universidade de Coimbra para cumprimento dos requisitos necessários à obtenção do grau de Mestre em Biologia Celular e Molecular, realizada sob a orientação da Doutora Ksenija Slavic (Instituto de Medicina Molecular, Faculdade de Medicina, Universidade de Lisboa) e da Doutora Emília Duarte (Departamento de Ciências da Vida, Universidade de Coimbra)

Aparajita Lahree

2015

TABLE OF CONTENTS

ACKNOWLEDGEMENTS

I would like to extend my heartfelt gratitude to Dr. Ksenija Slavic for her infallible supervision and persistent motivation towards practicing good science and enjoying the same and, to Prof (Dr). Maria Manuel Mota for giving me the opportunity and the encouragement to pursue my Master's thesis in the Malaria Parasite-Biology and Physiology lab; at Instituto de Medicina Molecular (IMM), Faculdade de Medicina, Universidade de Lisboa. I shall be failing in my duty if I do not express my gratefulness to all the members of the Maria Mota lab for their patient and unfailing support both professionally and personally.

I am especially grateful to Dr. Sofia Marques for help with transfection and flow cytometry related work, to Ana Parreira for providing and maintaining the mosquitoes used in this project and to Dr. Marija Markovic for the ookinete culture preparation. I would also like to extend my appreciation to António Temudo and Ana Margarida Nascimento from the IMM Bioimaging unit for their support with all the microscopy related work and, to Dr. Joana Marques and Iolanda Moreira for assistance with rodent handling.

I am also thankful to Dr. Paco Pino (Dominique Soldati-Favre lab, University of Geneva) for kindly providing the Inducible Knockdown Plasmid constructs and to Dr. Gunnar Mair for providing the plasmids for C-terminal *myc* tagging. I am indebted to Prof (Dr). Emilia Duarte, my academic tutor at Universidade de Coimbra; for assistance with the thesis documentation.

Last but certainly not the least I am grateful to the funding agencies for their financial support. This project was carried out under the following scientific funding grants:

2014/2015 "The role of Iron in *Plasmodium* life cycle and disease" – Fundação para a Ciência e Tecnologia (EXPL/BIM-MET/0753/2013), Coordinator: Daniel Carapau. 50.000 €

2012/2017 "Nutrient sensing by Parasites" – European Research Council, Starting Grant (311502), funded by the European Commission. Coordinator: Maria M. Mota. 1.500.000 €

ABSTRACT

Malaria has long been a threat to survival and persistently challenging at vaccine development. With a stuttering rise in drug resistant strains of the human parasites - *Plasmodium falciparum* and *Plasmodium vivax*, it is of paramount concern to identify new drug targets, which would render infection unsustainable at the earliest stage. As an essential co-factor iron has a critical role in virtually every cell from the simplest prokaryotes to complex eukaryotes. In humans, the fine tuning of iron homeostatic mechanism also dictates the outcomes to various infections. *Plasmodium* with its intricate life cycle and immense replication potential exhibits a high demand for iron at multiple stages during its development. During its intra-erythrocytic development *Plasmodium* has several possible iron reservoirs at its disposal in the host cell such as the iron bound in ferritin, the cytosolic labile iron pool and hemoglobin. The parasite's mechanism for iron uptake from the host and, its storage still remain shrouded due to the complexity in relating genome sequence of *Plasmodium spp.* to specific proteins and function. In this thesis project we have attempted to explore the function of two novel iron transporters in *Plasmodium:* Divalent metal transporter (DMT1) and Vacuolar iron transporter (VIT) homologues and, investigate the effect of compromise of their function on parasite development and virulence. Understanding the iron transport mechanism will shed some light on possible methods to target such machinery, if found essential.

Keywords: Malaria, Iron transport, *Plasmodium*, Divalent Metal transporter, Vacuolar iron transporter

RESUMO

A malária continua a ser uma ameaça à sobrevivência e persiste ao desafio da formulação de uma vacina. Com o aumento da prevalência das estirpes de *Plasmodium falciparum* e *Plasmodium vivax* resistentes aos fármacos disponíveis, torna-se cada vez mais relevante a identificação de novos alvos moleculares para o desenvolvimento de fármacos que inibam a infeção em fases precoces. O ferro, um co-factor essencial, tem um papel fundamental em virtualmente todas as células, desde o mais simples procariota até ao mais complexo eucariota. No Homem, a regulação da homeostase do ferro determina o resultado de várias infeções. Dado o seu ciclo de vida complexo e o seu grande potencial replicativo, *Plasmodium spp.* requerem uma grande disponibilidade ferro durante o seu desenvolvimento. Durante a sua maturação nos eritrócitos, *Plasmodium* tem na célula hospedeira várias reservas de ferro disponíveis, tais como, o ferro ligado à ferritina, o ferro livre no citosol e o ferro contido na hemoglobina. Os mecanismos utilizados pelo parasita na obtenção de ferro a partir do hospedeiro e no seu armazenamento continuam elusivos. Um obstáculo reside em parte na dificuldade em relacionar uma dada sequência genómica de *Plasmodium spp.* com a função da proteína resultante. Neste trabalho, tentámos explorar a função de dois transportadores de ferro identificados em *Plasmodium*: o Transportador de metais divalentes (do inglês, DMT) e o Transportador vacuolar de ferro (do inglês, VIT). Nesse âmbito estudámos o efeito da disrupção da sua função no desenvolvimento e na virulência do parasita. A melhor compreensão desta maquinaria do parasita, se considerada essencial, elucidará possíveis métodos para a modular e utilizar como alvo terapêutico.

Palavras Chave: Malaria, Transporte de ferro, *Plasmodium*, Transportador de metais divalentes, Transportador de ferro vacuolar.

LIST OF ABBREVIATIONS

Abbreviation/Notation	Description	Abbreviation/Notation	Description
ATc	Anhydrotetracycline	PBS	Phosphate buffered saline
ACT	Artemisinin combination therapies	PCR	Polymerase chain reaction
BLAST	Basic Local Alignment Tool	PFA	Paraformaldehyde
CCC1	Calcium complemeter superfamily 1	PfATP6	*Plasmodial* endoplasmic ATPase
CCM	Complete culture medium	*pfcrt*	CQ resistance transporter gene
CQ		pfmdr1	*Plasmodium falciparum* multidrug resistance gene
DcytB	Duodenal cytochrome B reductase	PMSF	Phenylmethyl sulfonyl fluoride
DD	Destabilization domain	*Pfu*	*Pyrococcus furiosus* DNA polymerase
DDT	Dichlorodiphenyltrichloroethane	PV	Parasitophorous vacuole
DFO	Desferroxamine	Pyr	Pyrimethamine
DHFR	Dihydro-folate reductase	RBC	Red blood cell
DHODH	Dihydroorotate dehydrogenase	RIPA	Radio-immunoprecipitation assay
DHPS	Dihydropteroate synthase	ROS	Reactive oxygen species
DMSO	Dimethyl Sulfoxide	rpm	Revolutions per minute
DMT1	Divalent metal transporter 1	RT	Room temperature
2E6	*Plasmodium* cytosolic Heat shock protein 70	SDS	Sodium dodecyl sulphate
EEF	Exo-erythrocytic form	SOB	Super optimal culture broth
ER	Endoplasmic reticulum	SP	Sulphadoxine-Pyrimethamine
GFP	Green fluorescent protein	TBST	Tris buffered saline containing Tween-20
HA	Hemagglutinin	TM	Transmembrane
H_2O_2	Hydrogen peroxide	TMD	Transmembrane domain
HRP	Horseradish peroxidases	TMP	Trimethoprim
IFA	Immunofluorescence assay	TRAD	Tetracycline repressor activating domain
iKo	Inducible knock-down	Uis4	Upregulated in infective sporozoite 1 protein
IMM	Instituto de Medicina Molecular	UMA	Unidade de Malaria
i.p	Intra-peritoneal	VIT	Vacuolar iron transporter
iRBC	Infected Red Blood cell	%v/v	Percent Volume by volume
i.v	Intra-venous	WB	Western Blot
LB	Luria-Bertani broth/agar	WHO	World Health Organization
LSM	Laser Scanning Microscope	% w/v	Percent Weight by volume
Msp1	Merozoite surface protein 1	YFP	Yellow fluorescent protein
myc	c-myc peptide tag	ZIP	ZRT/IRT-like Protein
US NIAID	United states of America-National Institute of Allergy and Infectious Diseases		
PAGE	Polyacrylamide gel electrophoresis		

I. INTRODUCTION

1. Malaria at a glance

Malaria is among the most notorious infectious diseases in the world today, with an incidence of 198 million cases and a mortality rate of 524000 individuals in 2013[1]. The death toll of malaria is most severe in sub-Saharan Africa, with Asia and Latin America next in line (Figure 1). The causative agents comprise of protozoan parasites belonging to the genus *Plasmodium*. The parasite is transmitted exclusively by mosquitoes of the genus *Anopheles to* vertebrate hosts such as humans, monkeys and mice during the mosquito's obligatory blood meal. There are five *Plasmodium* species known to infect humans and causing malaria of different degrees. The most fatal manifestation is the malignant malaria caused by *Plasmodium falciparum*; which is endemic in Africa, South America and Central and Southeast Asia, with highest prevalence in sub-Saharan Africa[2]. The other common variant of Clinical malaria is caused by *Plasmodium vivax* which is classified by acute febrile illness and anemia; and mostly prevalent in parts of Asia, Oceania and South America[3].The closely related monkey parasite, *Plasmodium knowlesi,* which has recently been classified as the fifth human malaria parasite can attain high peaks of parasitemia quickly due to its 24 hour life cycle and if not timely diagnosed, can lead to severe illness and death. This parasite was shown to be capable of transmission between vertebrate hosts (from monkey to humans) and demonstrated as fatal in Rhesus monkey (*Macaca mulatta*). *Plasmodium knowlesi* is common in Southeast Asia, possibly by virtue of abundance of its invertebrate host *Anopheles balabacencis* in that region[4]. The other species such as *Plasmodium ovale* rarely cause a serious disease[5] while *Plasmodium malariae* infections cause fevers with 3-day intervals. While relatively less severe, in the long term a lack of treatment may lead to glomerulonephropathy due to formation of immune-complexes.

Though malaria in its early stages does not demonstrate a very clinically conspicuous profile, it may later accelerate into fatal conditions such as metabolic acidosis, severe malarial anemia and cerebral malaria. Deaths due to malaria can be a result of organ failure or systemic shock.

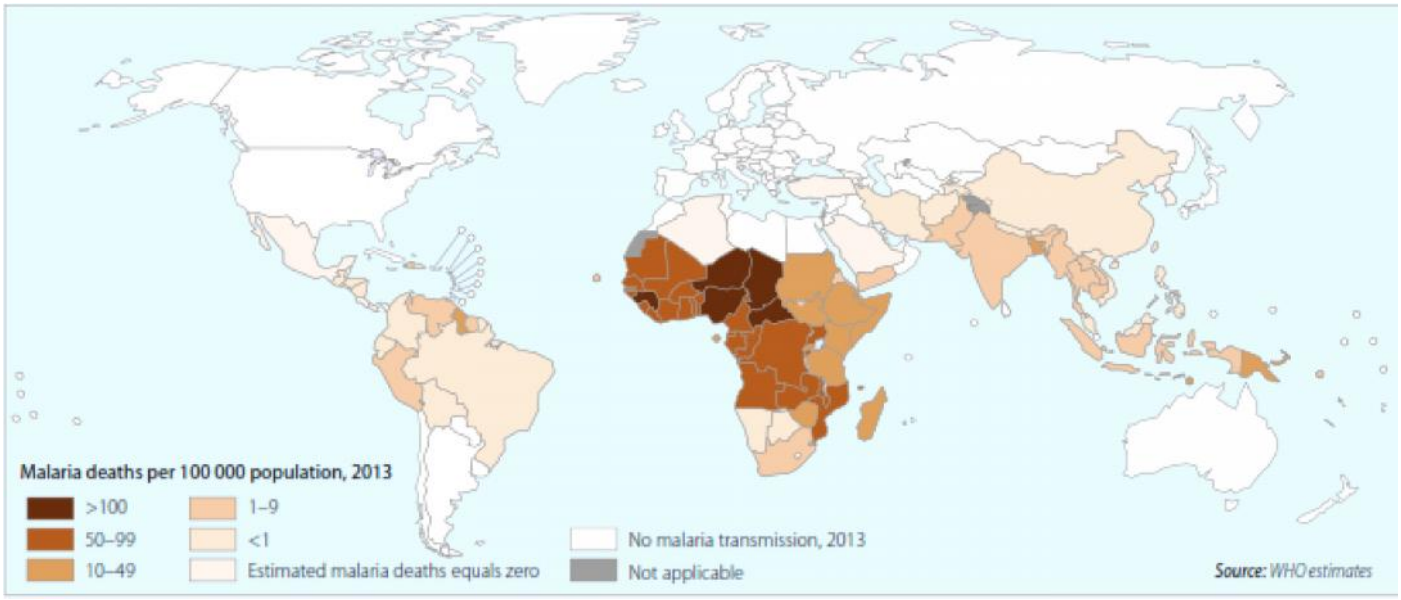

Figure 1. Malaria deaths per 100,000 (Image adapted from WHO World Malaria Report-2014)

Despite the persisting challenges in treatment and transmission control undertakings, there are optimistic reports indicating 26% reduction in the frequency of malaria infection, and reduction by 47% of the malaria induced mortality with respect to the malaria statistics in 2000; globally (Figure 2). The WHO predicts a further decrease by 8% in mortality rates by 2015, if the current trends for decline in mortality are maintained[1].

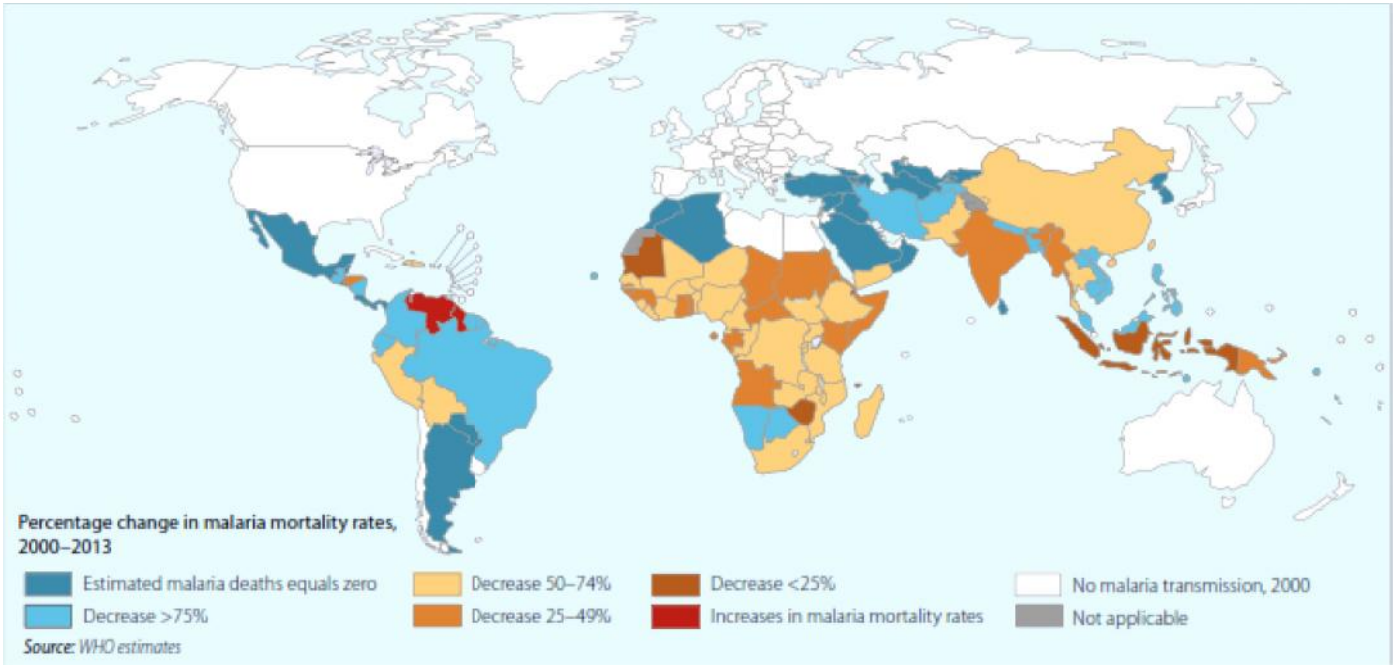

Figure 2. Percentage change in Malaria mortality rate: 2000-2013 (Image adapted from WHO World Malaria Report- 2014)

1.1. Plasmodium species Life cycle

Plasmodium exemplifies an intricate life cycle, involving two obligatory hosts: the mosquito and a vertebrate to complete its sexual and asexual developmental stages respectively (Figure 3).

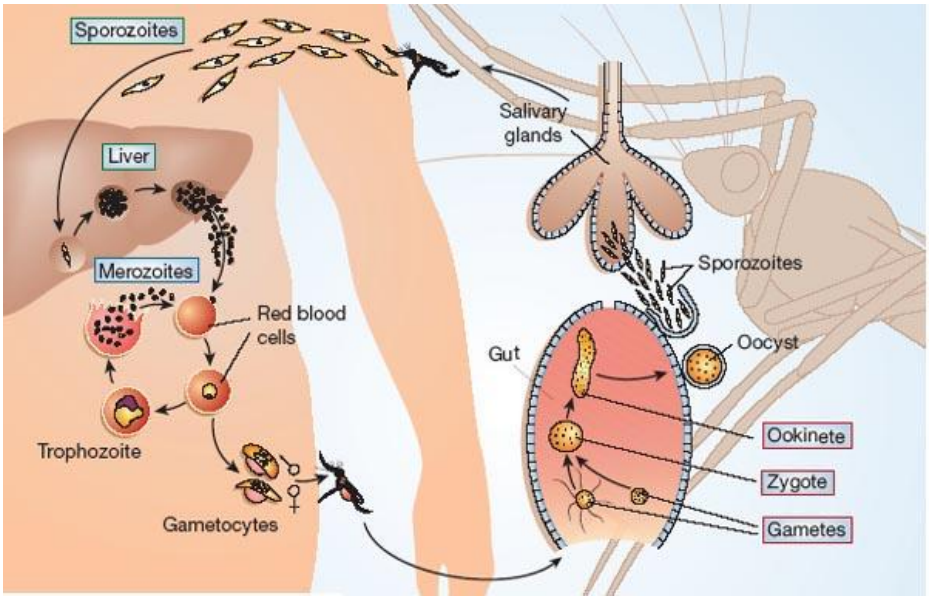

Figure 3. Plasmodium life cycle in the mosquito and the vertebrate host. [Image adapted from Ménard, 2005 [6]]

The transmission to a vertebrate host is initiated during a blood meal, wherein an infected female *Anopheles* mosquito releases saliva containing anti-coagulants into the victim and along with it, the *Plasmodium* parasite in its sporozoite form. The sporozoites move through circulation to reach the liver where they may traverse through Kupffer cells and several hepatocytes before infecting a final hepatocyte[6]. Upon entry into a hepatocyte, the sporozoite subsequently undergoes a large number of nuclear divisions (asexual) within a host cell derived vacuolated structure called the parasitophorous vacuole (PV). This stage is known as the exo-erythrocytic form (EEF) and each infected hepatocyte can contain up to new 20,000-30,000 merozoites, formed from one infectious sporozoite. The infected hepatocyte eventually ruptures and releases the merozoites into the blood circulation where these invade RBCs. The following development of the parasite constitutes the erythrocytic cycle, wherein it matures from an initial ring like structure to a vacuolated trophozoite. Mature trophozoites can undergo rapid asexual replication giving rise to schizont forms each of which can contain 6-32 merozoites depending on the *Plasmodium* species or, develop into gametocytes (the mosquito-transmitted form of the parasite). The former causes the infected RBC to eventually rupture in a synchronous manner and release thousands of merozoites (leading to typical malaria fevers) that further colonize more RBCs and continue the erythrocytic cycle. This blood stage replication of parasites is responsible for the symptoms associated with this disease.

When a pregnant female *Anopheles* mosquito takes her blood meal from an infected vertebrate host, the *Plasmodium* parasites in their gametocyte stage are also taken up. Within the mosquito stomach the lowering of ambient temperature, elevated pH and other mosquito-specific factors, trigger the maturation of the gametocytes into the male and the female gametes; eventually leading to fertilization. The fertilized cell transforms into a motile and invasive form called the ookinete which crosses the midgut wall of the mosquito to form stationary spherical structures known as the oocysts, just below the basal lamina of the midgut. The oocysts in turn produce several hundreds of motile forms of the parasite (Sporozoite) that migrate to the mosquito's salivary glands. The bite of such infected female *Anopheles* hence transfers the *Plasmodium* sporozoites into a vertebrate host and re-initiates development of the parasite paving way for malaria[7].

1.2. Treatment of Malaria and unforeseen consequences

The WHO indicates malaria to be a preventable and treatable disease with the primary aim being removal of parasite from the blood of patients. Thus, most anti-malarial drugs currently in therapeutic application target the blood stage of the parasite. The liver stage in contrast is asymptomatic but presents an attractive target for parasite clearance and prophylactic treatments[8].

In the 1950s the WHO devised large scale projects for malaria eradication through indoor residual spraying and mass use of anti-malarials like chloroquine (CQ) and sulphadoxine-pyrimethamine (SP). Such medical urgency paved way for inconsiderate application; eventually paralyzing this mammoth effort and falling prey to dichlorodiphenyltrichloroethane (DDT) resistant variants of *Anopheles* mosquitoes and CQ - SP resistant variants of *Plasmodium*[9].

CQ is a synthetic derivative of quinine that was derived from barks of *Cinchona* trees and used in traditional treatments. However, in the 1960s, CQ resistant variants were detected to this first-line treatment in Southeast Asia and South America. After decades of investigations into the mechanism underlying the chloroquine resistance, transfection studies have shown that point mutations in CQ resistance transporter gene (*pfcrt*) and mutations in other genes like *Plasmodium falciparum* multidrug resistance (*pfmdr1*) gene confer the resistance to CQ in *Plasmodium falciparum*[10,11]. Mutations and increased copy number of *pfmdr1* gene has also been attributed to confer resistance against other quinoline antimalarials, e.g. mefloquine and halofantrine[10,12]. Due to CQ resistance, SP was introduces in the 1970s. Not so ironically, resistance to SP developed rapidly in the areas of South Asia and CQ –SP multi-drug resistance spread to other parts of Asia and Africa as well[9]. Sulphadoxine and pyrimethamine belong to the group of antifolate anti-malarials which interfere with the parasite DNA replication through blockade of folate and pyrimidine biosynthesis. Pyrimethamine and biguanides inhibit the *Plasmodium* dihydrofolate reductase-thymidylate synthase (DHFR-TS), and sulphonamides /sulfones disrupt the target enzyme dihydropteroate synthase (DHPS). Point mutations in the DHFR-TS and DHPS genes were found to confer the resistance to

pyrimethamine and sulphonamides, respectively[13,14]. Thus, the resistance of Plasmodium spp. to the first line anti-malarials and mosquitoes to insecticides has been a critical medical concern.

In such a globally burned out zone of anti-malarials, the endoperoxide artemisinin derived from ancient Chinese herbal medicine was discovered as a potent drug during second half of the 20th century by Chinese scientists[15]. The artemisinin-combination therapies (ACTs) today represent the first-line treatment and include derivatives of artemisinin such as dihydroartemisinin, artesunate (hydrophilic), arteether and artemether (hydrophobic). The metabolically active agent of artesunate and artemether is dihydroartemisinin. Artemisinin and its derivates are potent antimalarial drugs and tolerated well overall.

Artemisinin and its derivatives however, come with their own share of pros and cons. They are powerful drugs that are cytotoxic to gametocytes in early development stages and clear out parasites from the blood relatively rapidly compared to quinine derivatives. The limitation of however, is their short half-life, thus given alone without a partner drug artemisinins may cause parasite recrudescence as its metabolic derivates are rapidly cleared out in humans. The cidal effect of artemisinin can be attributed to several interactions of the drug with high molecular weight proteins in the parasite. Artemisinins are proposed to be activated by ferrous iron or heme molecules arising from Plasmodial hemoglobin catabolism[16] through disruption of the endoperoxide bridge. The resulting free radicals have been proposed to interact with several malarial proteins, one of which is translationally controlled tumor protein (TCTP)[17]. Artemisinin has also been shown to interact with and inhibit the Plasmodial endoplasmic ATPase (PfATP6)[18–20] which is a SERCA orthologue Ca^{2+} pump localized to the membrane of sarco/endoplasmic reticulum and involved in Ca^{2+} homeostasis [21,22]. Nevertheless, the exact mechanism of action of artemisinin drugs remains a matter of scientific debate.

The WHO recommends the use artemisinin in combination with partner drugs in order to have a balance between the pharmacokinetic effects, the blood parasite clearance rate and the ease of parasite recrudescence. Nevertheless, artemisinin resistance began emerging recently in countries of the Greater Mekong Subregion[1]. Though the observed decrease in efficacy of artemisinins is still not at the level of classical drug-resistance (isolated parasites were still susceptible to drugs in vitro), it has been observed that parasite clearance in the treated patients is prolonged. The proposed causes are believed to include the use of low quality artemisinin singly for a long period of time, or in case of combination therapies use of partner drug to which resistance already exists. Currently artemisinin combination therapy (ACT) is suggested as the first line for treatment of uncomplicated *P.falciparum* malaria[23]. Combinations recommended by the WHO for ACT include artemether-lumifantrine, artesunate-mefloquine, artesunate-amodiaquine and artesunate-sulfadoxine/pyrimethamine[24]. The financially worrisome component of ACT is the associated cost which can be much higher in comparison with non-artemisinin or artemisinin only therapies. Also, in the near future there appears to be hardly any sign of lowering of treatment cost per person. This is a major roadblock in convincing developing countries to establish ACT in full swing, despite such regions being the ones worst affected by malaria[25].

1.3. Drug Discovery, Malaria Vaccines and future prospects

With the rivers running dry in the area of malaria treatment, there is a burning need for novel potent candidates. Drug discovery platforms now enable synthesis of small molecule drugs and provide repositories of structurally diverse molecules to target a plethora of entities in an organism. The challenging component to confirming a molecule as a therapeutic agent is the identification of an appropriate target through genetic and biochemical manipulation of the organism, and subsequent validation through functional characterization and high-throughput inhibition assays. Drug discovery approaches come in two flavors: target based screens and phenotypic screens. While target based screens offer greater operational feasibility through studying the target ex-vivo in terms of structure and chemistry; it mandates the identification of a target as priority. The screen then enables an array of molecules to be tested on the target for detection of those that can significantly inhibit the target function. Target based screens have been developed for Plasmodium proteins such as Dihydrofolate reductase (DHFR), Heat shock protein 90 (Hsp90) and Dihydroorotate dehydrogenase (DHODH) among others[25].

On the other hand, advantages of phenotypic screens over target-based high throughput screens are that compounds active against all targets of the parasite are identified and that "hits" will possess the necessary requirements regarding cell permeability and activity in the cellular context. With relevance to malaria, the predominant phenotypic screen involves studying parasite growth in RBCs. Molecules such as DNA and stage-specific parasite proteins can be studied by fluorescent probe, PCR and antibody based detection. This screening method does not focus on molecular mechanism of target inhibition, which makes it difficult to interpret drug specificity. Its target identification capacity is also redundant, yielding previously known targets frequently[25].

While the blood stage of the parasite has understandably been in the limelight of treatments, the liver stage, though still under-investigated is a feasible and interesting target. Drugs that clear out parasite from both the blood and liver of the host are seemingly meager (e.g.: primaquine). The liver as a target to clear parasites is attractive considering that clearing parasite burden at this stage, which is several folds lower than in the blood, prevents the onset of symptoms of malaria disease and also prevents transmission. Additionally, drugs targeting this stage are at lower imminent threat of resistance. Additional challenge for antimalarial drug development present reservoirs of latent forms of malaria parasites, called hypnozoites, that reside in hepatocytes and can lead to a potential relapse even years after the infective mosquito bite[26]. Of the Plasmodium species infecting humans, hypnozoite forms only are only produced by *P. vivax* and *P. ovale.* The identification of compounds active against the hypnozoites has been severely limited due to the challenges of culturing these parasite forms in vitro[27].

Studies on the differential genomic and proteomic profiles of Plasmodium at different developmental stages in all its hosts uncovered a promising number of liver stage specific players that can act as potential drug targets (Figure 4)[28].

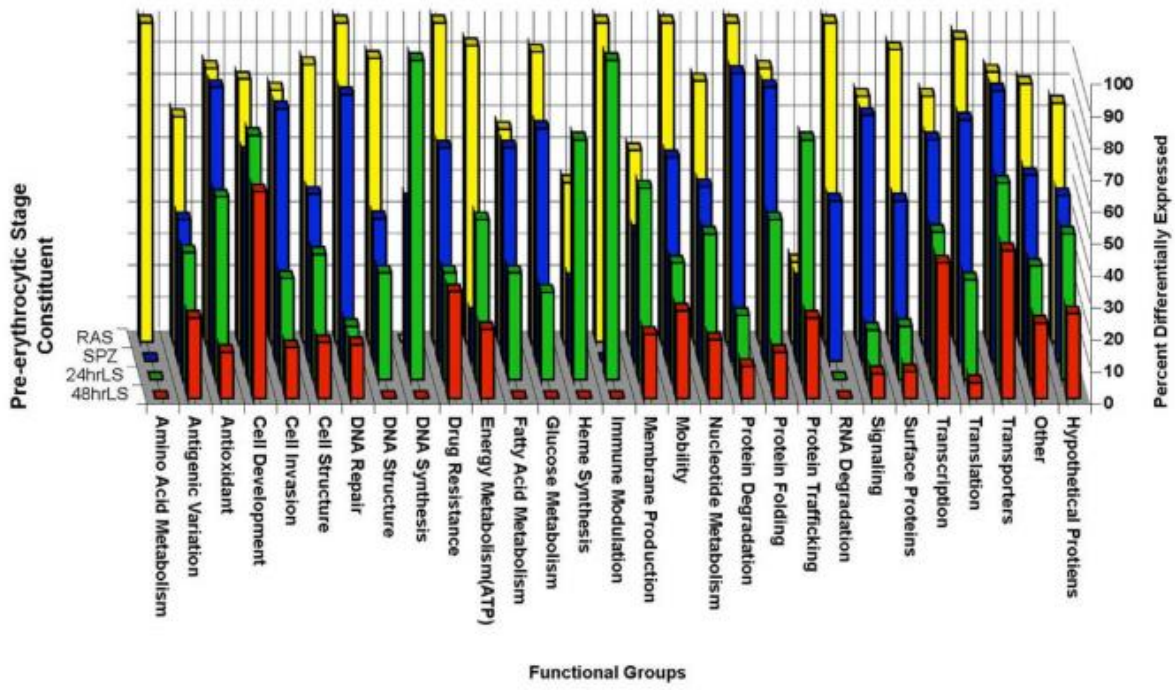

Figure 4. Functional grouping of genes differentially expressed during pre-erythrocytic stage of *Plasmodium yoelii*. (RAS- Radiation attenuated strain, SPZ- Salivary gland sporozoites, 24/48 hr LS – time specific liver stage parasites. Figure adapted from Williams *et al*[29]*)*

A highly exigent area of study in parallel with drug development in malaria has been that of vaccine strategies. It has been observed that continuous exposure to malaria parasite at an early age initially manifests into parasitemia and later confers protection against severe malaria and clinical symptoms. Though, such exposure must be repeated in order to maintain the infection associated immunity, the γ-globulin fraction from such semi-immune individuals has been shown to have protective effect against disease in non-immunized individuals[29]. Found mostly in malaria endemic area, such immunity rarely confirms protection against the liver stage parasite[29].

The primary goals for vaccine benefit, as outlined by the Malaria Vaccine Technology Roadmap in 2006 were 50% efficacy rate of a vaccine against the fatal forms of malaria with protection covering at least 12 months and a vaccine with long term effect and 80% efficacy against clinical malaria. However, these goals may be farfetched with respect to the available technological platforms which do not promise malaria control or eradication. The past decade has been a period of major makeover in the face of funding and cooperation in malaria vaccines. Major research and funding institutions such as the Bill and Melinda Gates foundation, Wellcome trust (UK), US NIAID, Medical research Council UK, European Vaccine initiative and WHO have contributed towards the stabilization of economic grounds and opportunities for large scale clinical trials. Some vaccine candidates currently in clinical trial RTS,S/AS01 as the most advanced malaria vaccine to date[30], Circumsporozoite protein targeting antibodies, adenovirus vectored vaccine expressing circumsporozoite protein and multiple epitope-thrombospondin-related adhesion protein (ChAd63-MVA CS and ChAd63-MVA ME-TRAP, respectively),Attenuated whole organism vaccine and Adch63/Mva Me-TRAP.

2. The multiple facets of Iron and Plasmodium infection

Nutrient sensing and homeostasis is at the heart of survival, *Plasmodium* being no exception. Molecular players involved in nutrient uptake, storage and utilization pathways are valid candidates towards identification of novel drug targets. Iron is an essential micronutrient for *Plasmodium*; however knowledge of its acquisition, transport or storage remains unknown.

Iron is of particular interest because of its transitional chemistry. Within eukaryotic cells, iron is either sequestered in proteins such as ferritin or in vacuoles as Fe^{3+} form[31–33]. Cellular iron reservoirs maintains an equilibrium between the cellular Fe^{3+} and Fe^{2+} pools to keep Fe^{2+} concentration below explosive thresholds[33]. Fe^{2+} is extremely reactive and can generate large amounts of hydroxyl radicals through the Fenton reaction (Equation 1). $OH\cdot$ is among the most reactive free radicals and capable of inducing lipid peroxidation and oxidation of proteins.

$$Fe^{2+} + H_2O_2 \rightarrow Fe^{3+} + OH\cdot + OH^- \qquad \text{Equation (1)}$$

This observation paves way for the fundamental question as to how does *Plasmodium* acquire iron from such a tight host regulated circuitry and moreover, not enter into an oxidative catastrophe. Dey *et al*[34] showed the inhibition of hepatocyte mitochondrial aconitase on infection with *Plasmodium yoelii* and associated elevation in superoxide radical and depletion of mitochondrial GSH in Balb/c mice hepatocytes. They also show the disruption of mitochondrial Fe-S clusters and release of Fe^{2+} that is later believed to induce apoptosis in such infected hepatocytes. While speculative, it is tempting to believe that some parasite strains have robust mechanisms to mobilize and sequester host cytosolic iron without causing an immediate oxidative surge in the parasite compartment or any chaos in its host hepatocyte.

In what seems to be a complicated host-pathogen relationship, the susceptibility and progression of malaria has been shown to be affected by the iron availability in the host[35], especially in the hepatocyte and the erythrocyte. In addition, the iron status also exerts implication on the host immune response to infection. The participation of iron in complex biological functions such as immunological response and host-parasite interaction are recent revelations, making this micronutrient stand out in a whole new perspective in addition to being a co-factor.

While a great amount of work and interest has been invested in research of how different hemoglobinopathies affect malaria[36], the iron metabolism of the malaria parasite and competition with the host for iron procurement is a relatively nascent domain of research. In malaria endemic areas of Africa, the occurrence of anemia in children represents a serious concern regarding impact on health and growth. The clinical trial conducted in Pemba, Zanzibar, aimed at managing the morbidity and mortality due to anemia in children between 1-35 months, through oral supplementation of iron, folic acid and zinc. The trial had to be interrupted mid-way due to death and high morbidity in children receiving iron and folic acid supplementation. This region is holoendemic for malaria (with *Plasmodium falciparum* accounting for majority of severe cases) with a mean of 405 infective bites per person per year. The

children showing adverse reactions displayed increased infection susceptibility (both malarial and non-malarial). The study hence, concluded that iron supplementation to counter iron deficiency in children must be managed with malaria prevention in areas of high malaria incidence[37]. Finding the most adequate iron supplementation regime for malaria endemic regions remains a matter of debate until present day. The mechanisms of how iron deficiency potentially protects from malaria infection and iron supplementation increases risk of infection remain unclear[35]. With respect to this, identification of molecular mechanisms in *Plasmodium* for iron uptake and metabolism are crucial for understanding the parasite-host competition for this micronutrient that is essential for both organisms.

With respect to the involvement of iron availability in parasite survival, a study by Gordeuk *et al* demonstrated enhanced clearance of *P.falciparum* from patients treated with Desferroxamine B (DFO-B)[38] (CHEBI: 4356), which is a siderophore (iron chelator) derived from the actinobacteria *Streptomyces pilosus*. There was however a relapse of malaria in most of the patients. A more detailed study on the effect of iron deprivation during various developmental stages of *P.falciparum* by Whitehead and Peto elucidated that the effect of iron withdrawal was most detrimental to parasites in pigmented trophozoites and early schizogony stages, whereas the young non pigmented or ring trophozoites were completely unaffected by it[39]. It has been observed that parasite maturation in RBC is accompanied by increased permeability of the RBC plasma membrane[40]. DFO-B is a polar compound; hence the lack of effect of DFO mediated iron chelation on young parasitic forms in erythrocytes is not the chief indicator of dispensability of iron at ring or trophozoite stages of *Plasmodium* development, as the erythrocyte membrane is less permeable.

Through dissection of phenotypes into molecular pathways, Painter *et al* outlined one of the critical molecular functions of iron in the electron transport chain of *P.falciparum*. The electron transport chain (comprising of iron and iron-sulfur clusters as essential co-factors) was shown to be indispensible to the parasite, as it was the primary centre for the regeneration of ubiquinone. Ubiquinone is necessary as the electron acceptor for dihydroorotate dehydrogenase (DHOD), the latter being a crucial enzyme in pyrimidine biosynthesis. Considering the rapid proliferation of the parasite within infected cells, nucleotide biosynthesis is at the heart of its survival[41]. A related study by Ferrer *et al* substantiated the observation that withdrawal of available iron with another high affinity iron chelator – FBS0701 in *Plasmodium falciparum* reduces the blood stage parasitemia. Additionally they also outlined a developmental arrest of stage V gametocytes and associated decline in transmission efficiency to mosquitoes[42].

An attempt to appreciate iron metabolism in the parasite would be futile without an understanding of the iron homeostatic pathways in the mammalian host. In mammals, most of the iron is bound to hemoglobin in the circulating RBCs and the rest is divided into - iron stores that can be mobilized on demand and, iron bound to muscle myoglobin and enzymes. The cellular mechanisms for recycling and storing iron are tightly regulated, outlining a critical requirement for maintenance of homeostasis. Iron requirement varies with age, and iron deficiency can have severe effects on growth, cognitive development and immune function[43].

2.1. Iron Acquisition and homeostasis in Mammals

Dietary iron (Fe^{3+}) is absorbed in the duodenum via the divalent metal transporter 1 (DMT 1) on the enterocyte apical membrane; and as bound to heme through heme transporters. The iron must exist in Fe^{2+} form for it to be transported by the enterocytes and this is achieved through the activity of surface ferrireductases, such is duodenal cytochrome B reductase (DcytB). Within the enterocytes, the iron is either stored or transported to the basolateral membrane based on the systemic iron demand. Iron is released into the circulation via the only known mammalian iron exporter- ferroportin. Exported iron is reoxidized to Fe^{3+} state, either by the action of hephaestin or ceruloplasmin[43].

The circulating iron is picked up by soluble iron scavenging protein- transferrin. The iron-transferrin complex on interaction with the surface transferrin receptor 1 (TfR1) (on liver and erythroid precursor cells mainly) is endocytosed into the cell. Acidification of the endocytosed vacuole by H^+ ATPase leads to the dissociation of bound iron. The vacuole matures into recycling endosome and transports the Apo-transferrin bound to TfR1 back to cell surface. The iron is then mobilized to the cytosol by the vacuolar Divalent Metal Transporter 1. In the cytosol the iron can either be stored as bound to ferritin or transported to mitochondria where it is incorporated into heme or iron-sulphur clusters.

Another major compartment for iron fluxing through circulation is represented by the macrophages (Figure 5). Since, there is no known mechanism for excretion of iron from the body (it is mainly lost during blood loss through menstruation, injury and sloughing of enterocytes), macrophages are key players in recycling systemic iron. Circulating and tissue macrophages extract iron from senescent or damaged RBC and from circulating hemoglobin bound to its carrier haptoglobin. The endocytosis of RBC or hemoglobin-haptoglobin complex is followed by the degradation of heme to release iron via the action of heme oxygenase I. The transport of Fe^{2+} from the phagosome to cytosol is facilitated through Fe^{2+} specific transporters namely DMT1 (also known as Nramp II) and Nramp I. The cytosolic Fe^{2+} ions are reactive and toxic molecules that must either be exported or confined into the cytosolic iron store of ferritin. Depending on the iron demand or infection status of the body the iron is mobilized accordingly. Similar to that in the enterocytes, export of Fe^{2+} from macrophage to circulation is through ferroportin. The major sink of iron in the body is the bone marrow which uses it for erythropoeisis[44].

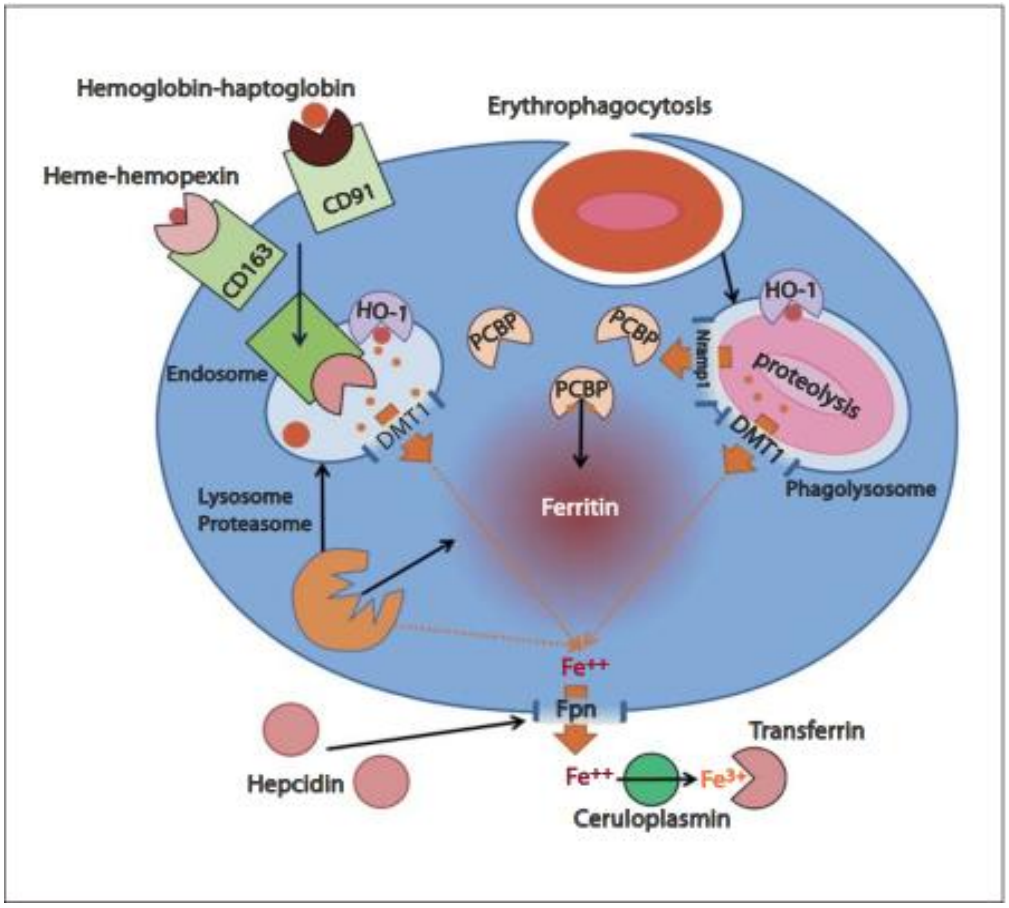

Figure 5. Schematic representation of macrophage based iron scavenging and recycling (Image adapted from T.Ganz, 2012[45])

The signaling entity that regulates the partitioning of iron from macrophages and enterocytes to blood is a 25 amino acid liver synthesized hormone known as hepcidin. Hepcidin exerts its effect by binding to ferroportin and flagging it for endocytosis and subsequent degradation. The effect hence, translates into sequestration of iron in macrophages and enterocytes leading to restricted iron bioavailability. This in turn paves way for anemia. Hepcidin expression is strictly regulated by sensing of erythroid demand, systemic iron status and inflammatory profile[45].

In the event of an infection, inflammatory cytokines such as IL-6, upregulate the expression of hepcidin[45] and other iron scavenging proteins (haptoglobin, siderocalin, ferritin). Increased hepcidin levels lead to sequestration of iron in macrophages and enterocytes. The resulting systemic hypo-ferrimia is protective against pathogen invasion especially for agents heavily dependent on iron for growth and survival.

2.2. Iron Acquisition and homeostasis in Plasmodium

The particular nature of the iron sources of *Plasmodium* within the Hepatocyte/RBC during its different stages of development is still hazy. While the hepatocytes are metabolically active cells with abundant iron and protein reserve, the RBCs, which become the long term residence for the parasite with disease progression, lack active

biosynthetic machinery. In order to replicate extensively, there is a high demand on the parasite's end for amino acids, nucleotides and also iron. During the erythrocytic stage, *Plasmodium* derives most of the amino acids from digestion of endocytosed hemoglobin by the action of parasite aspartic/cysteine proteases, metalloproteases and aminopeptidases in its digestive vacuole (Figure 6). The heme prosthetic group that is released through the digestion of hemoglobin is highly toxic to the parasite. The vast majority of heme is polymerized and sequestered into inert crystalline structures known as hemozoin. This process may be the sole way to detoxify heme, for the recently discovered *Plasmodium falciparum* putative heme oxygenase I[46] was shown to lack degradative effect on heme[47]. The small amount of heme uncoupled from hemozoin crystallization, can be degraded non-enzymatically by H_2O_2 within the parasite digestive vacuole releasing Fe^{3+} ions which may be a possible source of iron. However such oxidation of free heme moiety is also a source for ROS[48]. Apart from RBC cellular reserves, *Plasmodium* can derive nutrients and iron from the serum through permeabilization of the RBC cell membrane[49,50].

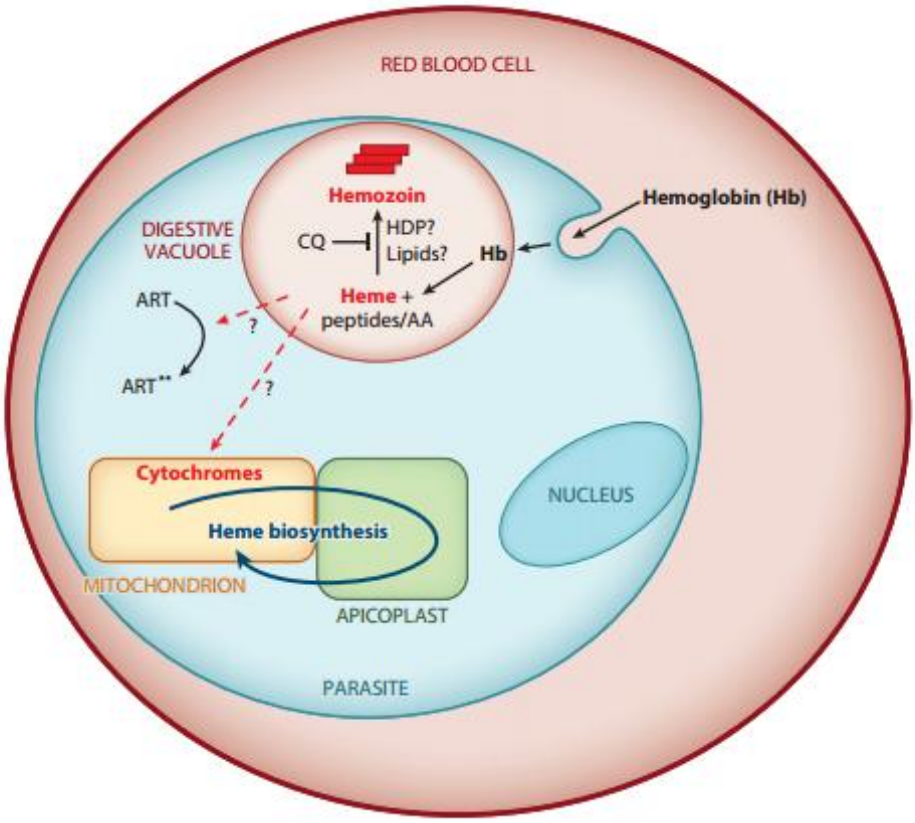

Figure 6. Schematic representation of heme metabolism of Plasmodium in the erythrocyte. [Image adapted from Siaga *et al*, 2012[52]]

The iron circuitry in the parasite has only begun to be unveiled and is an exciting area of research with promising prospects of drug target discovery.

3. Excavating molecular players and pathways: Plasmodium iron homeostasis

The whole chromosome shotgun sequencing of the *P.falciparum* genome revealed large datasets of genetic information for prediction of a putative proteome based on sequence homology and domain conservation[51] (Table 1).

Feature	Number	Per cent
Total predicted proteins	5,268	
Hypothetical proteins	3,208	60.9
InterPro matches	2,650	52.8
Pfam matches	1,746	33.1
Gene Ontology		
Process	1,301	24.7
Function	1,244	23.6
Component	2,412	45.8
Targeted to apicoplast	551	10.4
Targeted to mitochondrion	246	4.7
Structural features		
Transmembrane domain(s)	1,631	31.0
Signal peptide	544	10.3
Signal anchor	367	7.0
Non-secretory protein	4,357	82.7

Table 1. Schematic Plasmodium falciparum proteome predicted from genome sequence[53]

The proteome so outlined boasted of a large number of entities unique to the organism, however with a greater inclination of homology to eukaryotic proteins than prokaryotic ones. A Gene Ontology (GO) term classification based on biological process and molecular function (Figure 7) identified an optimistic percentage of transport proteins. Within the modest repertoire of membrane transporters, the fraction of solute carriers appeared further infrequent; therefore narrowing the boundaries of identifying cation transporters by prediction alone. Nonetheless, a more stringent analysis yielded a hit with Nramp divalent cation transporter like protein that may have specificity to manganese or iron transport[51].

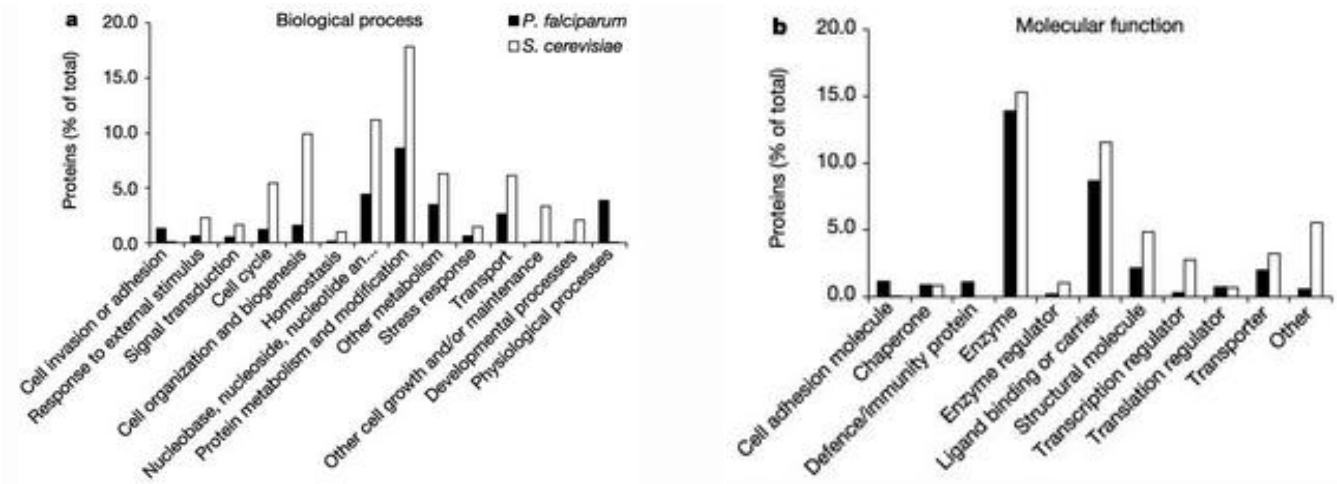

Figure 7. Classification of *P.falciparum* proteins according to the (a) biological process and (b) molecular function ontologies of the Gene Ontology system[53]

The scarcity of both experimental data and bioinformatics data on membrane transporters, especially inorganic ion transporters, remains a challenge to reckon with. The permeome analysis of *Plasmodium falciparum* by Martin *et al* aided in excavating several more candidate transporters through prediction of multiple pass transmembrane domains and secondary structure homology with known transporter superfamilies in eukaryotes[52]. The presence of transporters for vitamins, amino acids, nucleosides and solutes were confirmed in parasite plasma membrane and/or intracellular membrane bound compartments. Such transporters were previously postulated to be absent in *Plasmodium*[51]. There still remain ample plasma membrane transporters, with insignificant sequence and structural homology to classical transporters, yet showing hydropathy plots indicative of known transporters. Such transporters are believed to be unique to *Plasmodium* and open new avenues for specific drug target identification[52].

Though interesting, the bioinformatics based knowledge requires experimental confirmation to connect the dots and elucidate nutrient homeostasis pathways in the parasite and effects of disrupting such equilibrium.

The modus operandi in present practice involves the identification and characterization of macromolecules participating in the iron regulatory pathway from predicted putative transporter candidates annotated in the *Plasmodium* genome. This bottom-up approach will enable creation of a pool of molecular players and information regarding their position in iron homeostasis in the parasite during different developmental stages. Among the current findings with respect to this include the ZRT/IRT-like Protein (ZIP) domain-containing protein (ZIPCO) that was shown to be involved in iron/zinc uptake and on knockout, severely impairs the liver stage parasite development[53]. Plasma membrane iron transporters belonging to the ZIP family have also been identified in the protozoan parasite *Leishmania* and shown to participate in aiding survival in macrophages[54]

In this work we attempt to identify and characterize two more iron transporters in the rodent parasite *Plasmodium berghei* that maybe involved in iron uptake and/or detoxification. Among them one belongs to the Nramp family of Divalent Metal transporters (DMT1/NrampII) and the other to the CCC1 superfamily of Vacuolar Transition Metal ion transporters.

II. MATERIALS AND METHODS

1.1. Ethics Statement

All in vivo protocols were approved by the internal animal care committee of the Instituto de Medicina Molecular and were performed according to national and European regulations.

1.2. Animals

Mice were housed in the Rodent facility of the IMM. C57BL/6J WT and Balb/c WT mice were purchased from Charles River® Breeding Laboratories.

Anopheles stephensi WT were obtained from the breeding facility at IMM. Housing and infections were performed at IMM.

1.3. Parasites

Plasmodium berghei ANKA strain was obtained from Wellcome Trust Sanger Institute, UK. Asexual parasitic forms were maintained through passage of infected blood in Balb/c mice. Stock of blood vials were maintained at -80°C for all parasite lines.

Sporozoites for infection were obtained by dissection of *Anopheles stephensi* mosquitoes 19-20 days post-infection of mosquitoes. For *in vitro* infection of Huh7 hepatoma cells, 50.000 sporozoites were used to infect 50.000 cells per well a 24-well plate.

1.4. Bacterial Transformation

Escherichia coli strains DH5α (IMM_UMA developed strain) and XL-10 gold ultracompetent cells (Agilent Technologies®) were employed in cloning of modified *Plasmodium* DNA sequences. XL-10 gold cells were mixed with β-mercaptoethanol at 4%v/v, prior to use.

Competent cells were kept at 4°C and ligation mixture was added to aliquoted cells at 5% v/v. The mixture was swirled gently and maintained at 4°C for 30min, followed by heat shock at 42°C for 45 seconds and then for 2 minutes at 4°C. 900µL of pre-warmed (42°C) SOC medium (Super optimal broth supplemented with 20mM Glucose)

was added to heat shocked transformation cocktail and allowed to incubate at 37°C, 200rpm for 1 hour. The bacteria were then plated on Luria-Bertani (LB) Agar containing Ampicillin (1µg/mL) and incubated overnight at 37°C.

1.5. Molecular cloning

1.5.1 Generation of plasmids for Conditional knockdown of DMT

A. Protein level knockdown: Destabilization Domain (DD) method

For the generation of parasites expressing PbDMT_DD or PbDMT_HA_DD fusion protein – the DD sequence was amplified by PHUSION® High fidelity PCR kit (Thermo Scientific®) (Appendix) from the pBMN DHFR (DD)-YFP (Addgene®) plasmid with the primers UMA1803 and UMA1804 (Appendix List of primers) for PbDMT_DD and the primers UMA1959 and UMA1804 (Appendix List of primers) for PbDMT_HA_DD. The PCR product was resolved on 1% agarose gel to verify the amplicon size and followed by purification of the PCR product (Qiagen QIAquick® PCR Purification Kit). The blunt end PCR product was then ligated to pJet 1.2 blunt (CloneJET® PCR Cloning Kit-Life Technologies) intermediate cloning vector and transformed into *E.coli* DH5α competent cells. Transformed colonies were transferred to LB-Ampicillin (1µg/mL) broth and incubated overnight at 37°C and 200rpm. Plasmid DNA was extracted from cells in culture (Promega Wizard® Plus SV Minipreps DNA Purification System) and quantified by spectrophotometry at 260nm (Thermo Scientific Nanodrop 2000®). Preliminary verification of insert was performed by sequential digestion of plasmid DNA from the transformed bacteria with ApaI and NotI (New England Biolabs®) and resolving the digestion mixture on 1% agarose. Clones with appropriate insert size were sent for sequencing (454 sequencing- Stabvida®) to confirm the absence of mutations in the open reading frame of the DD/HA_DD insert.

Clones with negligible mutations and the target expression vector (PbDMT_GFP vector: previously developed) were sequentially digested with ApaI and NotI, which released the DD/HA_DD fragment from its pJet construct and the GFP fragment from the expression Vector backbone respectively. The digestion mixtures were resolved on 1% agarose. The DD/HA_DD fragment and the expression vector backbone were gel extracted and purified (Qiagen QIAquick® Gel Extraction Kit). Both Insert and Vector DNA samples were ligated (Appendix Routine protocol conditions) in the molar ratio 10:1 respectively, overnight using T4 ligase (Life technologies®). This ligation mixture was used to transform *E.coli* DH5α competent cells. Transformed colonies were transferred to LB-Ampicillin (1µg/mL) broth and incubated overnight at 37°C and 200rpm. Plasmid DNA was extracted from cells in culture and quantified by spectrophotometry. The complete construct was digested with BamH1 and Not1 to confirm appropriate size of insert in the complete expression vector construct. Selected clones were sequenced and the one with negligible mutations in the PbDMT_DD or PbDMT_HA_DD ORF was selected for parasite transfection.

For transfection in *P.berghei*; ≈ 30µg of the PbDMT_HA_DD construct (Appendix Maps of plasmids) was linearized with HindIII. DNA was extracted from the digestion mixture by acidification with 3M Sodium Acetate (pH 5.5, 0.1%v/v) followed by precipitation with 100% Ethanol (200% v/v) and incubation at 4°C, overnight. Precipitated DNA was obtained by centrifugation at 14000rpm for 5min at RT. The supernatant was discarded and the pellet washed with 70% Ethanol and centrifuged at 14000rpm for 1min at RT. The supernatant was decanted and the transparent pell*et al*lowed to air-dry. The air dried pellet was resuspended in 10-15 µL DNAse/RNAse free water and incubated overnight at 4°C to enhance solubility.

B. Transcriptional regulation based knockdown: Inducible knockdown system (iKo)

The plasmid construct backbone employed to generate Inducible knockdown DMT mutants in P.*berghei* (PbDMT_iKO) was kindly provided by Dr. Paco Pino (Soldati Lab, University of Geneva). A portion of the 5' UTR and the DMT gene was amplified from the *P.berghei* ANKA genomic DNA using primers UMA2233, UMA2234 and UMA2231, UMA 2232 respectively (Appendix List of primers). The respective amplicons were verified on 1% agarose for their size. PCR products were purified (Qiagen QIAquick® PCR Purification Kit) and then ligated into pJet1.2 (Life Technologies CloneJET® PCR Cloning Kit) blunt end immediate cloning vector through blunt end ligation. The ligation mixture was then used to transform *E.coli* XL-10 competent cells. Transformed colonies were transferred to LB-Ampicillin (1µg/mL) broth and incubated at 37°C and 200 rpm overnight.

Plasmid DNA was extracted from cells in culture (Promega Wizard® Plus SV Minipreps DNA Purification System) and quantified spectrophotometrically at 260nm (Thermo Scientific Nanodrop 2000®). Preliminary verification of insert was performed by double digestion of plasmid DNA from the transformed bacteria with SacII and NheI (New England Biolabs®) for *pbdmt* 5'UTR and NaeI and NheI (New England Biolabs®) for *pbdmt* gene and, resolving the digestion mixture on 1% agarose. Cloning of the UTR and the gene into the expression vector were done sequentially.

Clones with appropriate insert size were sent for sequencing (454 sequencing-Stabvida®) to confirm the absence of mutations in the target sequences. The 5'UTR clones with negligible mutations along with the expression vector were digested with SacII and NheI, which released the 5'UTR fragment from its pJet construct and a fragment from the expression Vector backbone respectively. The digestion mixtures were resolved on 1% agarose. The 5'UTR fragment and the expression vector backbone were gel extracted and purified (Qiagen QIAquick Gel Extraction Kit). Both Insert and Vector DNA samples were ligated in the molar ratio 10:1 respectively, overnight using T4 ligase (Life technologies®)(Appendix Routine protocol conditions). This ligation mixture was used to transform *E.coli* XL-10 competent cells. Transformed colonies were transferred to LB-Ampicillin (1µg/mL) broth and incubated overnight at 37°C and 200rpm. Plasmid DNA was extracted from cells in culture and quantified by spectrophotometry. The partial construct along with the *pbdmt*-pJet construct were further digested with NaeI and NheI to release a fragment from the partial construct and *pbdmt* gene from its pJet construct. Insertion of *pbdmt* into the partial expression construct was performed similar to its 5'UTR and the final expression construct was verified through enzymatic digestion and

sequencing. Clones with a stable and unaltered *pbdmt* 5'UTR and *pbdmt* gene fragment were selected and expanded to obtain the plasmid.

For transfection in *P.berghei*; ≈ 30µg of the PbDMT_iKO construct was linearized with NheI. DNA was extracted from the digestion mixture by acidification with 3M Sodium Acetate (pH 5.5, 0.1%v/v) followed by precipitation with 100% Ethanol (200% v/v) at 4°C, overnight. Precipitated DNA was obtained by centrifugation at 14000rpm for 5min at RT. The supernatant was discarded and the pellet washed with 70% Ethanol and centrifuged at 14000rpm for 1min at RT. The supernatant was decanted and the transparent pell*et al*lowed to air-dry. The air dried pellet was resuspended in 10-15 µL DNAse/RNAse free water and incubated overnight at 4°C to enhance solubility.

1.5.2 Generation of plasmids for Tagging of DMT and VIT : Localization in Plasmodium berghei

A. C-terminal *myc* tagged constructs

DMT and VIT sequences were amplified by *Pfu* (Thermo Scientific®) from the genomic DNA of *P.berghei* ANKA using the primers UMA1814 and UMA1815 (Appendix Primers list) for DMT and; UMA1812 and UMA1813 (Appendix List of primers) for VIT. The amplicons were resolved on 1% agarose gel and purified. The blunt end PCR products as well as the expression vector backbone (kindly provided by Dr. Gunnar Mair) were then digested with BamH1 and EcoRV (New England Biolabs®) to generate compatible sticky ends. The resulting DMT and VIT fragments were ligated individually into the *myc* vector backbone containing the *dhfr* selection cassette (kindly provided by Dr. Gunnar Mair) in the molar ratio of 10:1; using T4 ligase (Life technologies®). The ligation mixture was used to transform *E.coli* DH5α competent cells. Transformed colonies were selected with Ampicillin (1 µg/mL) and transformants were cultured in LB-Ampicillin (1 µg/mL) broth at 37°C, 200rpm, overnight. Plasmid DNA was extracted from the broth clulture of transformed colonies and digested with BamH1 and EcoRV to verify the presence and the size of the respective inserts (DMT/VIT). Clones with appropriate insert size were sent for sequencing and those with negligible mutations in the DMT_myc and VIT_myc ORF were selected for preparation of the transfection construct.

The transfection construct was prepared by linearzing the PbDMT_myc and PbVIT_myc plasmid constructs with HindIII and BstX1 (New England Biolabs®) respectively to generate fragments with suitable homology to the genomic counterparts of DMT/VIT respectively that would enable homologous recombination on transfection with linearized plasmid.

1.6. Plasmodium berghei transfection[55]

A. Preparation of Donor mice:

A Balb/c mouse was injected intraperitoneally with *P.berghei* infected blood from a cryopreserved vial and allowed to develop parasitemia of around 5%, following which the mouse was sacrificed and its blood collected by cardiac puncture (Heparin treated 1mL syringe-26G needle).

The blood so collected was immediately passaged into two Balb/c mice via intraperitoneal injection of 200µL of infected blood. The parasitemia in these mice was monitored by microscopic examination of Giemsa stained smears and, allowed to develop between 1-3%.

B. Preparation of schizont culture:

When the desired parasitemia was reached the donor mice were sacrificed and 1-2mL blood was collected via cardiac puncture (Heparin treated 1mL syringe-26G needle).

The blood was washed once in Complete culture medium (25% FBS supplemented RPMI) (CCM) at 2000 rpm. The Blood pellet was transferred to 50mL CCM and split equally between two 250mL culture flasks with filter paper lined screw caps. The flasks were incubated in horizontal position, at 37°C, 5% CO_2 for overnight.

The presence of normal schizonts was confirmed by microscopic examination of Giemsa stained thin smears prepared from the overnight cultures.

C. Isolation of Schizonts:

The medium was gently removed and the RBC were flushed and transferred to 50mL falcon tubes. Erythrocytes were harvested by centrifugation at 2000rpm for 5min; the supernatant was discarded. For separation of schizonts, the blood suspension was distributed equally between 4-5, 15mL falcon tubes. The tubes were positioned so as to minimize shear and a glass Pasteur pipette was inserted per tube. Using a micropipette, 7-8mL of 60% v/v Nycodenz (in PBS) was poured through each Pasteur pippete to gently underlay the blood such that the boundaries remain separate and visible. Nycodnez is used to separate the schizonts by density gradient centrifugation. The arrangement is centrifuged at 2058 rpm (450g- Eppendorf® 5810R) for 20 min in a swing-out rotor at RT without acceleration or brake (to minimize disturbance to separated fractions). The schizonts at this stage appear on a thin belt at the interface of the two larger fractions and were extracted gently with a pasteur pipette, taking care to avoid disturbing the fractions. The schizonts were then washed in CCM at 450g for 8min; the supernatant was discarded.

D. Schizont preparation and transfection:

The schizonts were carefully resuspended in 1mL of CCM. 9mL of CCM was further added to the schizont suspension and the final suspension was distributed equally between 10, 1mL microcentrifuge tubes.

Prior to electroporation, the mice to be infected were transferred to a fresh cage and warmed under an Infrared lamp to enable the swelling of the tail vein and subsequent ease in performing the intravenous injections. The electroporation working solution (EWS) was prepared by mixing the solutions provided by Amaxa® in the suggested dilutions. An aliquot of the schizont suspension was centrifuged at 2000rpm and the supernatant discarded. The schizont pellet was gently resuspended in the 100µL EWS and 10µL of the linearized DNA fragment intended to be inserted into the parasite genome was added. This solution was then transferred to the electroporation cuvette and inserted in the Amaxa Nucleofactor®. The transfection protocol U33 was activated. Post electroporation, 100µL CCM was immediately added to the contents of the cuvette, and the clear supernatant (100µL) removed with a plastic Pasteur pipette and transferred to a fresh microcentrifuge tube. A mouse was immobilized in a restrainer and intravenously injected with this suspension through the tail vein using an Insulin syringe. Since the vector backbone for all transfections performed, had a single *hdhfr* gene cassette, selection of mutant parasites was performed by supplying the infected mice with 70µg/mL Pyrimethamine (Pyr) in drinking water 1 day post-transfection.

E. Monitoring and verification of mutant parasites:

The appearance of parasites in the blood of the infected mice was monitored from day 4 post infection by examination of Giemsa stained blood smears. This was done until the parasitemia was around 2-5%. Most clones were visible on blood smear from 6-8 days post infection (dpi). Mice positive for clonal parasites were sacrificed and their blood collected via cardiac puncture for preparation of parasite glycerol stocks (to be maintained frozen at -80°C) and for extraction of genomic DNA. Total blood DNA was extracted (Qiagen® DNeasy Blood and Tissue Kit) and further used for parasite genotyping. The confirmation of appropriate integration of target sequence into parasite genome and elimination of WT locus containing parasites was performed by genotyping the total blood DNA with primers respective for the WT and the integration loci (Appendix Primers list).

1.7. Infections and parasitemias

Experimental infections in mice were performed through intravenous injection of 10^5 infected red blood cells through the tail vein.

Parasitemia in the blood was monitored by staining of methanol fixed blood smears in Giemsa (10% v/v) stain. All transgenic parasites carry constructs with the human Dihydrofolate Reductase (*hdhfr*) gene cassette [*hdhfr* gene cassette enables resistance against the drug Pyrimethamine used for eradication of wild type (WT) parasites] and mice infected with transgenic parasites were provided with 70 µg/mL Pyr in drinking water or intraperitonially injected with 40 mg/kg Pyr.

1.8. *In vitro ookinete culture*

Balb/c mice were infected with 10^5 PbDMT_myc or PbVIT_myc parasitized RBC and allowed to develop 20-30% parasitemia and around 1% gametocytemia. Thin smears were prepared on daily basis to monitor the exflagellation events (mobilization of the male gamete from infected RBC), till they were about 3-10 per microscopic field. At this stage the blood of these mice were collected and transferred to Ookinete medium (Appendix), at a dilution of 1:10. The blood in culture was maintained at 19°C for 22-24 hours, creating conditions conducive for fertilization of the mature gametes and formation of the zygote/ookinete.

1.9. *Parasite pellet extraction for Western Blotting*

Complete parasite pellet extraction protocol is performed at 4°C to minimize proteolytic activity and autodegradation of target protein. The whole blood samples were lysed in complete Radio-immunoprecipitation (RIPA) buffer (Appendix). The pellet is obtained by centrifugation of the lysed blood sample at 14000rpm for 3min. The supernatant was discarded and the pellet was washed twice in PBS containing 1X protease inhibitor cocktail (Roche® cOmplete Protease inhibitor tablets, EDTA free) and then resuspended in fresh complete RIPA buffer.

The pellet extract was then sonicated at 5 Ampμ (3×10 seconds) and the supernatant was collected. Quantification of the total protein content was performed spectrophometrically by measuring absorption at 280nm. Equal quantities of protein (40 μg) were boiled at 95°C for 10 minutes in Laemmli buffer. Denatured total parasite protein fractions were then resolved on 8% Polyacrylamide gel (SDS-PAGE). Resolved bands were transferred to a Nitrocellulose membrane via dry electro-transfer (iBlot® Dry Blotting System- Life Technologies). Protein transfer to membrane was confirmed by staining in Ponceau S solution, post electro-transfer. Blocking of membrane surface was performed in WB Blocking solution (Appendix) for 2 hours at RT.

The blot containing the proteins was incubated in primary antibody solution (prepared in blocking solution) overnight at 4°C. Primary antibodies used here were rabbit anti-HA antibody (Abcam 9110®, 1:1000) and mouse anti-Hsp70 (2E6, 1:100). Following incubation in the primary antibody, membranes were rinsed in 0.1% Tween 20 -Tris Buffer Saline (TBST) buffer and incubated in Horseradish Peroxidase (HRP)-conjugated secondary antibody solution (prepared in blocking solution, 1:5000) at RT for 1 hour. Protein bands were visualized post addition of Luminata Crescendo Western HRP substrate (Merck Millipore®) to the membrane; on the ChemiDoc XRS+ Gel imaging System (Bio-Rad®).

All quantification of protein on Nitrocellulose membranes were performed on Image Lab software (version 5.2.1) (Bio-Rad®)

1.10. Immuno fluorescence Assay (IFA) for localization studies

a. RBC were washed in PBS and fixed with 4% PFA containing 0.0075% glutaraldehyde at room temperature(RT) for 30min. Fixed cells were washed in PBS and permeabilized by 0.1% Triton X-100 in Phosphate buffered saline (PBST) treatment for 10 minutes at RT. Blocking of permeabilized RBCs was performed in 3% BSA (in PBS) for 2 hours at RT. Primary antibodies against targeted *Plasmodium berghei* transporter were prepared in blocking solution at respective dilutions (Appendix) and blocked samples were incubated overnight at 4°C. Post incubation with primary antibody(-ies) the samples were rinsed in PBS and incubated in secondary fluorophore conjugated antibody solution (prepared in blocking solution) for 1 hour at RT. Stained RBC were rinsed and finally resuspended in PBS followed by adhesion on Poly-D-Lysine coated coverslips. Excess RBCs were removed and the coverslips were mounted on glass slides with Fluoromount G™ (Southern Biotech). Prepared samples were allowed to dry overnight prior to imaging.

b. Hepatocytes (Huh7/HepG2) to be imaged were seeded on Poly-L lysine coated coverslips (50,000cells/well) in respective culture medium (complete RPMI/DMEM). Post infection, cells were washed in PBS and fixed at different time points with 4% PFA (in PBS) at RT for 15 minutes. Fixed hepatocytes were washed in PBS followed by blocking and permeabilization in BBT buffer (Appendix) for 2 hours at RT. Blocked hepatocytes were incubated in the primary antibody solution (prepared in BBT buffer, details in Appendix) for 2 hours followed by rinsing with 1X PBS and incubation in Secondary antibody solution (prepared in BBT buffer) for 1 hour at RT. Stained and rinsed coverslips were mounted on glass slides with Fluoromount G®.

1.11. Imaging

All localization imaging were performed on *Zeiss® LSM 710* Confocal point-scanning microscope at 100X (Plan Apochromat oil immersion) magnification for RBC and 40X and 63 X magnifications (EC-Plan Neofluar Oil immersion) for Hepatocytes. All images were captured at a pixel resolution of 1024×1024. Analysis and processing of confocal images was performed on Image J (version 1.49p)[56].

1.12. Quantifying Iron accumulation in iRBC on disrupting transporter function[57]

Labile iron pool of erythrocytes infected within WT and VITKO parasites was determined by flow cytometry method using Phen Green SK (Life Technologies®) fluorescent iron probe. Balb/c mice infected with WT and VITKO P.*berghei* were allowed to develop upto 1.5-2.8% parasitemia and then sacrificed to collect whole blood. Post rinsing in serum free RPMI (RPMI$^-$), the RBC were either used directly for the experiment or transferred to CCM, adjusted to 2-2.5%

hematocrit. Post overnight incubation, presence of schizonts was confirmed by microscopic examination of Giemsa stained smears from the cultures. The blood was rinsed once and stained in 10µM Phen Green SK in $RPMI^-$ for 45 minutes at RT. Stained cells were rinsed in PBS and incubated in $RPMI^-$ containing 0.5 µM Syto61 DNA stain, in the presence or absence of 100 µM DFO or 100µM $FeSO_4$ + 1mM ascorbic acid . Treated and stained cells were washed in PBS and analyzed on FACS Calibur (BD Biosciences®). Geometric mean of Phen Green SK fluorescence for FL1-H, FL4-H subset was determined for all samples and for each sample the amount of labile iron was estimated as relative to DFO condition (ΔMFI).

1.13. Statistical Analysis

Comparison of parasitemia between two experimental groups and the volumetric intensities on Western blot were performed using the Mann-Whitney U test at 95% confidence. Comparison of survival curves between two groups was performed by Log rank (Mantel-Cox) test at 95% confidence. All statistical analysis were performed on Graph Pad Prism 5 software[58].

III. RESULTS

1. Plasmodium Vacuolar Iron Transporter homologue

Iron is imperative for cellular processes; however it is useful in a fairly narrow range of concentration. Due to its transitional chemistry and the chemical environment within a cell, iron can be extremely reactive in its biologically relevant form (Fe^{2+}). Among the chief concerns regarding ferrous ion reactivity is the generation of Reactive Oxygen Species (ROS) that can rapidly oxidize proteins and lipids in the cell creating a biochemical chaos and eventually facilitating cell death. In the stringent homeostatic pathways for iron mobilization and utilization in cells, safe storage of iron is of special importance. Detoxification of any excess intracellular iron is typically attained through its sequestration by iron-binding/storage proteins, such as ferritin, or by its transport into separate organelles. Transport of excess intracellular iron into acidic vacuoles for storage and detoxification is particularly common in plants and fungi[59,60]

Vacuolar Iron transporters (VIT) are transmembrane proteins known to be present on vacuolar membranes and involved in transport of iron and manganese ions from the cytosol into vacuoles[31]. VITs are members of the CCC1 superfamily of proteins (InterPro family ID: IPR008217). The CCC1 (Ca^{2+} sensitive cross complementer 1) domain was first identified in the *Saccharomyces cerevisiae* CCC1 protein. *S.cerevisiae* mutants lacking CCC1 are sensitive to increased extracellular concentrations of iron. In addition to yeast, VITs have been best described in plants[61]. In *Arabidopsis* seeds, VIT1 was described to participate in vacuolar enrichment of iron in the embryo and maintaining a normal germination process[59,62] .

Presence of a VIT homologue in *Plasmodium* species was a recent observation that put forth several questions regarding its involvement in the parasite's iron homeostatic pathways, especially since *Plasmodium* lacks known homologues of the iron storage protein: ferritin. The latest ongoing work in our laboratory aims to characterize the function VIT in the iron homeostasis of *Plasmodium* species.

The *P.falciparum* homologue of VIT was previously annotated in the *Plasmodium* Genomic resource – PlasmoDB[63]. *P.berghei* homologue - gene PBANKA_143860 was identified through BLAST similarity to *P.falciparum* VIT gene. Prediction of transmembrane domains (TMD) for the protein encoded by PBANKA_143860 (PbVIT) was performed by employing Hidden Markov Model approach[64]. PbVIT was predicted to possess 5 TMDs (Figure 8), that is typical of the CCC1 family of proteins.

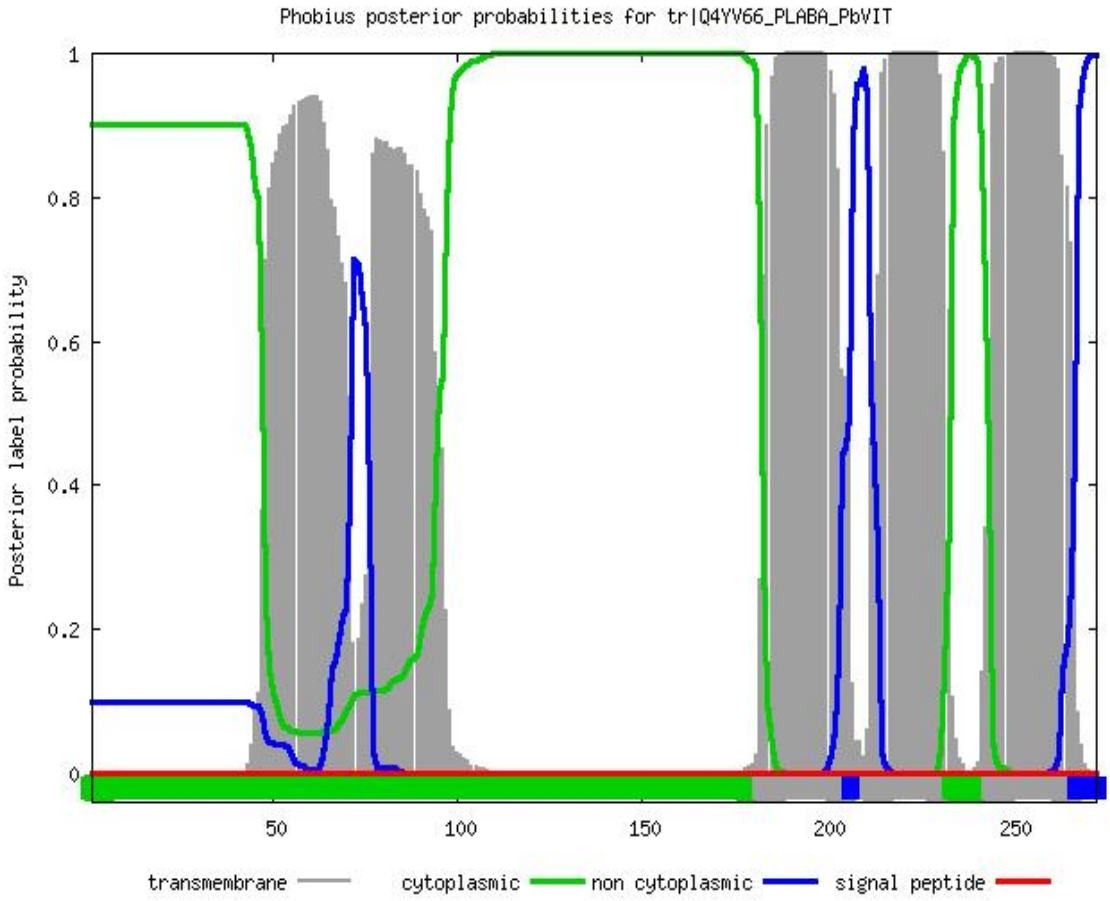

Figure 8. Probability distribution for predicted transmembrane domains along the length of PbVIT protein sequence

Constraint based alignment BLAST[65] of VIT homologues in *Plasmodium,* with *Arabidopsis thaliana*, *Saccharomyces cerevisiae* and other parasitic protists revealed high sequence similarity. To examine the phylogenetic distance between these homologues a phylogenetic tree was constructed (Figure 9)[66]. The VITs of the rodent malaria parasites *(P.berghei*, *P.yoelii* and *P.chabaudi*) were phylogenetically closest with minimum divergence; as were the primate parasites (P. *falciparum*, *P.*vivax and *P.knowlesi*). VITs of kinetoplastids (*Leishmania* and *Trypanosoma*) formed a separate branch from Apicomplexan species (*Plasmodium*, *Toxoplasma* and *Cryptosporidium*). Overall, *Plasmodium* VIT proteins showed greater homology to *Arabidopsis* than to *Saccharomyces* VIT homologues.

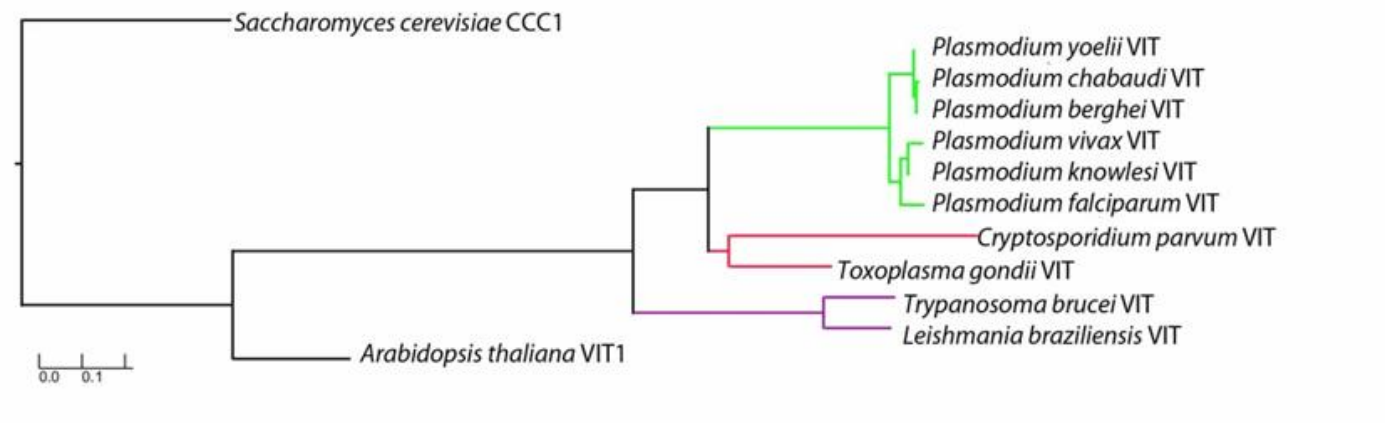

Figure 9. Phylogenetic tree highlighting the divergence between selected VIT homologues. *Saccharomyces cerevisiae* CCC1 has been used a root/out group.

Saccharomyces cerevisiae CCC1 was shown to be involved in vacuolar transport of iron and manganese ions and, mutants lacking this transporter were susceptible to toxicity at high extracellular iron concentrations. Slavic *et al* demonstrated that expression of yeast codon-optimized *Plasmodium falciparum* VIT gene (*pfvit*) was able to rescue strains of *Saccharomyces cerevisiae* lacking CCC1 (ΔCCC1) from iron toxicity at increased iron concentrations. The ability of PfVIT to rescue ΔCCC1 strains from iron toxicity implied its role in iron transport. To directly test the ability of PfVIT to transport Fe^{2+}, uptake of $^{55}Fe^{2+}$ into vacuolar vesicles isolated from transfected ΔCCC1 was measured. These experiments also confirmed the specificity of PfVIT for transport of iron, over other transition metal ions, such as zinc. In addition, iron transport by PfVIT was found to be pH (optimal around pH 7) and temperature-dependent. These studies demonstrated that PfVIT is indeed an iron transporter and have paved the way for future explorations of its role in *Plasmodium* iron homeostasis.

Therefore in the light of these recent findings in our laboratory, specific aims of my thesis project were to establish the localization of *P.berghei* homologue (PbVIT) throughout the parasite life cycle, and to investigate the role of this transporter in iron homeostasis of *Plasmodium* blood stages.

1.1. Localization of PbVIT in different developmental stages of Plasmodium berghei

The prime intent was to establish the expression and localization of PbVIT across the different developmental stages of *Plasmodium berghei*. Transcriptomics data indicated the elevation in PbVIT expression from the ring to the trophozoite stage followed by a relative decline in expression in the following erythrocytic stages[67]. To elucidate the nature of localization of PbVIT in different stages of parasite development, a C-terminal *myc* tag was added to the endogenous, PbVIT gene in *Plasmodium berghei* (PbVIT_*myc*) through a single crossover recombination at the WT PbVIT locus. In addition to PbVIT_*myc P.berghei* line, a previously generated transgenic *P.berghei* line expressing a C-terminal GFP fusion protein of PbVIT was employed in parallel to study the localization of the transporter by immunofluorescence assay (IFA).

Localization studies performed with both parasite lines yielded consensual results on the nature of localization of PbVIT during different erythrocytic stages. While there appeared to be some overlap between PbVIT and the parasite cytosolic Hsp70 protein (2E6), PbVIT did not have a uniform distribution as the latter. Rather, PbVIT appeared to be granular, possibly vesicular (Figure 10A). Moreover these vesicular structures did not seem to co-localize with the parasite plasma membrane either, as evident from the lack of overlap with the parasite plasma membrane marker- Merozoite Surface protein 1 (Msp1) (Figure 10B). In all the stages of erythrocytic development, there existed an elevated PbVIT signal confined to a region, which co-localized with *Plasmodium* endoplasmic reticulum (ER) resident protein-BiP (Figure 10C).

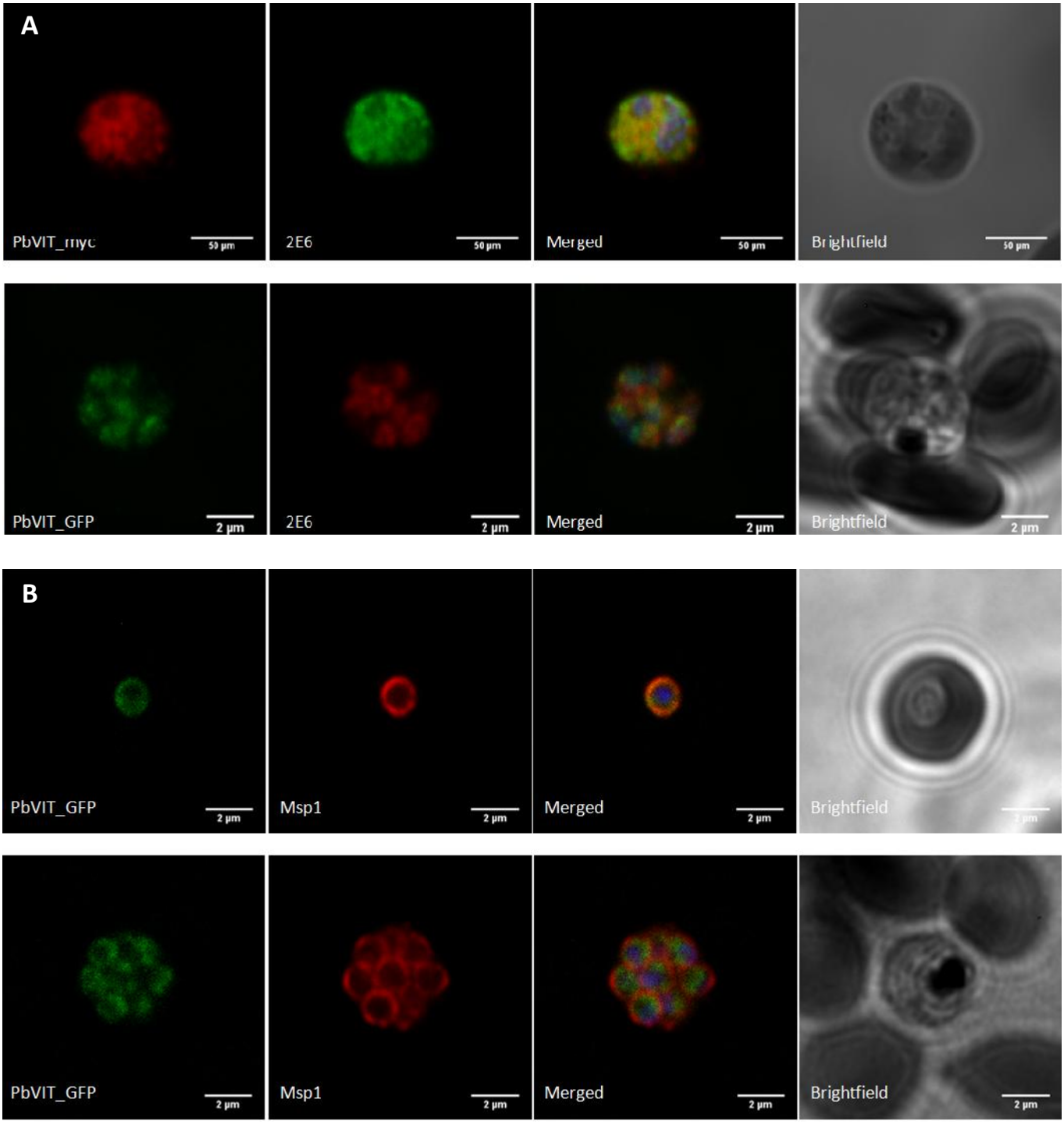
A
PbVIT_myc
50 µm
2E6
50 µm
Merged
50 µm
Brightfield
50 µm
PbVIT_GFP
2 µm
2E6
2 µm
Merged
2 µm
Brightfield
2 µm
B
PbVIT_GFP
2 µm
Msp1
2 µm
Merged
2 µm
Brightfield
PbVIT_GFP
2 µm
Msp1
2 µm
Merged
2 µm
Brightfield
2 µm

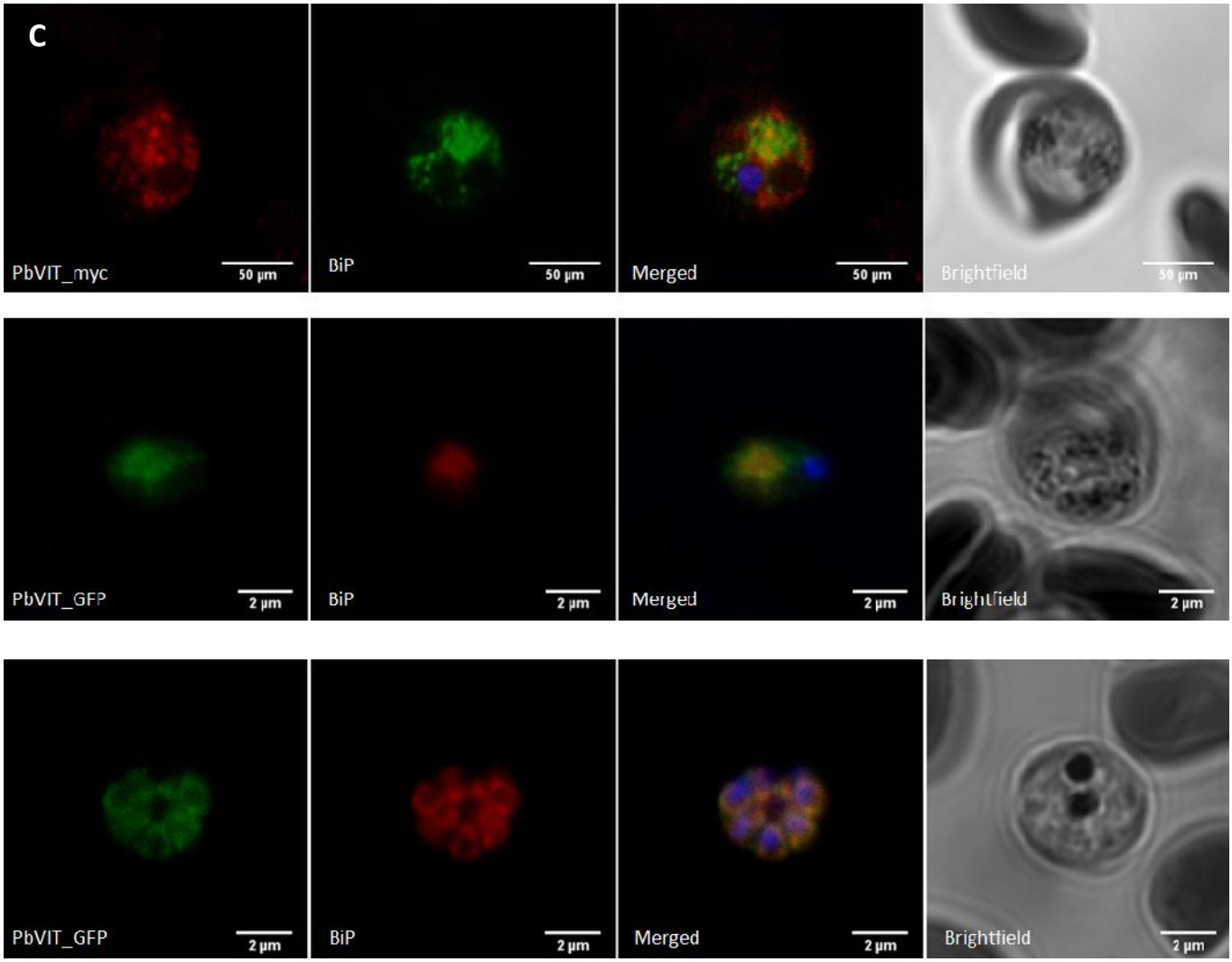

Figure 10. Localization of PbVIT using C-terminal myc or GFP tag respectively; in different stages of erythrocytic development with (A) cytosolic protein PbHsp70 (2E6); (B) Plasma membrane resident protein-Msp1; (C) Endoplasmic reticulum resident protein BiP using Point scanning Confocal Microscopy

To extend the investigation of PbVIT localization to other life cycle stages of malaria parasites, *P.berghei* ookinetes were obtained by culturing the infected RBCs in conditioned medium, to yield ookinetes *in vitro*. PbVIT_myc was then visualized along with PbHsp70 (2E6) by IFA. The region of greatest signal for PbVIT appeared to possess a structure, yet to be clearly identified through co-staining with other organellar markers (Figure 11). However, there also exist some diffuse signals in the rest of the ookinete cytosol. Therefore, PbVIT is not limited to the cytosol in ookinetes and presents itself in what seems to be reticular structures.

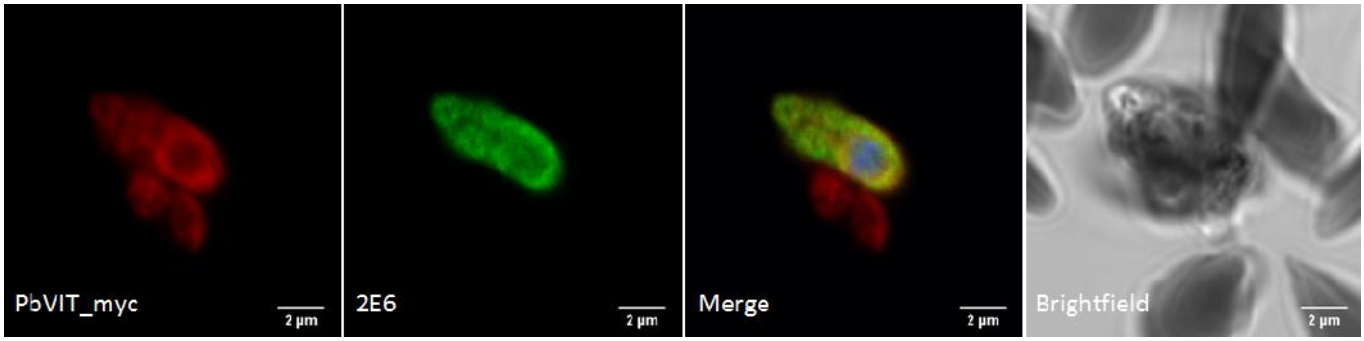

Figure 11. Localization of PbVIT containing C-terminal myc tag with Plasmodium Hsp70 (2E6) in ookinetes

Furthermore, to study the mosquito phase of the infection, the midguts of mosquitoes were analyzed 19 days post infection to localize the PbVIT pattern in sporulating oocysts. PbVIT appears to localize within the parasites (organized as radial stacks in mature oocysts) in an organized arrangement (Figure 12). It does not appear to co-localize with the PVM marker-Upregulated in infectious sporozoite 1 protein (Uis4) which has an apical organization at this phase, consistently forming an outer concentric arrangement with respect to PbVIT. However, as in the case of ookinetes, the precise nature of PbVIT localization remains to be deciphered through co-localization studies with other markers. Nevertheless, these experiments clearly demonstrate expression of the PbVIT protein during the parasite development inside the mosquito midgut.

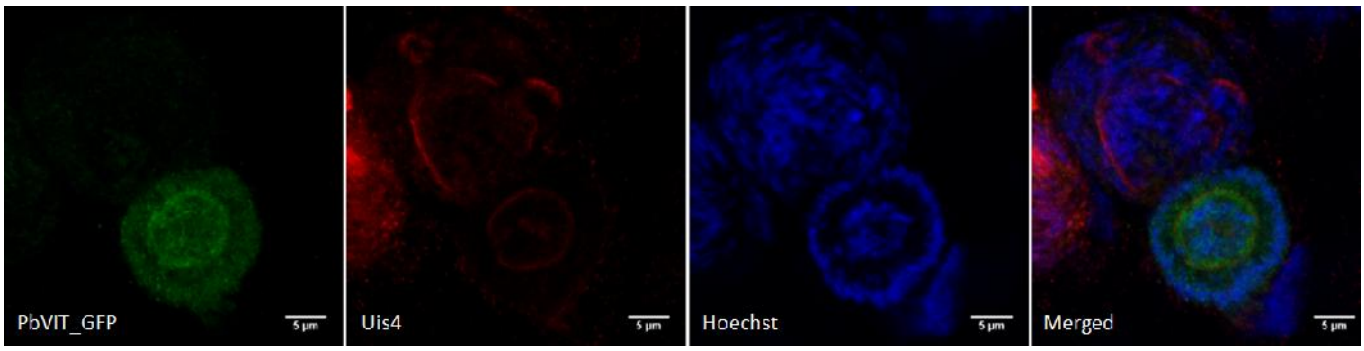

Figure 12. Localization of PbVIT containing a C-terminal GFP tag, withUis4, in sporulating midgut oocysts 19 days post infection

Extending the localization investigation to the exo-erythrocytic form of the parasite (liver stage of parasite development), PbVIT was monitored at different time points in Huh7 hepatoma cells infected with sporozoites (PbVIT_GFP). The different time points coincide with major developmental events and throughout all of them, the maximum PbVIT signal intensity appeared in foci that neatly co-localized with *Plasmodium* ER resident protein-BiP (Figure 13A). The signal was not solely limited to the ER, but extended as granular entities in the parasite cytosol. No visible overlap was noticed with the PVM protein marker Uis4, excluding a possible PVM localization of PbVIT for all the developmental stages studied (Figure 13B).

A

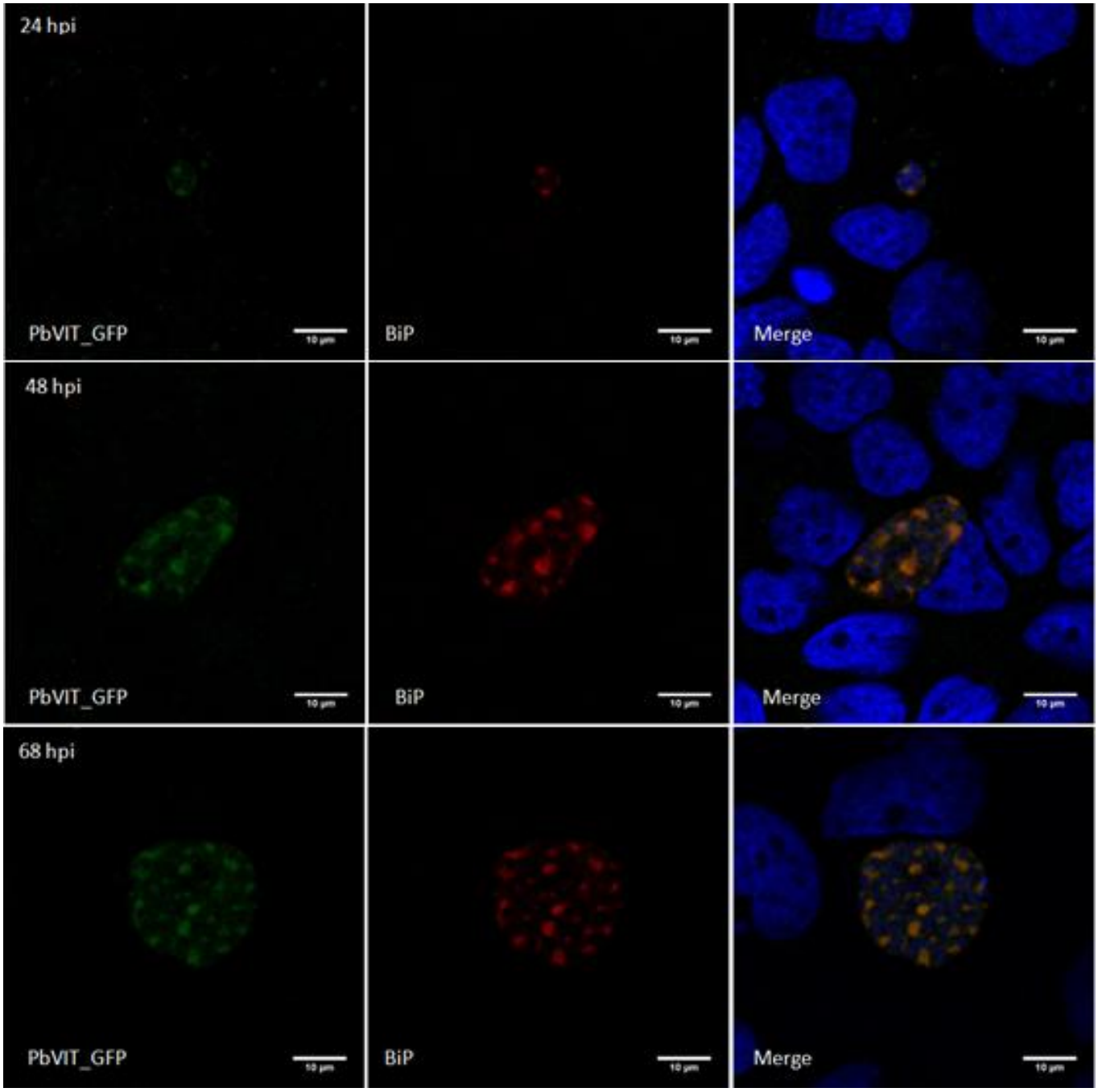
24 hpi
PbVIT_GFP
BiP
Merge
48 hpi
PbVIT_GFP
BiP
Merge
68 hpi
PbVIT_GFP
BiP
Merge

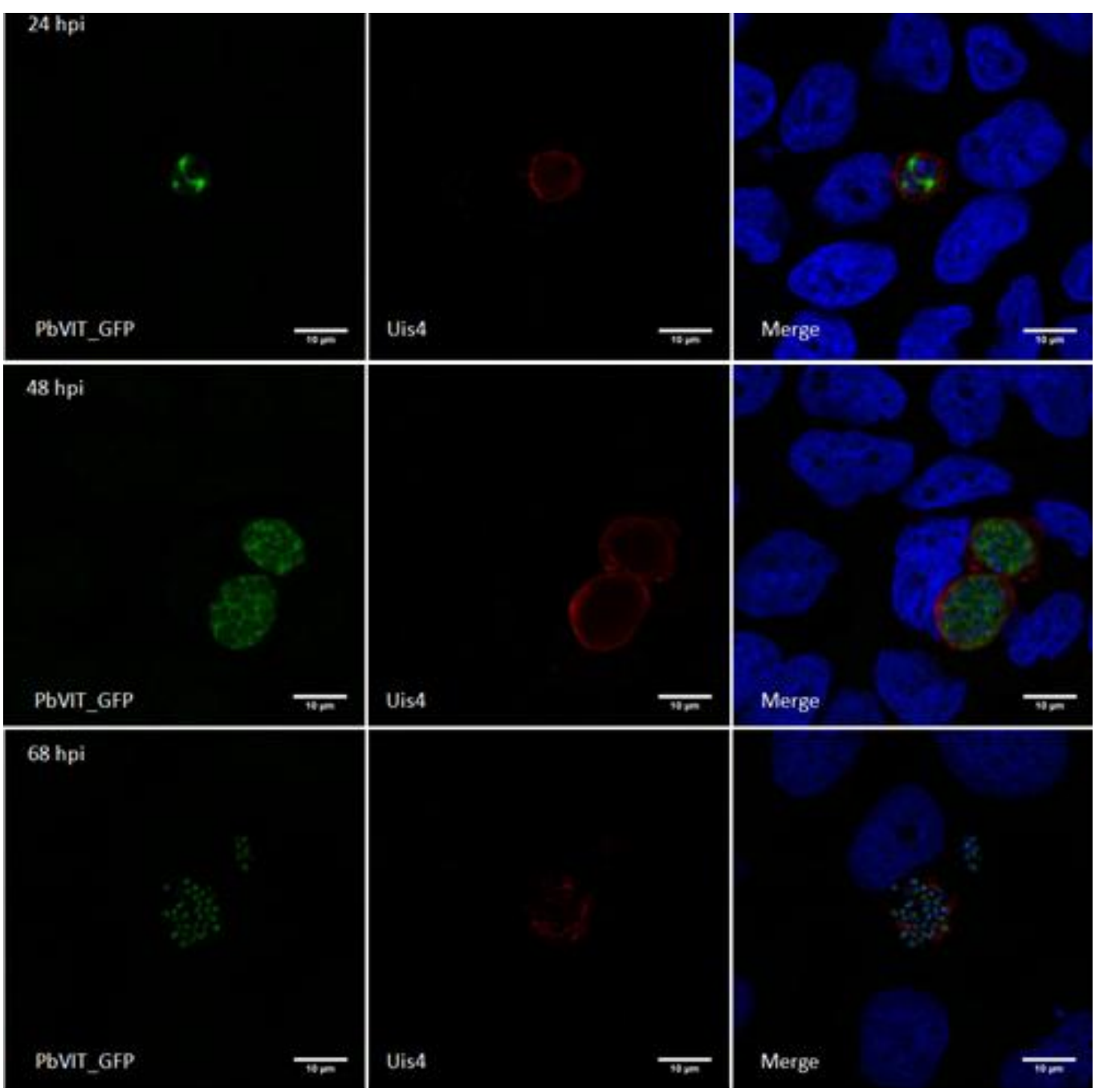

Figure 13. Localization of C-terminal GFP tagged PbVIT during liver stage infection (exo-erythrocytic forms) at developmentally distinguishing time points with (A) ER resident protein-BiP; (B) PVM marker protein-Uis4 using Point scanning Confocal Microscopy

While not completely transparent as to why PbVIT localizes to the ER, a possible doubt could be, whether the protein is arrested in the ER due to a large tag that affects its insertion into target membranes? To account for the certainty of PbVIT localization, a C-terminal *myc* tagged fusion protein of PbVIT was used in addition to the GFP tagged line. Imgaing in PbVIT_myc *P.berghei* infected hepatocytes is still under optimization.

The *myc* tag is considerably smaller compared to GFP and still presents similar results regarding ER localization and cytosolic granular distribution in erythrocytic stage parasites. The ideal situation would be to use an antibody

directed to PbVIT however, the currently available PfVIT antibody is not suitable due to its non-specific binding to off-target proteins in the parasite as shown in Figure 14.

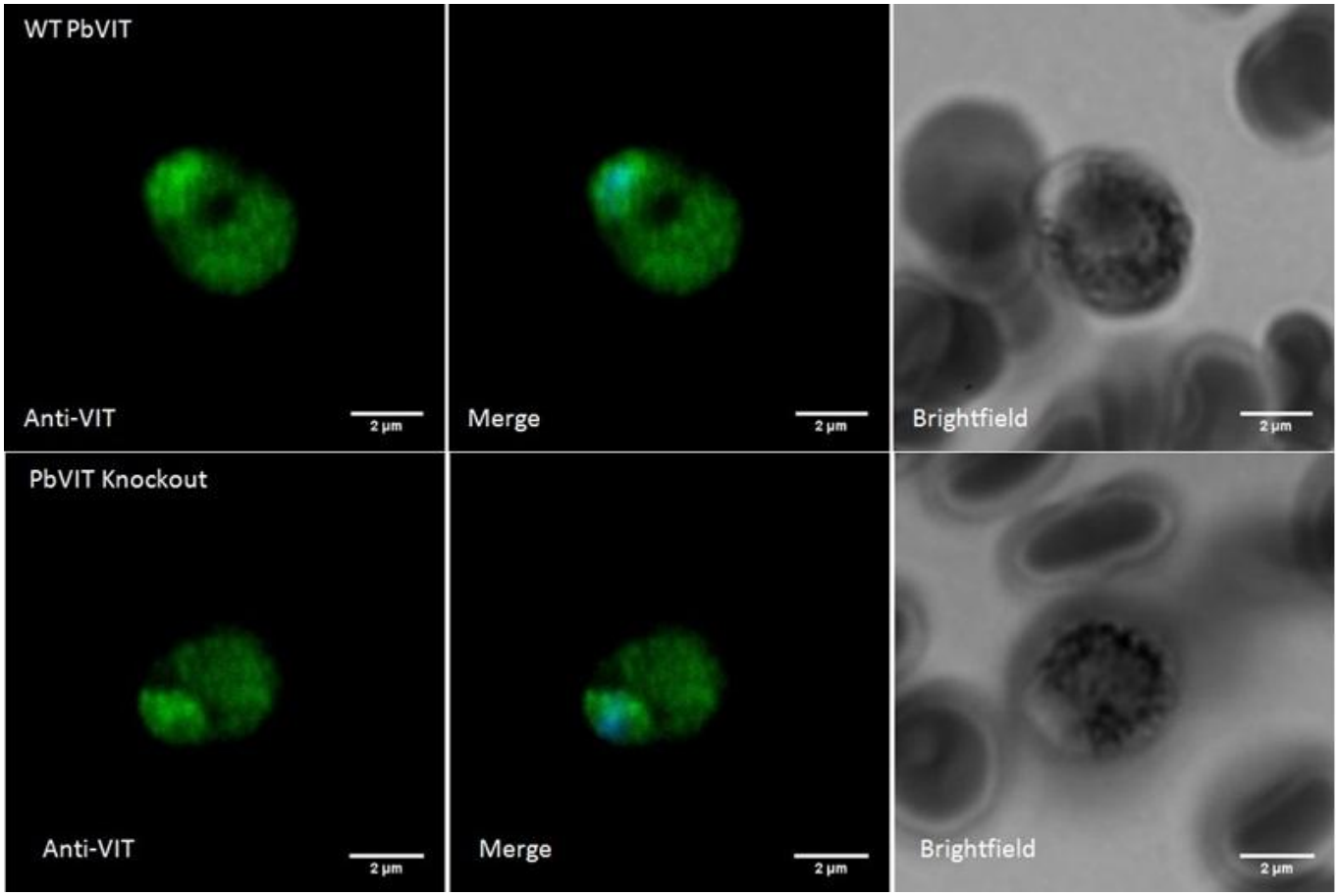

Figure 14. Immunofluorescence analysis of *P.berghei* WT and PbVITKO blood stage parasites, using PfVIT antibody

Recently, two plant transporters with demonstrated functional homology to CCC1 have also been localized to ER bodies with their proposed role in the metal ion homeostasis[68]. Thus, in addition to studies in plants, our study paves the way to explore further the role of the ER in iron detoxification.

1.2. Quantitative estimation of accumulation of ferrous ions in cytosol of WT and VITKO Plasmodium berghei[57]

It was previously observed in our laboratory that disruption of the PbVIT locus through a homologous double crossover recombination with *Toxoplasma dhfr* cassette providing resistance to pyrimethamine, did not eradicate parasite populations in the erythocytic stage. This indicated PbVIT to be dispensable in the blood stage of development. However, PbVIT knockout *P.berghei* (PbVITKO) produced a significantly lower parasite load in livers of mice infected with sporozoites, in comparison to those infected with the WT *P.berghei* sporozoites. It was also

demonstrated that PbVITKO were mildly compromised in induction of cerebral malaria in C57BL6/J mice; as well as demonstrated lower blood parasitemia with respect to their wild type counterparts.

With this present knowledge of parasite requirement for VIT to achieve normal development during both the blood and liver stages, the aim here was to understand the cause of lower parasite burden both at liver and blood stages of infection with PbVITKO parasites. With the established role of PfVIT in iron transport, the succeeding question was, what does VIT do in the parasite? Specifically, are *Plasmodium* VITs involved in uptake of iron across the parasite plasma membrane or detoxification of iron by transporting this metal into an organelle? In order to address this question, we proceeded to compare the levels of labile iron pools in WT and PbVITKO parasites.

To determine the parasite labile iron pool, we relied on flow cytometry approach based on a probe which fluorescence depends on the cellular iron content. Phen Green SK is an iron probe that permeates the cell membrane and its fluorescence is reversibly quenched in the presence of Fe^{2+}. Therefore, with the efficient removal of Fe^{2+} from cytoplasm by the addition of high affinity iron chelators, such as desferoxamine, iron is removed and the Phen Green SK probe fluorescence is consequently increased. Alternatively, the addition of excess iron quenches Phen Green SK fluorescence (Figure 15). Thus, comparison of Phen Green SK fluorescence of DFO-treated and untreated samples provides an effective method for assessing the relative labile iron content of cells.

In such settings, RBCs were taken from Balb/c mice infected with WT or VITKO parasites and were incubated under three experimental conditions: iron depleted (DFO treatment), untreated control and excess extracellular iron. All samples were then stained with a fluorescent iron probe - Phen Green® SK and a DNA stain SYTO 61 for further analyses by flow cytometry[57,69]. The RBCs infected with PbVITKO parasites were found to have a greater labile iron pool compared to the WT- parasitized RBCs (Figure 16). Therefore, these data indicate a role for PbVIT in cellular iron detoxification in blood stage parasites.

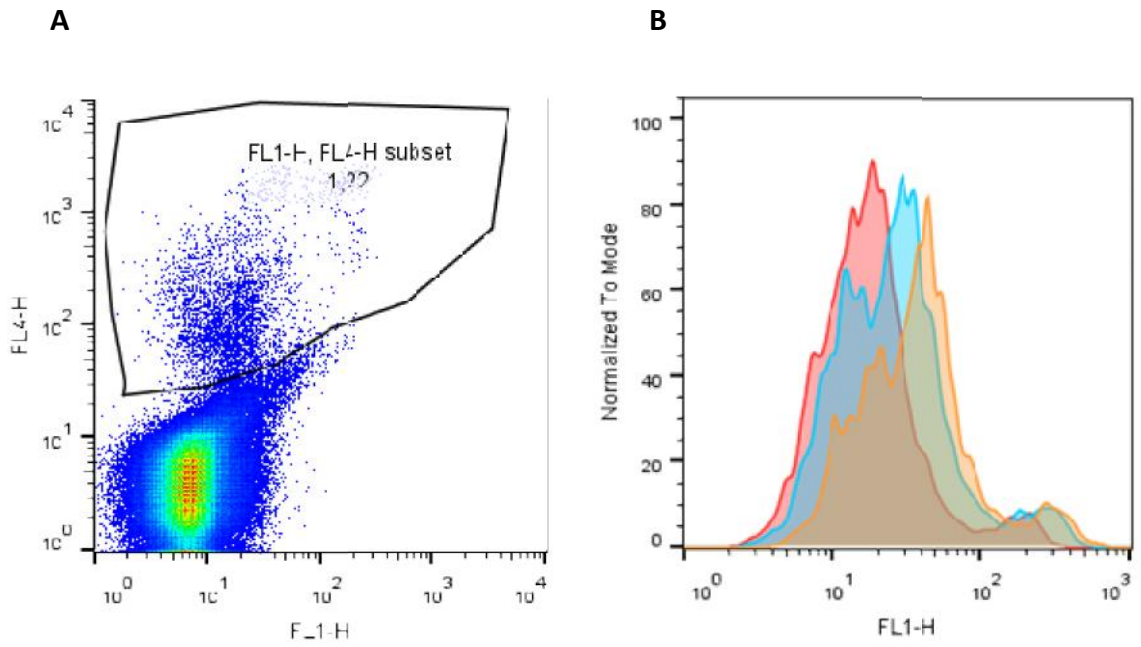

Figure 15. Representation of the flow cytometry method used for determination of labile iron pool of iRBC. A. Gating strategy used to select the P. *berghei*-infected RBC from non-infected RBC based on SYTO 61 DNA staining (FL 4). B. An example of histogram showing the Phen Green fluorescence intensity of Syto-61 positive subsets of $FeSO_4$ treated sample (red) and DFO treated sample (yellow)

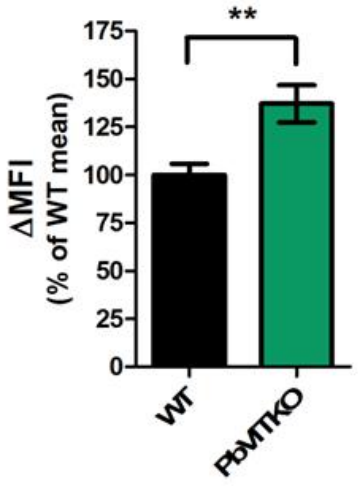

Figure 16. The labile iron pool (LIP) of *P.berghei* WT and PbVITKO-iRBCs analyzed by flow cytometry. ΔMFI was determined by evaluating the change in mean fluorescence intensity of Phen Green-loaded iRBCs (SYTO 61-positive subset), after incubation with 100 µM DFO (ΔMFI=MFIDFO-treated –MFIDFO-untreated). For each independent experiment, the MFI of PbVITKO-iRBCs was normalized to the mean MFI of WT-iRBCs. Shown is a pool of 4 independent experiments (N = 14), ** P = 0.0028 (unpaired, two-tailed Student's t test; WT mean ± SEM = 100 ± 6, PbVITKO mean ± SEM = 137.1 ± 10).

2. Plasmodium Divalent Metal transporter 1 homologue

The physiochemical property of iron in the extracellular fluid does not permit it to effortlessly cross lipid membranes around or within cells. Organisms therefore, have a variety of mechanisms for import of iron that enables effective acquisition and shuttling of iron at optimal oxidation state for storage or metabolic utilization. Among some of the most well studied players in acquisition of iron, is the Divalent metal transporter 1 (DMT1/Nramp II).

DMT1 was the first mammalian transmembrane iron transporter to be identified[70] and shown to be a proton-coupled metal ion transporter[71]. DMT1, also known as NrampII[70] possesses a conserved transmembrane structure characteristic to those in the Nramp family (InterPro ID: IPR001046) of proteins[72]. This family of proteins comprises of members involved in solute transport across membranes.

The NrampI gene was identified and classified originally as being involved in the natural resistance of mice to intracellular pathogen infections and expressed exclusively in macrophages and Polymorphonuclear leukocytes (PMNL)[73]. NrampII or DMT1 on the other hand is expressed ubiquitously and participates in uptake of dietary iron by enterocytes and transferrin dependent iron uptake in the periphery. DMT1 is highly conserved from bacteria to human. The presence of a 3' iron responsive element has been reported in some isoforms of DMT1 mRNA that account for its stabilization through interaction with iron regulatory proteins[74] and also indicates mechanisms of sensing systemic iron demand and subsequent regulation of DMT1 expression.

DMT1 is capable of transporting iron in Fe^{2+} state and thus, is accompanied by ferrireductase in its vicinity, to reduce extracellular iron (Fe^{3+})[75]. The intriguing finding that *Plasmodium* lacks transferrin or transferrin receptor homologues, sparked an interest as to how the parasite can acquire iron from its host especially considering the rapidly replicating parasite would dearly require this micronutrient?

A DMT1 homologue was identified in the genome of *Plasmodium falciparum*[51], which opened up avenues to understand the role of this putative iron transporter in iron acquisition and homeostasis. In addition to studies of *Plasmodium* VIT, elucidation of iron acquisition mechanisms in *Plasmodium* by DMT1 homologue is another area of active investigation in our laboratory.

The *P.berghei* gene PBANKA_123860 was identified via BLAST similarity to the *P.falciparum* DMT1 homologue. The resultant protein (PbDMT) was predicted to have 12 TMDs[64] (Figure 17), which are characteristic of the Nramp family proteins (10-12 TMDs) and, an unusually long cytosolic N-terminal domain which is poorly conserved in sequence across different species.

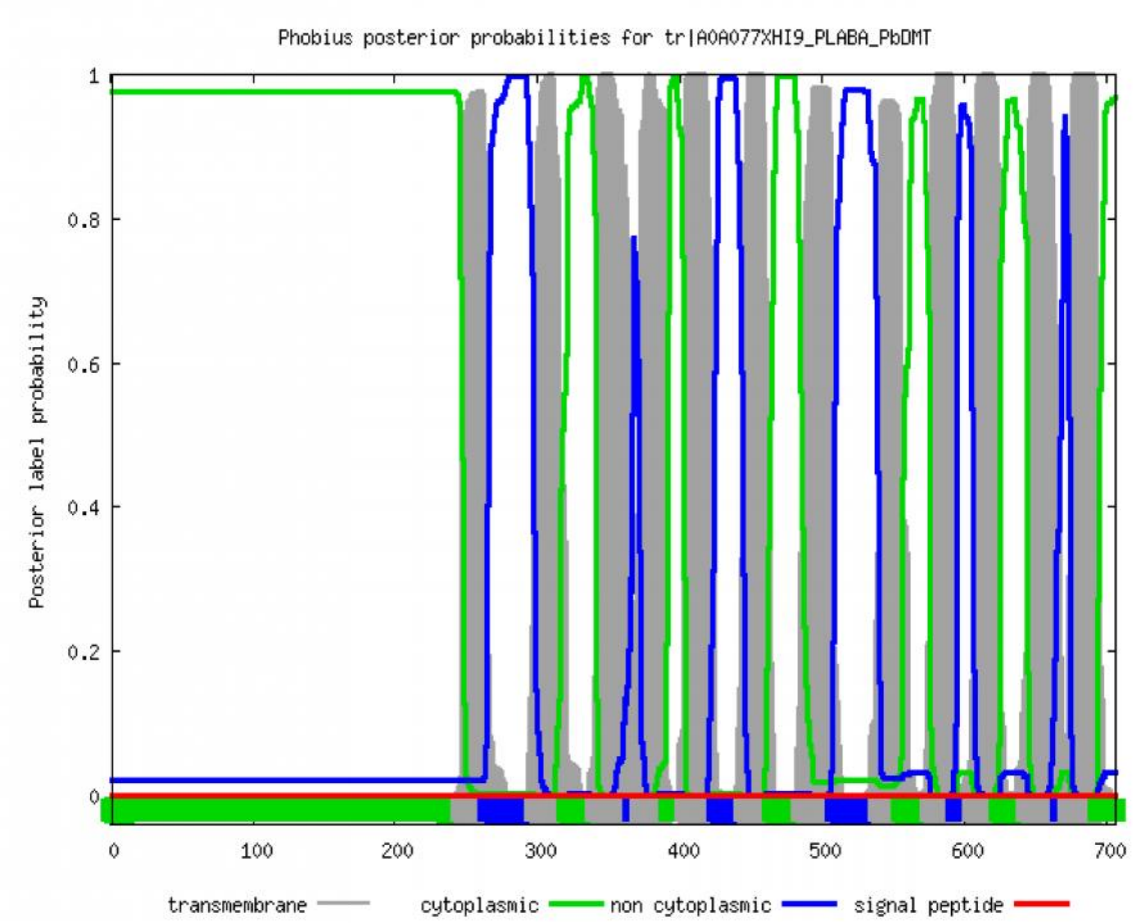

Figure 17. Probability distribution for predicted transmembrane domains along the length of PbDMT protein sequence

Ehrnstorfer *et al* recently described the crystal structure and key amino acids involved in chelation of Fe^{2+} in SLC11 (NRAMP) transporters in *Staphylococcus capitis*[76]. The signature comprises of an Aspartate (D) residue in close proximity of an Asparagine (N) residue in the first helix of the transmembrane domain and, a *thiol* containing residue in the sixth transmembrane helix. Constraint based Alignment BLAST[65] of DMT1 homologues from *Plasmodium* species and some other phylogenetically diverse organism (Figure 18) displayed a stretch of conserved sequence across the first transmembrane helix. Additionally the signature D and N arrangement was observed towards the end of the first TM sequence; except for TgDMT where the signature was in its second TM domain which may not be too disparate considering TgDMT has 13 TM domains. All TM domains for unreviewed protein sequences (*Plasmodia and Toxoplasma*) are strictly predicted by 'Hidden Markov-Model' posterior probabilities that work at over 95% sensitivity yet with an error window of 3-4 positions.

Figure 18. Identification of signature residues in the first TM helix of DMT homologues. Green underline marks the span of the first TM except for Toxoplasma where it is the second TM helix

To examine the phylogenetic distance the between these DMT1 homologues, a phylogenetic tree was constructed (Figure 19)[66]. The DMTs of rodent malaria parasites (*P.berghei, P. yoelii and P. chabaudi*) were minimally divergent; as were the primate parasites (P. *falciparum, P. vivax and P. knowlesi*). DMT1 homologues of Apicomplexan species (*Plasmodium* and *Toxoplasma*) were overall distant phylogenetically from other eukaryotic and prokaryotic DMT1 homologues.

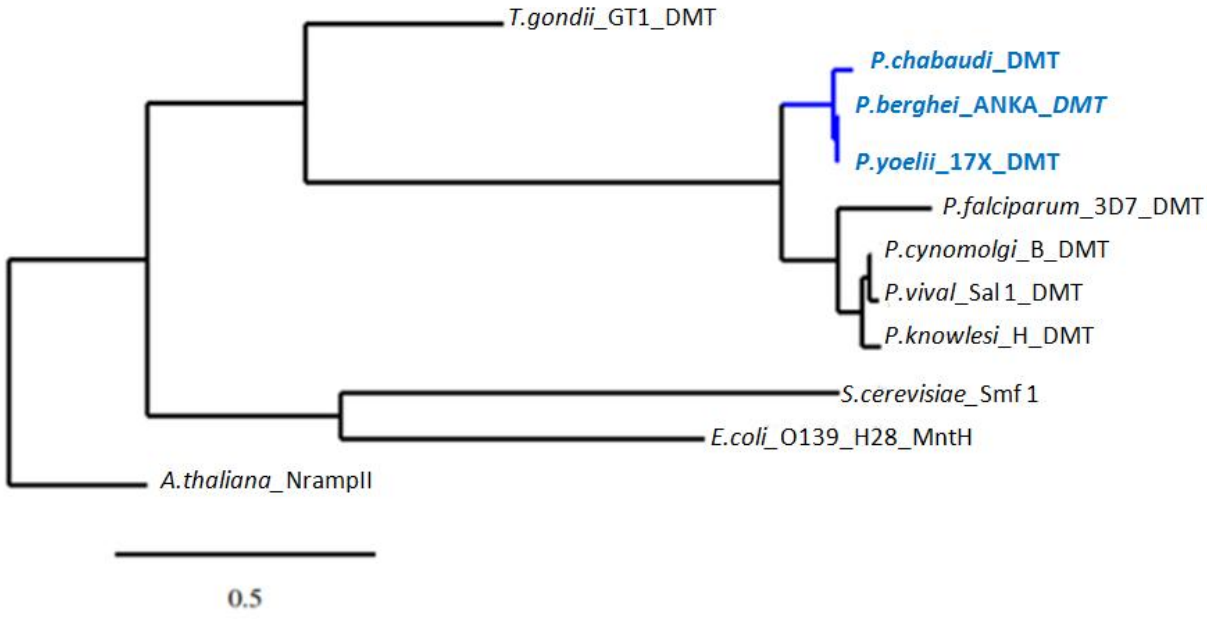

Figure 19. Phylogenetic tree highlighting the divergence between DMT1 homologues. *A.thaliana* NrampII has been used a root/out group

In addition to the above described VIT homologues, *S. cerevisiae* has also been successfully used as an expression system for functional characterization of DMT 1 homologues. *S. cerevisiae* Fet3 and Fet4 proteins were

demonstrated to be involved in uptake of Fe^{2+} at the plasma membrane and account for one of the chief iron transport systems. Fet3 is a component of the high affinity Fe^{2+} transport system with ferroxidase like function and essential during growth in iron scarce conditions[77]. Fet4 on the other hand is a low affinity Fe^{2+} transporter[78]. Disruption of the fet3 and fet4 loci in *S. cerevisiae* impairs growth on iron limiting media, a phenotype that was rescued by transfection with *P.falciparum* or *P.berghei* DMT 1 homologues to complement the Fet3Fet4 function [Slavic *et al* unpublished data]. The iron transport function of *P.berghei* DMT 1 homologue (PbDMT) was confirmed by uptake of $^{55}Fe^{2+}$ by PbDMT complemented Δfet3fet4 cells. Additionally, iron transport by PbDMT was found to be pH (optimal around pH 4-5) and temperature-dependent. These studies corroborated the role of PbDMT as an iron transporter and opened avenues into the investigation of the role of DMT 1 homologue in *Plasmodium* iron acquisition and homeostasis.

Recent studies in our laboratory suggest an essential role of PbDMT for the blood stage *P.berghei* parasites, as repeated attempts of *pbdmt* knock-out did not result in gene disruption. In order to unravel the effect of PbDMT disruption on both the erythrocytic and the exo-erythrocytic stages of parasite life-cycle, it would be necessary to demonstrate the correlation between the deficiencies of PbDMT function and associated developmental defects and whether revival of WT PbDMT function could rescue such parasites.

Thus, under the current revelations of DMT 1 homologues in *Plasmodium*, this thesis project aims to establish the role of the DMT 1 homologue in *Plasmodium* iron homeostasis pathways by studying its cellular localization through different life stages and by employing conditional gene knockdown systems to induce a reversible, inducible knockdown of PbDMT. However, transmembrane proteins have different post translational processing and degradation pathways than classical cytosolic proteins, making it difficult to deduce whether a certain technique would be superior to others. Hence, in this thesis two conditional knockdown systems were employed targeting different cellular machineries to obtain protein level knockdown.

2.1. Localization of PbDMT in different developmental stages of Plasmodium berghei

The primary aim here was to elucidate the distribution of the DMT 1 homologue in *Plasmodium berghei* through its different developmental phases. The localization was studied using three independent mutant parasite lines, where PbDMT was tagged with either a C-terminal GFP tag, a C-terminal *myc* tag or a C-terminal HA tag respectively. In the erythrocytic stage, PbDMT appeared to be granularly distributed in both the cytosol and close to the parasite periphery (Figure 20). This observation was agreeable in erythrocytic stage for different tagged mutant *P.berghei* lines. The cytosolic punctuate signals co-localized with PbHsp70 (2E6). However, while PbHsp70 signal was homogenous, the PbDMT signal indicated a somewhat punctuate distribution (Figure 21A). There was also a co-localization with parasite plasma membrane as elucidated by the overlap of PbDMT signal with Msp1 (Figure 21B). With respect to retention of PbDMT in the endoplasmic reticulum, no clear overlap was observed with the parasite ER resident protein BiP (Figure 21C).

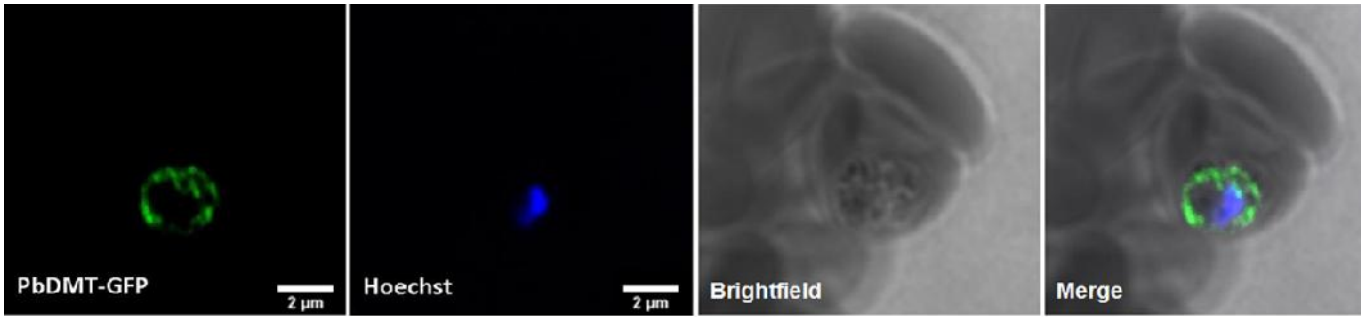

Figure 20. Localization of C-terminal GFP fusion protein of PbDMT in erythrocyte (trophozoite form)

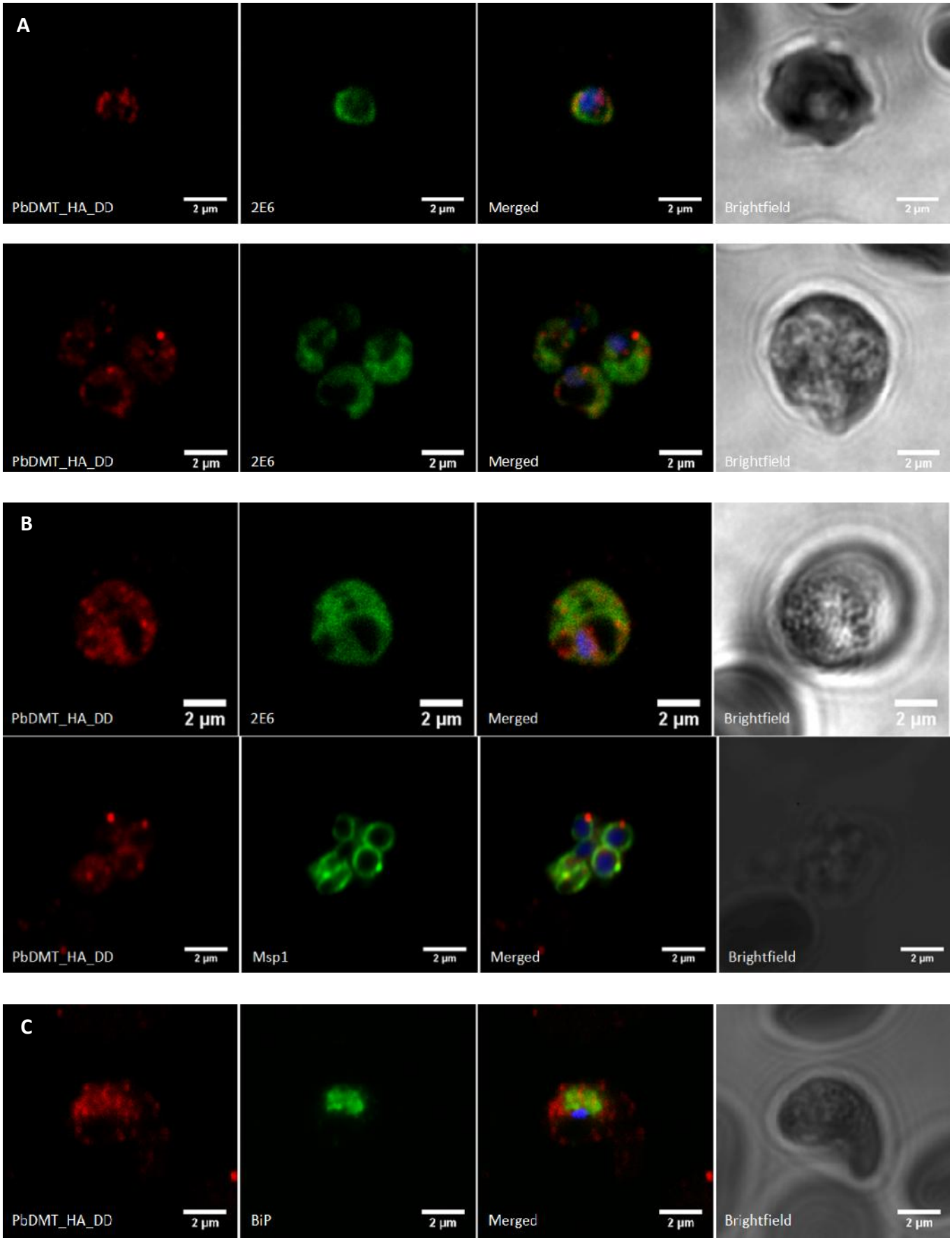

Figure 21. Localization of PbDMT using C-terminal HA or myc tag respectively; in different stages of erythrocytic development with (A)Cytosolic protein PbHsp70 (2E6); (B) Plasma membrane resident protein-Msp1; (C) Endoplasmic reticulum resident protein BiP using Point scanning Confocal Microscopy

To extend the investigation of PbDMT localization to other life cycle stages of malaria parasites, *P.berghei* ookinetes were obtained by culturing the infected RBCs in conditioned to generate ookinetes *in vitro*. PbDMT_myc was then visualized along with PbHsp70 (2E6) by IFA. The PbDMT_myc signal appeared to be spread through the ookinete cytosol and also co-localized with the cytosolic protein marker: PbHsp70 (2E6) (Figure 22).

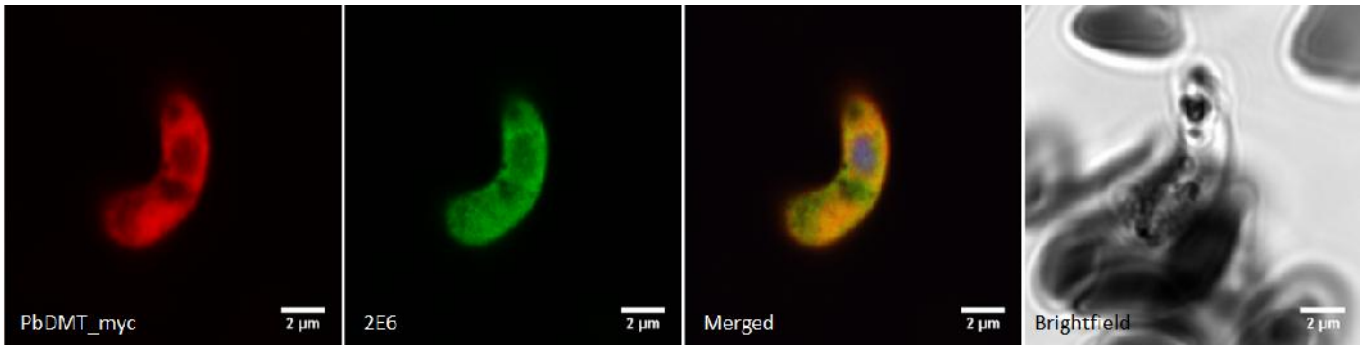

Figure 22. Localization of PbDMT containing C-terminal myc tag with Plasmodium Hsp70 (2E6) in ookinetes

Proceeding with the localization studies into the liver stage of parasite development; the exo-erythroctic forms were studied in *P.berghei* sporozoites infected HepG2 hepatoma cells at developmentally relevant time points. PbDMT possessed a strongly peripheral arrangement that overlaps with Msp1, though slimly excluding Uis4 considering the proximity of parasitophorous vacuole membrane (PVM) and parasite plasma membrane (PPM) and, the resolution achieved with the current optical settings (Figure 23). The co-localization of PbDMT with Msp1 is faint after formation of individual merozoites and PbDMT signals appear more punctuate, indicating its possible allocation during ctyokinesis in the parasite. It is known about nutrient transporters to reside in plasma membrane as well as in vesicles involved in nutrient delivery and mobilized on cellular nutrient demand. The punctuate signals of PbDMT that may or may not totally merge with the Msp1 signal, may abide to a similar pattern.

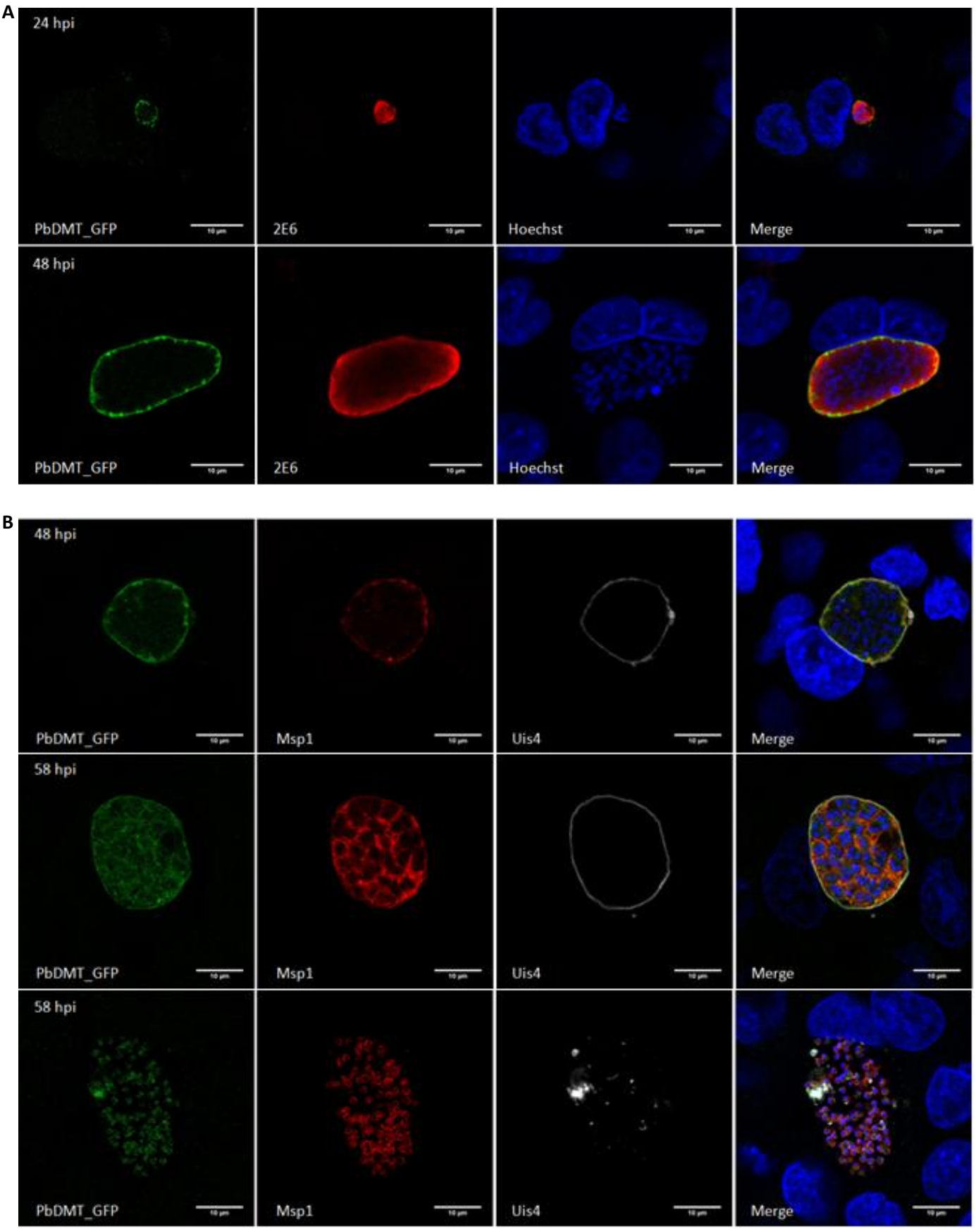

Figure 23. Localization of C-terminal GFP tagged PbDMT during liver stage infection (exo-erythrocytic forms) at developmentally distinguishing time points with (A) PbHsp70 and (B) Plasma membrane marker-Msp1 and PVM marker protein-Uis4 using Point scanning Confocal Microscopy [Slavic *et al* unpublished data]

The localization observed in this study is in alignment with the DMT protein distribution patterns seen in other eukaryotic cells[79,80]. *Plasmodium* does not possess any transferrin receptor homologues, which further complicates the understanding of how it is able to transport iron at the host-parasite interface.

2.2. Effect of PbDMT knockdown on survival and parasitemia in mice

A. *Destabilization Domain (DD) strategy*

The working principle of this technique involves the fusion of a modified *Escherichia coli* DHFR sequence (DD) to the C-terminal of the target protein. The DD is inherently unstable causing misfolding of the entire fused protein and targets it to the proteasome. However, in the presence of a small molecule (Trimethoprim in this case), the DD is stabilized and supposedly does not interfere with target protein structure of function. The knockdown is therefore, induced on removal of trimethoprim (TMP), directly at the protein level making this technique quick to bring about a phenotype caused by depletion of a target protein[81] .In this thesis project, we employed two independent DD lines namely PbDMT_DD and PbDMT_HA_DD. Integration of transgenic locus containing 3'-DD or 3'-HA_DD in to the parasite genome was confirmed by genotyping PCR (Figure 24).

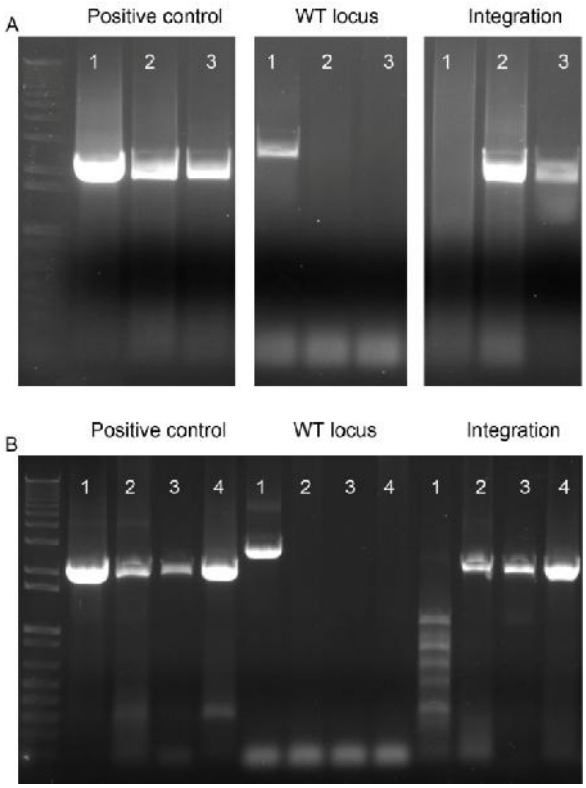

Figure 24. Genotyping PCR confirming pure populations of (A) PbDMT_DD, 1-WT *P.berghei* ANKA; 2-PbDMT_DD clone 1; 3-PbDMT_DD clone 2 and (B) PbDMT_HA_DD, 1-WT *P.berghei* ANKA; 2-PbDMT_HA_DD clone 1; 3-PbDMT_HA_DD clone 2 ; 4-PbDMT_HA_DD clone 3 of *Plasmodium berghei*

Following the successful generation of the transgenic *P.berghei* lines expressing PbDMT-DD or PbDMT-HA-DD fusion proteins, the following step was to examine the effect of PbDMT destabilization on the parasite development and the outcome of infection. To this end, C57BL/6J male mice were infected with 10^5 PbDMT_DD or PbDMT_HA_DD *P.berghei* parasitized RBC and mice survival along with parasitemia were followed daily. . In both the DD parasite **l**ines, the destabilization of the transporter by removal of trimethoprim did not result in any statistically significant difference in survival of infected mice; nor protection against cerebral malaria compared to its stabilized counterpart (Figure 25B and 26B).

With respect to the effect of PbDMT knockdown on progression of parasite load; parasitemia in blood was monitored in C57BL/6J mice throughout the experiment. In addition to C57BL/6J mice which develop cerebral malaria, parasitemia was monitored in Balb/c mice which do not develop cerebral malaria and succumb to very high levels of parasitemia instead. Balb/c mice were also infected with 10^5 iRBC (*i.v*). In C57BL6/J mice infected with PbDMT_DD *P.berghei*, destabilization of the PbDMT-DD by trimethoprim removal led to significant decrease in parasitemia on days 3 to 6 post-infection, compared to the PbDMT-DD stabilized condition (Figure 25A). However, with progression of infection death of mice by cerebral malaria reduced the number of animals in the experiment, thus the difference in parasitemia was no longer significant. In infected Balb/c mice, the parasitemia patterns appeared similar to that in C57BL6/J mice with the stabilized PbDMT parasite maintaining a higher parasitemia throughout the course of infection (Figure 25C). The difference in parasitemia was significant over a longer period than in C57BL6/J mice. Due to the lack of a dedicated antibody against PbDMT and the absence of a fusion tag in the PbDMT_DD line, the knockdown could not be quantified at the protein level through Western blotting. Therefore, the experiments were reiterated with the PbDMT_HA_DD *Plasmodium berghei* line that would enable quantification of the extent of knockdown on PbDMT destabilization, and associate the same to the observed phenotype in parasitemia.

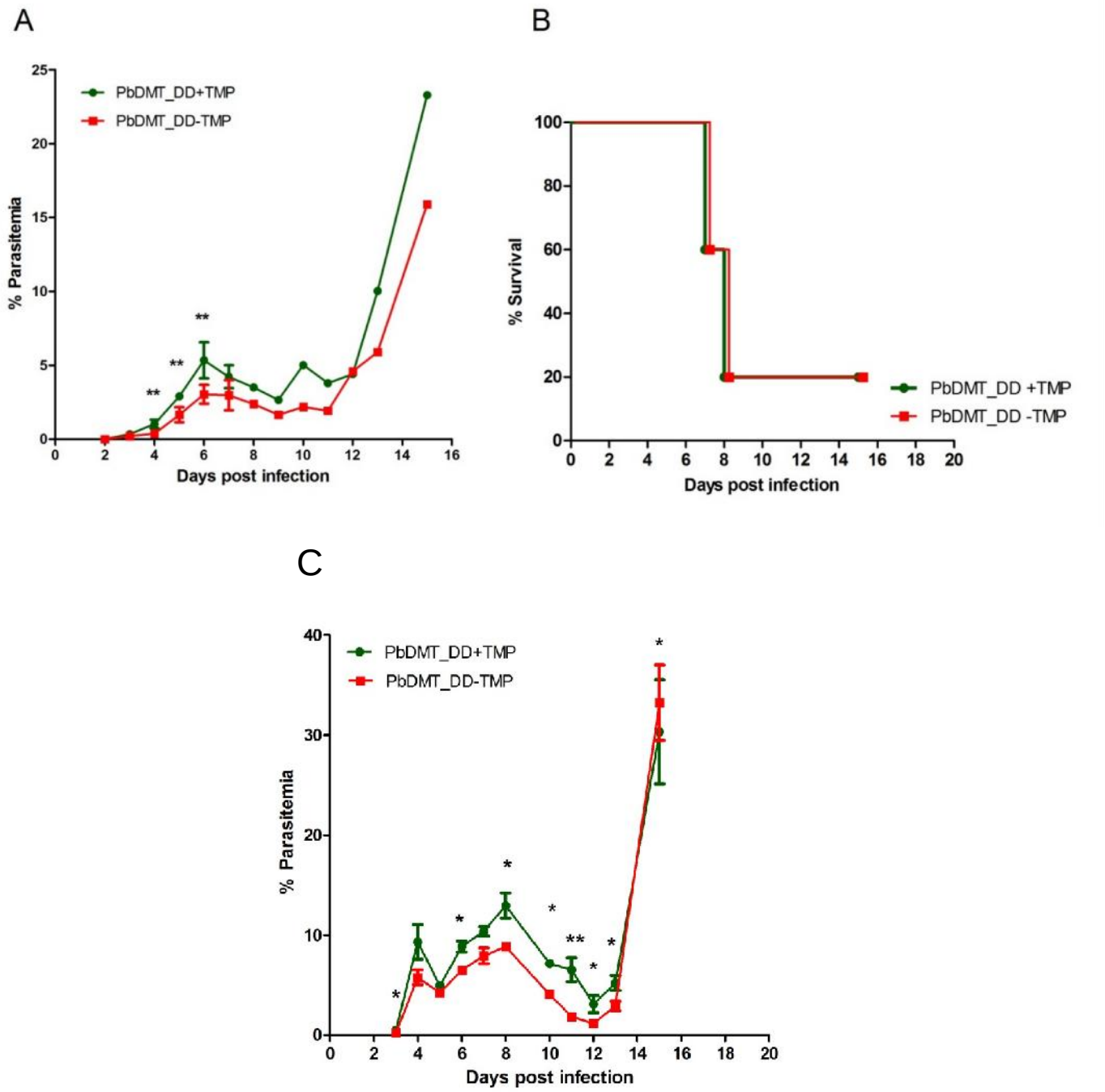

Figure 25. Parasitemia and survival proportions mice infected with PbDMT_DD P. berghei line, on stabilization and destabilization of PbDMT in (A) Parasitemia of C57BL/6J mice upon infection with 105 iRBC *i.v.*, ** p<0.01, Mann Whitney test (B) Survival of C57BL/6J mice upon infection with 105 iRBC *i.v.*, (C) Parasitemia of Balb/c mice upon infection with 105 iRBC *i.v.*, * p<0.05, ** p<0.01, Mann Whitney test. N=5

The trend of parasitemia in C57BL6/J mice infected with PbDMT_HA_DD *Plasmodium berghei*, though initially slower, with the destabilization of PbDMT; did not consistently progress as such throughout the experiment (Figure 26A). A similar trend of parasitemia was observed in the Balb/c mice infection model, where the parasite with destabilized PbDMT initially kicked off with a lower blood parasite load compared to its stabilized counterpart, but did not consistently remain lower throughout the experiment (Figure 26C).

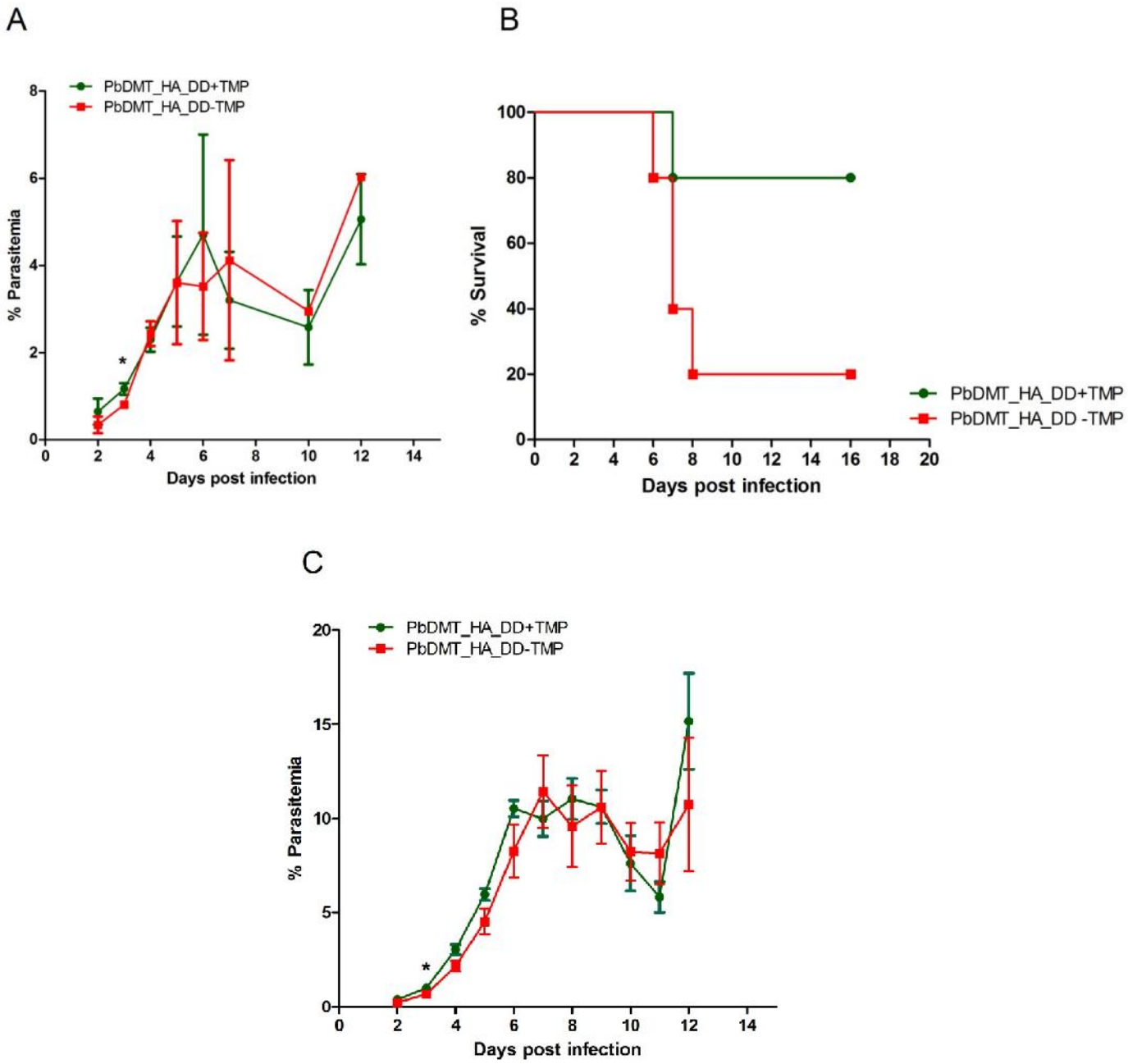

Figure 26. Parasitemia and survival proportions mice infected with PbDMT_HA_DD P. berghei line, on stabilization and destabilization of PbDMT in (A) Parasitemia of C57BL/6J mice upon infection with 10^5 iRBC *i.v.*, (B) Survival of C57BL/6J mice upon infection with 10^5 iRBC *i.v.*, (C) Parasitemia of Balb/c mice upon infection with 10^5 iRBC *i.v.*, * p<0.05, , Mann Whitney test. N=5

Visualization of the extent of knockdown was performed by antibody based detection of HA-tagged PbDMT from whole parasite extracts, obtained from the blood of infected Balb/c mice (14 days post infection). Normalized to the PbHsp70 (Loading control), there appeared to be no significant statistical difference between the volumetric intensity of the signal from the stabilized and destabilized forms of PbDMT (Figure 27). The effect of destabilization did not appear to strikingly reduce the levels of the PbDMT protein, which explains the lack of notable differences in infection phenotype in terms of parasitemia.

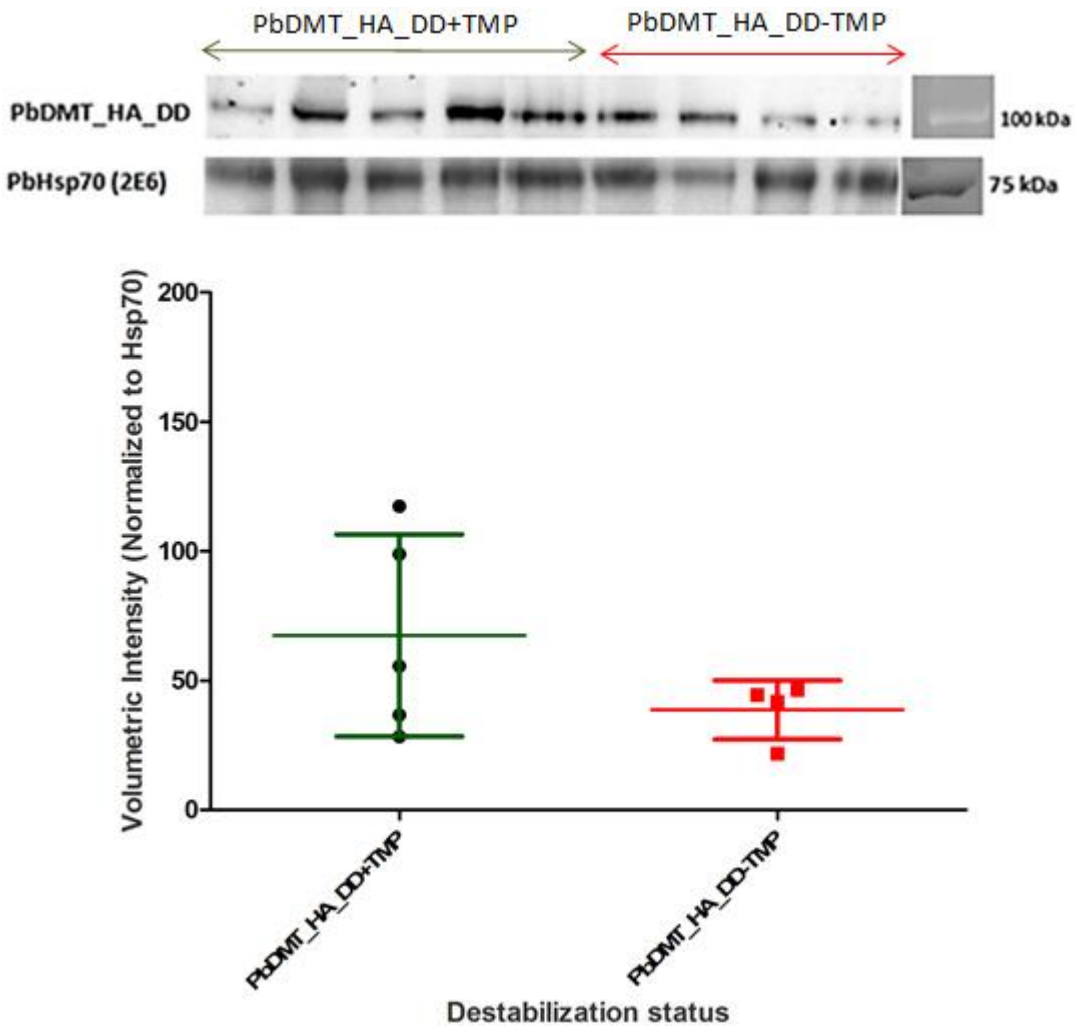

Figure 27. Quantification of knockdown in destabilized PbDMT with respect to stabilized PbDMT ($p>0.05$,Mann Whitney Test)

B. *Inducible knockdown through transcriptional regulation of gene expression (iKo)*[82]

The inducible knockdown technique employs the principle of promoter modification, upstream of the target gene such that it can be inducibly controlled by addition of a small molecule like tetracycline. The organization of the recombined locus comprises of the native promoter being followed by a coding sequence for a fusion protein composed of Tetracycline Repressor and transactivating domain (TRAD) (Figure 28). The binding of the TRAD to the TetO7 promoter sequence which is placed upstream of the gene of interest, activates transcription of the target gene. However, in the presence of tetracycline or its derivative anhydrotetracycline (ATc), the interaction between TRAD and TetO7 is disrupted by severe reduction in affinity of the former to the latter, eventually leading to a plummeting transcription of the gene or even a transcriptional shutdown. This system is however reversible depending on addition of tetracycline enabling the possibility of rescuing the parasite from the knockdown of essential gene.

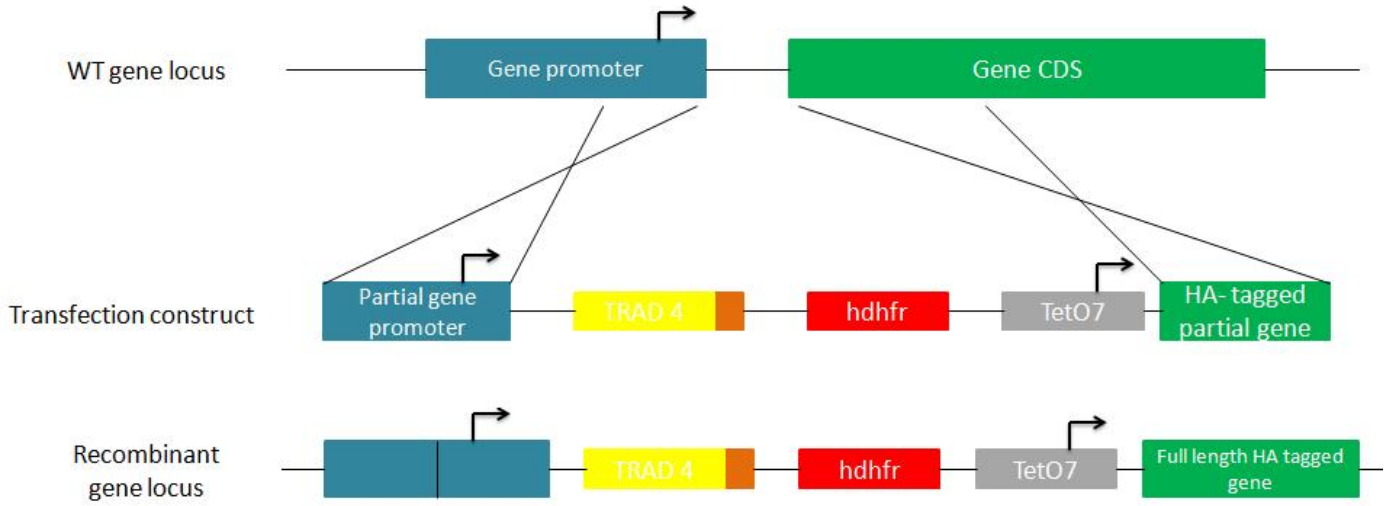

Figure 28. Schematic representation of the working principle of transcriptional repression mediated Inducible knockdown of a gene in *Plasmodium berghei*

In this work, we tested the inducible knockdown system for PbDMT gene promoter in *P.berghei* . The desired construct was introduced into *P.berghei* genome via a double cross-over recombination followed by Pyrimethamine treatment of infected mice to pressure the removal of non-transgenic parasites *in vivo.* Confirmation of integration at desired genomic loci and removal of wild type parasites was performed by genotyping PCR (Figure 29)

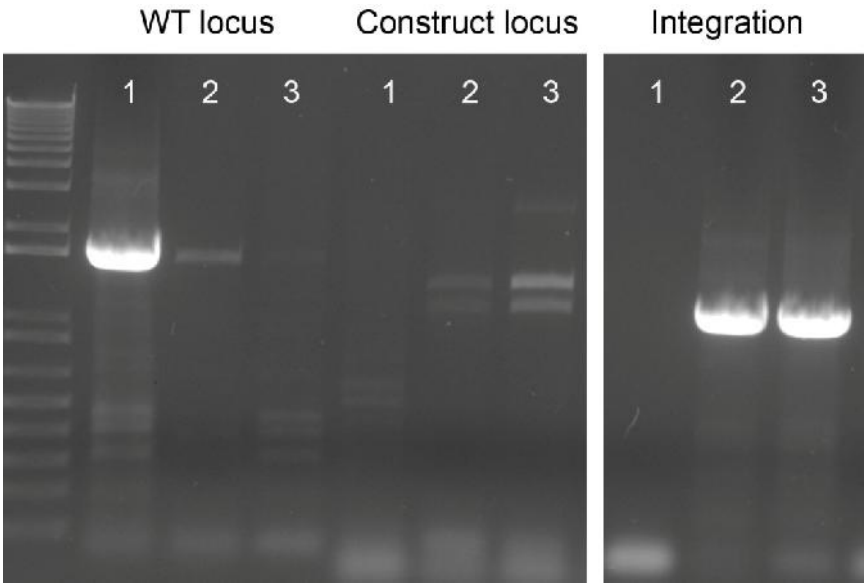

Figure 29. Genotyping PCR confirming clonal populations of PbDMT_iko, 1-WT P.berghei ANKA; 2-First generation of PbDMT_iko parasite line (PbDMT_iko parasites were still mixed with a small population of WT parasites); 3- Second passage of PbDMT_iko transgenic parasites with additional round of pyrimethamine drug pressure

Upon generation of transgenic population of PbDMT_iko parasites without detectable WT P. *berghei* population, containing the TRAD-TetO7 construct in the 5'UTR region of the *pbdmt* gene; we proceeded to examine the effect of transcriptional knockdown of PbDMT on the parasite development and outcome of infection. The experiments were performed in C57BL/6J mice. Infection was carried out by intravenous injection of 10^5 PbDMT_iko parasitized RBC into the mice and monitoring the parasitemia and survival on a daily basis. The knockdown group received ATc in drinking water containing 5% sucrose w/v, while the untreated control were maintained on 5% w/v sucrose in drinking water.

The group under knockdown conditions exhibited a significantly lower parasitemia than its non-induced counterpart on 3, 5 to 7 and 11 days post infection (Figure 30A). There was no statistical difference in survival between the two groups (Figure 30B), however the mortality rate in both groups were very low, with 100% survival in the knockdown induced group. Comparison of survival and parasitemia to WT *P.berghei* infected mice with and without ATc, is proposed to be done shortly to deduce whether alteration of PbDMT promoter alone produced a protective phenotype.

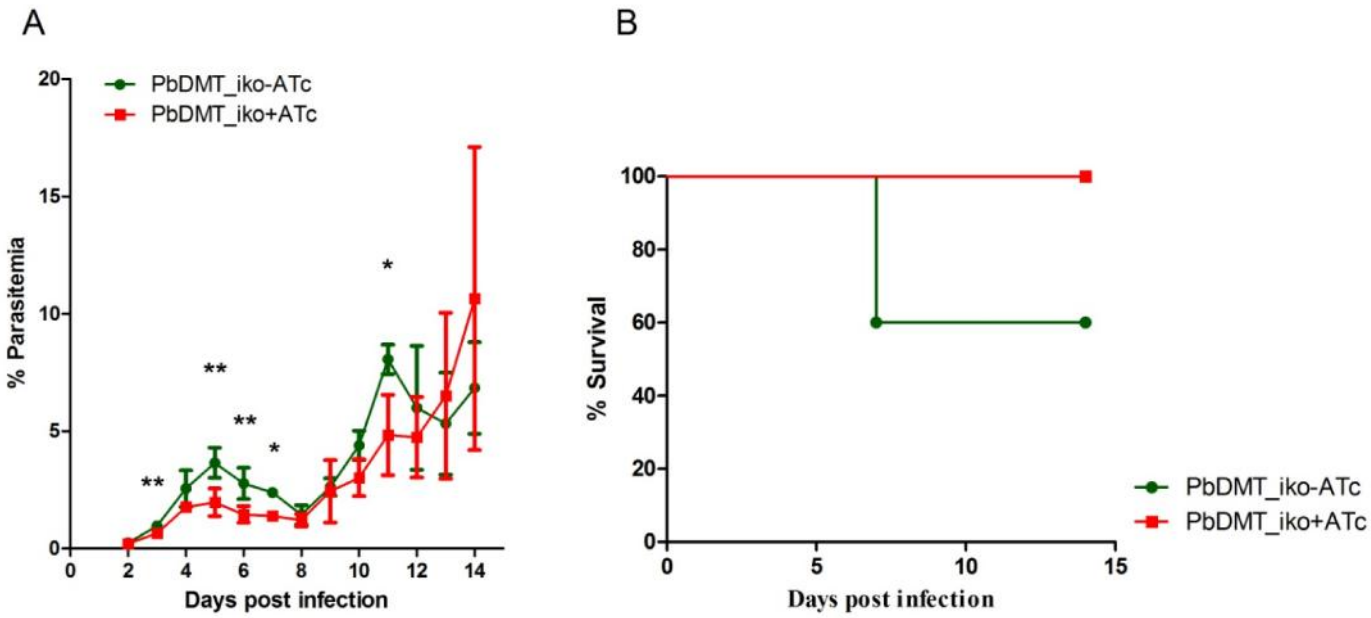

Figure 30. Parasitemia and survival proportions mice infected with PbDMT_iko *P.berghei* line in the presence or absence of transcriptional knockdown (A) Parasitemia of C57BL/6J mice upon infection with 10^5 iRBC *i.v.*, **p<0.01, * p<0.05, Mann Whitney test. N=5 (B) Survival of C57BL/6J mice upon infection with 10^5 iRBC *i.v.*,p>0.05, Log Rank (Mantel-Cox) test

IV. DISCUSSION

Iron is an essential nutrient for *Plasmodium* as well as the host cells however, the biochemical pathways involved in acquisition and mobilization of iron in the parasite remain little divulged. With experimental evidence indicating iron availability as a limiting factor for parasite proliferation and survival, understanding the molecules and their role in the *Plasmodium* iron homeostasis will yield significant knowledge to develop a new class of anti-malarial drugs. In this study we have explored two novel iron transporters in *Plasmodium*.

Presence of a CCC1 homologue (VIT) was previously identified in the *Plasmodium* genome VIT homologues in *Plasmodium* are predicted to possess 5 TMD, which conforms to the structural properties of the CCC1 superfamily. Estimation of the phylogenetic distance between the different CCC1 homologues denotes greatest conservation of VIT between *Plasmodium* species that infect similar hosts. This in turn could possibly hint towards a host specific adaptation of the *Plasmodium* VIT sequence. *Plasmodium* VIT was confirmed to be specific for the transport of Fe^{2+}. VIT was dispensable in the blood stage and the knockout parasite could progress from erythrocytic stage to the mosquito phase and subsequently to form exo-erythrocytic forms (EEF) *in vivo* and *in vitro*. However, the VIT knockout parasites demonstrated a lower blood parasitemia *in vivo*, as well as reduced liver load as estimated by qRT-PCR and counting EEF in liver slices. The EEF of the knockout parasites were also smaller when compared to their WT counterpart. Considering the homology of *Plasmodium* VIT to those in plants and yeast, it was hypothesized that the former may be involved in vacuolar Fe^{2+} shunting hence, detoxification of cytosolic iron as in plants and yeast. The hypothesis was tested by subjecting WT or VIT knockout parasitized RBC to iron excess or depleted conditions and then estimating indirectly the cytosolic labile iron pool in both parasite strains by flow cytometry approach using an iron-sensitive fluorescent probe. The rationale behind this measurement was to quantify the ability of the VIT knockout parasite to maintain its basal cytosolic iron concentration under iron overload stress. In agreement with the role of VIT in plants and yeast, the VIT knockout parasite presented with a somewhat compromised ability to detoxify cytosolic iron. At this juncture, the primary concern became the localization of VIT and the same was then examined through the different developmental stages of *Plasmodium berghei*. In the erythrocytic form, the limit of optical resolution only allowed the deduction that PbVIT localized in the parasite's endoplasmic reticulum and in addition in what seemed to be punctuate structures/vesicles in the cytoplasm. In mosquito midguts, sporulating oocysts appeared to have a rather reticular arrangement of PbVIT that was apical to Uis4. While the sporozoites had a cytosolic distribution of PbVIT, the EEF in Huh7 hepatoma cells distinctly showed ER localization of PbVIT; in addition to presence in grainy structures.

The apparent vesicular distribution of VIT presents an interesting possibility, especially on the nature of these vesicular structures. *Plasmodium berghei* has several food vacuoles containing hemozoin, yet the VIT appears to localize in other vesicular bodies. Equating the role of VIT as a possible iron detoxifier to that of possible reservoirs of inorganic ions in the parasite, a plausible location could be Acidocalsiosomes. Acidocalsiosomes are acidic organelles, containing electron dense matrix and are found from bacterial to complex eukaryotic cells. These compartments are

rich in phosphorous available as polyphosphates or pyrophosphates with inorganic cations; primarily calcium. In Apicomplexan parasites, of which *Plasmodium* is a member; acidocalsiosomes were shown to store calcium, magnesium, sodium, potassium, and zinc. In addition the acidocalsiosome membrane is decorated with inorganic ion pumps and exchangers[83]. The structure serves as a reservoir for phosphate and inorganic ions, which are utilized by the organism depending on its developmental or metabolic requirement[84]. Iron rich acidocalsiosomes were identified in trypanosomatids such as *Trypanosoma cruzi*[85] and *Phytomonas françai*[84], thus opening up possibilities for acidocalsiosomes storing Iron in *Plasmodium* species. However, there are no committed antibodies against acidocalsiosomes, and verifying the possibility of VIT being present on this organellar membrane is a task for the near future.

Thus, VIT though not essential to any of the parasite developmental stages, is involved in its iron homeostasis pathway and its absence leads to compromised growth of the parasite at both in blood and liver. There may exist other proteins that may complement the function of VIT, thus compensating for the lack of the same.

The existence of NrampII (DMT) homologue was predicted upon the whole genome sequencing of *Plasmodium falciparum*[51]. *Plasmodium* DMT was predicted to possess 12 TMDs, which is within the characteristic range for members of the SLC11 superfamily. DMT 1 homologues in most *Plasmodium* species had the signature D and N residue in their first TMD, which has been shown to be critical for chelation of Fe^{2+} by members of the SLC11 superfamily[76]. Phylogenetic analysis revealed that DMT as in VIT was less divergent within *Plasmodium* species, and in addition, more conserved among species infecting similar hosts. Overall the DMT 1 homologues from diverse organism groups appeared to be highly conserved in the TM regions (Appendix whole alignment). *Plasmodium* DMT was confirmed to transport Fe^{2+} at the plasma membrane most favorably around pH 4-5. PbDMT was found refractory to genetic deletion in the blood stage infection which indicated a possible essential role for DMT in the erythrocytic development of *Plasmodium berghei*. To establish if DMT is indeed essential for the development and survival of malaria parasites, two different inducible knock-down approaches were attempted in this project.

Conditional knockdown of PbDMT by fusion of a Destabilization domain did not show any significant differences in survival of C57BL6/J mice infected with the mutant parasites under destabilizing conditions (withdrawal of stabilizing drug TMP). Parasitemia in Balb/c mice infected with the transgenic parasite was significantly lower under destabilizing conditions when compared to the parasite with stabilized PbDMT, though the trend was not consistent among different clones of the DD tagged PbDMT lines of *P.berghei*. Quantification of protein level knockdown, failed to show a striking reduction in PbDMT under destabilizing conditions. The conclusion therefore was that direct protein knockdown through the destabilization domain method did not yield a satisfactory level of knockdown nor presented with any striking phenotypes in terms of protection from cerebral malaria and parasitemia *in vivo*. Similar observation has been reported in a DD based conditional knockdown in *Plasmodium yoelii* recently[86], thus this work contributes to the understanding of the limitations of using DD in *P.berghei* despite its successful application in *P.falciparum*. A curious observation in the destabilization domain in vivo experiments was the reversion of the mutants to WT *pbdmt* locus on withdrawal of Pyrimethamine, indeed suggesting the parasites' requirement for an

intact *pbdmt* locus. Pyrimethamine was the drug used to maintain a selection pressure, since the PbDMT_DD mutants were generated via a single crossover recombination where it is possible to regain the WT locus by recombining out the transgenic locus. The preference to maintain the WT *pbdmt* locus indicates that destabilization of PbDMT was a stress to the parasite and when opportune, the transgenic locus was excised. Eukaryotic cells have a plethora of protein editing mechanisms and chaperone mediated rescue of misfolded proteins, which could account for one of the possible reasons for the failure of protein level knockdown. Another possibility could involve upregulation of transcription/translation machinery to cope with the reduced transporter function.

In order to obtain a greater stringency in the knockdown, the Promoter modification based inducible knockdown system was applied. Upon induction of the knockdown by addition of ATc, there appeared to be a reduction in parasitemia in comparison to the un-induced group. The trend was consistent through the exponential growth phase of the parasite maintaining a significant difference in parasitemia between the two groups. However, the difference was overridden in the later days of infection. A possible explanation could be that the parasites were not a pure clonal line therefore; a residual sub-population of WT *P.berghei* could have thrived as ATc does not have any antibiotic activity. Repetition of experiments with pure clone populations may serve to address this apparent anomaly. C57BL/6J mice infected with the PbDMT_iko parasite did not show a significant difference between the knockdown-induced and un-induced groups. A curious observation here was the complete lack of occurrence of cerebral malaria in the knockdown induced group. The uninduced group was not markedly different, as majority of mice did not develop cerebral malaria

There are no known homologues of Transferrin receptor in *Plasmodium*, which fuels hypotheses towards the possible machinery involved in uptake of iron at the host-parasite interface. The presence of a DMT homologue in *Plasmodium*, and confirmation of its ability to transport Iron makes it a strong candidate for iron acquisition at the host-parasite boundary. Localization studies throughout the developmental stages of *Plasmodium berghei* were performed, employing three differently tagged lines. In the erythrocytic stage, PbDMT appeared in foci close to the parasite periphery. Co-localization with a plasma membrane marker protein confirmed the presence of PbDMT in the parasite plasma membrane as well as in foci in the parasite cytosol, which may possibly be vacuolar structures. In the ookinete stage, PbDMT mostly co-localized with the cytosolic Hsp70, but presented higher signals around the nucleus. In the EEF form within HepG2 hepatoma cells, PbDMT localized on parasite periphery, that appeared to be on the plasma membrane at 24 and 48 hours post infection. At later time point, PbDMT was also found on the newly synthesized merozoite membranes. Drawing from the degree of structural and functional conservation of DMT through bacteria to human, the localization of DMT could be similar among different cell types. With regard to this, the distribution of DMT in mammalian cells does not strictly follow plasma membrane localization, rather DMT is also found in lysosomal membrane as well in the perinuclear region[79]. In *Saccharomyces cerevisiae* the DMT1 homologues appear on the plasma membrane, though their localization may vary from plasma membrane to cytosolic vesicles during metal starvation[87]. In line with these observation the PbDMT, appears to follow a similar

trend, however the precise nature of its distribution needs to be visualized by Immuno- transmission electron microscopy.

V. CONCLUSIONS AND FUTURE DIRECTIONS

The pressing requirement for new-anti malarial drugs in a globally burned out zone of potent anti-malarial therapies fuels the need to study and characterize novel drug targets in the parasite. With recent studies indicating the criticality of iron homeostasis for parasite development and virulence in the host, the prospect of exploring molecular players involved in the *Plasmodium* iron regulatory system for novel drug targets is an attractive one.

The present work comprises of characterizing two iron transporters in *Plasmodium* and contributes to the understanding of iron partitioning in the parasite cell. While only the DMT 1 homologue was found to be essential, exploring the functions of VIT has unraveled interesting details on the ability of the parasite to cope with acute iron overload stress. Among the major conclusions drawn from this study is the probable involvement of *Plasmodium* VIT homologue in iron detoxification and further confirmation of such function will be performed in the near future through *in vitro* iron challenge in *Plasmodium falciparum* and estimating the rate of clearance in wild type and VIT knockout parasite strains. Another area of profound curiosity was the localization of VIT in *Plasmodium* during its different developmental stages, especially to correlate whether the localization would agree with those found in other Apicomplexan organisms such as *Eimeria* and *Toxoplasma*, and its proposed function. Current work in the laboratory aims to examine the VIT localization using other peptide tags and other *Plasmodium* specific organellar markers.

Characterization of the Plasmodium DMT homologue has been especially challenging by virtue of its essentiality in the blood stage development of the parasite. Construction of conditional knockdown systems in the experimental model used in this project (*P.berghei*) is known to be demanding and few cases of absolute success have been reported. We faced similar road blocks in developing a conditional knockdown system for the DMT 1 homologue in *P.berghei.* While the Inducible knockdown method appeared to promising from the phenotypic aspect, there is a need to develop pure clonal strains and replicating the experiments to observe whether the phenotype on inducing the knockdown (iKo) is preserved. There also remains the mammoth task of then proceeding to examine the ability of the PbDMT_iKo parasites to progress through the mosquito phase and whether a knockdown in that phase would have any effect on parasite fecundity and transmission. Last but not the least, the effect of knockdown in the liver stage awaits scrutinization once the phenotype is confirmed to be robust in the blood and mosquito phase of parasite life-cycle. The localization of PbDMT, in alignment with that of PbVIT has been intriguing and demands further investigation with more *Plasmodium* organellar markers. We also hope to be able to catch in action the compromise of iron uptake in PbDMT knockdown strains, once the phenotype is characterized completely. An optimistic and distant aim is to screen libraries of small molecule inhibitors of DMT 1 homologues to identify possible candidates for drug development.

Though extremely exigent, the exploration of DMT and VIT homologues in *Plasmodium berghei* has yielded better insights into the complexity of the parasite's iron homeostasis and yet more possibilities to chalk out novel drug targets.

BIBLIOGRAPHY

1. WHO | World Malaria Report 2014. *WHO* at <http://www.who.int/malaria/publications/world_malaria_report_2014/en/>
2. Hay, S. I. *et al.* A World Malaria Map: Plasmodium falciparum Endemicity in 2007. *PLoS Med* **6,** e1000048 (2009).
3. Schofield, L. & Grau, G. E. Immunological processes in malaria pathogenesis. *Nat. Rev. Immunol.* **5,** 722–735 (2005).
4. White, N. J. Plasmodium knowlesi: The Fifth Human Malaria Parasite. *Clin. Infect. Dis.* **46,** 172–173 (2008).
5. Strydom, K.-A., Ismail, F. & Frean, J. Plasmodium ovale: a case of not-so-benign tertian malaria. *Malar. J.* **13,** 85 (2014).
6. Prudêncio, M., Rodriguez, A. & Mota, M. M. The silent path to thousands of merozoites: the Plasmodium liver stage. *Nat. Rev. Microbiol.* **4,** 849–856 (2006).
7. Bray, R. S. & Garnham, P. C. C. The Life-Cycle of Primate Malaria Parasites. *Br. Med. Bull.* **38,** 117–122 (1982).
8. Hoffman, S. L. & Doolan, D. L. Malaria vaccines–targeting infected hepatocytes. *Nat. Med.* **6,** 1218–1219 (2000).
9. Talisuna, A. O., Bloland, P. & D'Alessandro, U. History, Dynamics, and Public Health Importance of Malaria Parasite Resistance. *Clin. Microbiol. Rev.* **17,** 235–254 (2004).
10. Reed, M. B., Saliba, K. J., Caruana, S. R., Kirk, K. & Cowman, A. F. Pgh1 modulates sensitivity and resistance to multiple antimalarials in Plasmodium falciparum. *Nature* **403,** 906–909 (2000).
11. Sidhu, A. B. S., Verdier-Pinard, D. & Fidock, D. A. Chloroquine Resistance in Plasmodium falciparum Malaria Parasites Conferred by pfcrt Mutations. *Science* **298,** 210–213 (2002).
12. Price, R. N. *et al.* Mefloquine resistance in Plasmodium falciparum and increased pfmdr1 gene copy number. *The Lancet* **364,** 438–447 (2004).
13. Wang, P., Read, M., Sims, P. F. G. & Hyde, J. E. Sulfadoxine resistance in the human malaria parasite Plasmodium falciparum is determined by mutations in dihydropteroate synthetase and an additional factor associated with folate utilization. *Mol. Microbiol.* **23,** 979–986 (1997).
14. Plowe, C. V. *et al.* Mutations in Plasmodium falciparum Dihydrofolate Reductase and Dihydropteroate Synthase and Epidemiologic Patterns of Pyrimethamine-Sulfadoxine Use and Resistance. *J. Infect. Dis.* **176,** 1590–1596 (1997).
15. Krishna, S., Bustamante, L., Haynes, R. K. & Staines, H. M. Artemisinins: their growing importance in medicine. *Trends Pharmacol. Sci.* **29,** 520–527 (2008).
16. Klonis, N., Creek, D. J. & Tilley, L. Iron and heme metabolism in Plasmodium falciparum and the mechanism of action of artemisinins. *Curr. Opin. Microbiol.* **16,** 722–727 (2013).
17. Pandey, A. V., Tekwani, B. L., Singh, R. L. & Chauhan, V. S. Artemisinin, an Endoperoxide Antimalarial, Disrupts the Hemoglobin Catabolism and Heme Detoxification Systems in Malarial Parasite. *J. Biol. Chem.* **274,** 19383–19388 (1999).

18. Eckstein-Ludwig, U. *et al.* Artemisinins target the SERCA of Plasmodium falciparum. *Nature* **424,** 957–961 (2003).
19. Uhlemann, A.-C. *et al.* A single amino acid residue can determine the sensitivity of SERCAs to artemisinins. *Nat. Struct. Mol. Biol.* **12,** 628–629 (2005).
20. Pulcini, S. *et al.* Expression in Yeast Links Field Polymorphisms in PfATP6 to in Vitro Artemisinin Resistance and Identifies New Inhibitor Classes. *J. Infect. Dis.* **208,** 468–478 (2013).
21. Meshnick, S. R. Artemisinin: mechanisms of action, resistance and toxicity. *Int. J. Parasitol.* **32,** 1655–1660 (2002).
22. Golenser, J., Waknine, J. H., Krugliak, M., Hunt, N. H. & Grau, G. E. Current perspectives on the mechanism of action of artemisinins. *Int. J. Parasitol.* **36,** 1427–1441 (2006).
23. WHO | World Health Organization. *WHO* at <http://www.who.int/Malaria/media/artemisinin_resistance_qa/en/>
24. Mutabingwa, T. K. Artemisinin-based combination therapies (ACTs): Best hope for malaria treatment but inaccessible to the needy! *Acta Trop.* **95,** 305–315 (2005).
25. Derbyshire, E. R., Prudêncio, M., Mota, M. M. & Clardy, J. Liver-stage malaria parasites vulnerable to diverse chemical scaffolds. *Proc. Natl. Acad. Sci.* **109,** 8511–8516 (2012).
26. Dembele, L. *et al.* Towards an In Vitro Model of Plasmodium Hypnozoites Suitable for Drug Discovery. *PLoS ONE* **6,** (2011).
27. Dembélé, L. *et al.* Persistence and activation of malaria hypnozoites in long-term primary hepatocyte cultures. *Nat. Med.* **20,** 307–312 (2014).
28. Williams, C. T. & Azad, A. F. Transcriptional Analysis of the Pre-Erythrocytic Stages of the Rodent Malaria Parasite, Plasmodium yoelii. *PLoS ONE* **5,** e10267 (2010).
29. Cohen, S., McGREGOR, I. A. & Carrington, S. Gamma-Globulin and Acquired Immunity to Human Malaria. *Nature* **192,** 733–737 (1961).
30. The RTS,S Clinical Trials Partnership. A Phase 3 Trial of RTS,S/AS01 Malaria Vaccine in African Infants. *N. Engl. J. Med.* **367,** 2284–2295 (2012).
31. Kwok, E. & Kosman, D. in *Molecular Biology of Metal Homeostasis and Detoxification* (eds. Tamas, M. J. & Martinoia, E.) 59–99 (Springer Berlin Heidelberg, 2005). at <http://link.springer.com/chapter/10.1007/4735_92>
32. Briat, J.-F., Duc, C., Ravet, K. & Gaymard, F. Ferritins and iron storage in plants. *Biochim. Biophys. Acta BBA - Gen. Subj.* **1800,** 806–814 (2010).
33. Mackenzie, E. L., Iwasaki, K. & Tsuji, Y. Intracellular Iron Transport and Storage: From Molecular Mechanisms to Health Implications. *Antioxid. Redox Signal.* **10,** 997–1030 (2008).
34. Dey, S. *et al.* Malarial infection develops mitochondrial pathology and mitochondrial oxidative stress to promote hepatocyte apoptosis. *Free Radic. Biol. Med.* **46,** 271–281 (2009).

35. Clark, M. A., Goheen, M. M. & Cerami, C. Influence of host iron status on Plasmodium falciparum infection. *Front. Pharmacol.* **5,** (2014).

36. Taylor, S. M., Cerami, C. & Fairhurst, R. M. Hemoglobinopathies: Slicing the Gordian Knot of Plasmodium falciparum Malaria Pathogenesis. *PLoS Pathog.* **9,** (2013).

37. Sazawal, S. *et al.* Effects of routine prophylactic supplementation with iron and folic acid on admission to hospital and mortality in preschool children in a high malaria transmission setting: community-based, randomised, placebo-controlled trial. *The Lancet* **367,** 133–143 (2006).

38. Gordeuk, V. R. *et al.* Iron chelation with desferrioxamine B in adults with asymptomatic Plasmodium falciparum parasitemia [see comments]. *Blood* **79,** 308–312 (1992).

39. Whitehead, S. & Peto, T. E. Stage-dependent effect of deferoxamine on growth of Plasmodium falciparum in vitro. *Blood* **76,** 1250–1255 (1990).

40. Ginsburg, H., Kutner, S., Krugliak, M. & Ioav Cabantchik, Z. Characterization of permeation pathways appearing in the host membrane of Plasmodium falciparum infected red blood cells. *Mol. Biochem. Parasitol.* **14,** 313–322 (1985).

41. Painter, H. J., Morrisey, J. M., Mather, M. W. & Vaidya, A. B. Specific role of mitochondrial electron transport in blood-stage Plasmodium falciparum. *Nature* **446,** 88–91 (2007).

42. Ferrer, P. *et al.* Antimalarial Iron Chelator, FBS0701, Shows Asexual and Gametocyte Plasmodium falciparum Activity and Single Oral Dose Cure in a Murine Malaria Model. *PLoS ONE* **7,** e37171 (2012).

43. Abbaspour, N., Hurrell, R. & Kelishadi, R. Review on iron and its importance for human health. *J. Res. Med. Sci. Off. J. Isfahan Univ. Med. Sci.* **19,** 164–174 (2014).

44. Ganz, T. Macrophages and Systemic Iron Homeostasis. *J. Innate Immun.* **4,** 446–453 (2012).

45. Nemeth, E. *et al.* IL-6 mediates hypoferremia of inflammation by inducing the synthesis of the iron regulatory hormone hepcidin. *J. Clin. Invest.* **113,** 1271–1276 (2004).

46. Okada, K. The novel heme oxygenase-like protein from Plasmodium falciparum converts heme to bilirubin IXα in the apicoplast. *FEBS Lett.* **583,** 313–319 (2009).

47. Sigala, P. A., Crowley, J. R., Hsieh, S., Henderson, J. P. & Goldberg, D. E. Direct Tests of Enzymatic Heme Degradation by the Malaria Parasite Plasmodium falciparum. *J. Biol. Chem.* **287,** 37793–37807 (2012).

48. Francis, S. E., Sullivan, D. J. & Goldberg, and D. E. HEMOGLOBIN METABOLISM IN THE MALARIA PARASITE *PLASMODIUM FALCIPARUM*. *Annu. Rev. Microbiol.* **51,** 97–123 (1997).

49. Sanchez-Lopez, R. & Haldar, K. A transferrin-independent iron uptake activity in Plasmodium falciparum-infected and uninfected erythrocytes. *Mol. Biochem. Parasitol.* **55,** 9–20 (1992).

50. Breuer, W. V., Kutner, S., Sylphen, J., Ginsburg, H. & Cabantchik, Z. I. Covalent modification of the permeability pathways induced in the human erythrocyte membrane by the malarial parasite Plasmodium falciparum. *J. Cell. Physiol.* **133,** 55–63 (1987).
51. Gardner, M. J. *et al.* Genome sequence of the human malaria parasite Plasmodium falciparum. *Nature* **419,** 498–511 (2002).
52. Martin, R. E., Henry, R. I., Abbey, J. L., Clements, J. D. & Kirk, K. The 'permeome' of the malaria parasite: an overview of the membrane transport proteins of Plasmodium falciparum. *Genome Biol.* **6,** R26 (2005).
53. Sahu, T. *et al.* ZIPCO, a putative metal ion transporter, is crucial for Plasmodium liver-stage development. *EMBO Mol. Med.* **6,** 1387–1397 (2014).
54. Dean, P., Major, P., Nakjang, S., Hirt, R. P. & Embley, T. M. Transport proteins of parasitic protists and their role in nutrient salvage. *Front. Plant Sci.* **5,** (2014).
55. Janse, C. J., Ramesar, J. & Waters, A. P. High-efficiency transfection and drug selection of genetically transformed blood stages of the rodent malaria parasite Plasmodium berghei. *Nat. Protoc.* **1,** 346–356 (2006).
56. Schneider, C. A., Rasband, W. S. & Eliceiri, K. W. NIH Image to ImageJ: 25 years of image analysis. *Nat. Methods* **9,** 671–675 (2012).
57. Clark, M., Fisher, N. C., Kasthuri, R. & Cerami Hand, C. Parasite maturation and host serum iron influence the labile iron pool of erythrocyte stage Plasmodium falciparum. *Br. J. Haematol.* **161,** 262–269 (2013).
58. GraphPad Software,. GraphPad Prism version 5.00 for Windows. at <www.graphpad.com>
59. Kim, S. A. *et al.* Localization of Iron in Arabidopsis Seed Requires the Vacuolar Membrane Transporter VIT1. *Science* **314,** 1295–1298 (2006).
60. Li, L., Chen, O. S., Ward, D. M. & Kaplan, J. CCC1 Is a Transporter That Mediates Vacuolar Iron Storage in Yeast. *J. Biol. Chem.* **276,** 29515–29519 (2001).
61. Shoji, K., Momonoi, K. & Tsuji, T. Alternative Expression of Vacuolar Iron Transporter and Ferritin Genes Leads to Blue/Purple Coloration of Flowers in Tulip cv. 'Murasakizuisho'. *Plant Cell Physiol.* **51,** 215–224 (2010).
62. Briat, J.-F., Curie, C. & Gaymard, F. Iron utilization and metabolism in plants. *Curr. Opin. Plant Biol.* **10,** 276–282 (2007).
63. Aurrecoechea, C. *et al.* PlasmoDB: a functional genomic database for malaria parasites. *Nucleic Acids Res.* **37,** D539–543 (2009).
64. Käll, L., Krogh, A. & Sonnhammer, E. L. L. A combined transmembrane topology and signal peptide prediction method. *J. Mol. Biol.* **338,** 1027–1036 (2004).
65. Papadopoulos, J. S. & Agarwala, R. COBALT: constraint-based alignment tool for multiple protein sequences. *Bioinforma. Oxf. Engl.* **23,** 1073–1079 (2007).

66. Dereeper, A. *et al.* Phylogeny.fr: robust phylogenetic analysis for the non-specialist. *Nucleic Acids Res.* **36,** W465–469 (2008).

67. Otto, T. D. *et al.* A comprehensive evaluation of rodent malaria parasite genomes and gene expression. *BMC Biol.* **12,** 86 (2014).

68. Petrat, F., Rauen, U. & de Groot, H. Determination of the chelatable iron pool of isolated rat hepatocytes by digital fluorescence microscopy using the fluorescent probe, phen green SK. *Hepatol. Baltim. Md* **29,** 1171–1179 (1999).

69. Gruenheid, S., Cellier, M., Vidal, S. & Gros, P. Identification and characterization of a second mouse Nramp gene. *Genomics* **25,** 514–525 (1995).

70. Gunshin, H. *et al.* Cloning and characterization of a mammalian proton-coupled metal-ion transporter. *Nature* **388,** 482–488 (1997).

71. Cellier, M. *et al.* Nramp defines a family of membrane proteins. *Proc. Natl. Acad. Sci.* **92,** 10089–10093 (1995).

72. Govoni, G. & Gros, P. Macrophage NRAMP1 and its role in resistance to microbial infections. *Inflamm. Res. Off. J. Eur. Histamine Res. Soc. Al* **47,** 277–284 (1998).

73. Shawki, A., Knight, P. B., Maliken, B. D., Niespodzany, E. J. & Mackenzie, B. H(+)-coupled divalent metal-ion transporter-1: functional properties, physiological roles and therapeutics. *Curr. Top. Membr.* **70,** 169–214 (2012).

74. Choi, J. *et al.* Duodenal reductase activity and spleen iron stores are reduced and erythropoiesis is abnormal in Dcytb knockout mice exposed to hypoxic conditions. *J. Nutr.* **142,** 1929–1934 (2012).

75. Ehrnstorfer, I. A., Geertsma, E. R., Pardon, E., Steyaert, J. & Dutzler, R. Crystal structure of a SLC11 (NRAMP) transporter reveals the basis for transition-metal ion transport. *Nat. Struct. Mol. Biol.* **21,** 990–996 (2014).

76. Silva, D. M. D., Askwith, C. C., Eide, D. & Kaplan, J. The FET3 Gene Product Required for High Affinity Iron Transport in Yeast Is a Cell Surface Ferroxidase. *J. Biol. Chem.* **270,** 1098–1101 (1995).

77. Dix, D., Bridgham, J., Broderius, M. & Eide, D. Characterization of the FET4 Protein of Yeast EVIDENCE FOR A DIRECT ROLE IN THE TRANSPORT OF IRON. *J. Biol. Chem.* **272,** 11770–11777 (1997).

78. Tabuchi, M., Yoshimori, T., Yamaguchi, K., Yoshida, T. & Kishi, F. Human NRAMP2/DMT1, Which Mediates Iron Transport across Endosomal Membranes, Is Localized to Late Endosomes and Lysosomes in HEp-2 Cells. *J. Biol. Chem.* **275,** 22220–22228 (2000).

79. Picard, V., Govoni, G., Jabado, N. & Gros, P. Nramp 2 (DCT1/DMT1) Expressed at the Plasma Membrane Transports Iron and Other Divalent Cations into a Calcein-accessible Cytoplasmic Pool. *J. Biol. Chem.* **275,** 35738–35745 (2000).

80. Muralidharan, V., Oksman, A., Iwamoto, M., Wandless, T. J. & Goldberg, D. E. Asparagine repeat function in a Plasmodium falciparum protein assessed via a regulatable fluorescent affinity tag. *Proc. Natl. Acad. Sci.* **108,** 4411–4416 (2011).

81. Pino, P. *et al.* A Tetracycline-Repressible Transactivator System to Study Essential Genes in Malaria Parasites. *Cell Host Microbe* **12,** 824–834 (2012).

82. Miranda, K. *et al.* Acidocalcisomes of Phytomonas françai possess distinct morphological characteristics and contain iron. *Microsc. Microanal. Off. J. Microsc. Soc. Am. Microbeam Anal. Soc. Microsc. Soc. Can.* **10,** 647–655 (2004).

83. Corrêa, A. S., Andrade, L. R. & Soares, M. J. Elemental composition of acidocalcisomes of Trypanosoma cruzi bloodstream trypomastigote forms. *Parasitol. Res.* **88,** 875–880 (2002).

84. Pei, Y. *et al.* Plasmodium yoelii inhibitor of cysteine proteases is exported to exomembrane structures and interacts with yoelipain-2 during asexual blood-stage development. *Cell. Microbiol.* **15,** 1508–1526 (2013).

85. Portnoy, M. E., Liu, X. F. & Culotta, V. C. Saccharomyces cerevisiae Expresses Three Functionally Distinct Homologues of the Nramp Family of Metal Transporters. *Mol. Cell. Biol.* **20,** 7893–7902 (2000).

APPENDIX

1.1. Reagents and Drugs Composition

1.1.1. Ookinete Culture medium : in RPMI1640 medium(Gibco® Life Technologies)

25mM HEPES
10% Fetal Bovine Serum
2g/L Sodium Bicarbonate
11mM Glucose
0.4mM Hypoxanthine
100µM Xanthurenic acid
50000U/L Penicillin
50mg/L Sreptomycin
pH 7.6-7.8

1.1.2. Western Blotting: Reagents composition

a. **RBC Lysis buffer** : 0.05% w/v Saponin and 1X protease inhibitor cocktail (Roche® cOmplete Protease inhibitor tablets, EDTA free) in PBS
b. **Parasite pellet Lysis Buffer** : Complete Radio Immunoprecipitation buffer (in PBS)-RIPA
   30mM Tris-HCl pH 8
   1mM EDTA
   0.5% v/v Triton X-100
   0.1% w/v SDS
   0.5% w/v Sodium deoxycholate
   1mM PMSF
   1X Protease inhibitor cocktail
c. **Sample washing buffer** : 1X protease inhibitor cocktail in PBS
d. **SDS-PAGE loading composition** : 40µg protein in 1X Laemlli buffer (Nzytech®)
e. **Blocking Solution** : 5% w/v Non fat dry milk in 0.1% TBST
f. **Blot membrane wash solution :** 0.1% Tween-20 in Tris Buffered Saline (TBS)

1.1.3. Immunofluorescence: Reagents composition

a. **Fixing Solution for erythrocytes** : 4% Paraformaldehyde and 0.0075% glutaraldehyde in PBS
b. **Fixing Solution for hepatocytes** : 4% Paraformaldehyde in PBS
c. **Permeabilization buffer for erythrocytes** : 0.1% v/v Triton X-100 in PBS
d. **Permeabilization buffer for hepatocytes** : 0.1% v/v Triton X-100 and 2% BSA in PBS (BBT)
e. **Blocking Solution for erythrocytes** : 3% BSA in PBS
f. **Blocking Solution for hepatocytes** : BBT

1.1.4. Frozen Vials Preparation

a. **Bacterial stocks** : 0.6% v/v Bacterial culture in 50% glycerol in Luria broth
b. **Blood stocks** : 0.4% v/v whole blood in 30% glycerol in PBS

1.1.5. Giemsa stain working solution

a. Giemsa stain modified solution (Sigma-Aldrich®) in distilled water – 1:10 dilution

1.1.6. Drug preparations

a. **Intraperitoneal injections :** 100µL of 1mg/mL Pyrimethamine in DMSO

b. Oral Administration

i. 70µg/mL Pyrimethamine in water

ii. 250µg/mL Trimethoprim in water

iii. 200µg/mL Anhydrotetracycline with 5% w/v Sucrose in water

c. Other applications

i. 100µg/mL Ampicillin in LB broth/agar

ii. 1:300 Fungizone in RPMI/DMEM for cell culture

1.2. Routine Protocol Conditions

a. Restriction Digestion: Overnight incubation of substrate DNA in digestion buffer at recommended reaction temperature for respective restriction enzyme (New England Biolabs®).

b. Ligation Reaction: Incubation of Insert and Vector DNA in ligation buffer and T4 DNA ligase (Thermo Scientific® Life Technologies), for 2 hours at 37°C followed by overnight incubation of ligation cocktail at 4°C.

c. Genotyping PCR temperature cycle: 95°C (3min) → 92°C (30 sec) → 56°C (45 sec) → 68°C (2min) : 34 cycles(red)
followed by final extension at 68°C (10 minutes).

d. PbDMT_DD PCR temperature cycle: 95°C (3min) → 92°C (30 sec) → 56°C (45 sec) → 68°C (2.5min) : 34 cycles(red)
followed by final extension at 68° (10 minutes).

e. PbDMT_iko PCR temperature cycle: 95°C (3min) → 92°C (30 sec) → 54°C (45 sec) → 68°C (2.5min) : 34 cycles(red)
followed by final extension at 68° (10 minutes).

1.3. Lists

1.3.1. Antibodies

Primary Antibody	Source organism	Target protein	Solvent	Application	Dilution (ratio)
Rab_anti-HA	Rabbit	HA tag	3%BSA in PBS	IFA/ Immumo-TEM /WB	1:300/1:100/1:1000
Rab_anti-myc	Rabbit	c-myc tag	3%BSA in PBS	IFA/Immumo-TEM	1:300/1:100
Rab_anti-Msp1	Rabbit	*Plasmodium berghei* PVM resident protein Msp1	3%BSA in PBS	IFA	1:300
Rab_anti-BiP	Rabbit	*Plasmodium berghei* ER resident protein BiP	3%BSA in PBS	IFA/WB	1:500/1:1000
Rab_anti-GFP	Rabbit	Green Fluorescent Protein	3%BSA in PBS	IFA/Immuno-TEM	1:500
Mou_anti-myc	Mouse	c-myc tag	3%BSA in PBS	IFA	1:300
Mou_anti-2E6	Mouse	*Plasmodium berghei* cytosolic Hsp70 like protein	3%BSA in PBS	IFA	1:100
Mou_anti-GFP	Mouse	Green Fluorescent Protein	3%BSA in PBS	IFA	1:500
Goat_anti-Uis4	Goat	*Plasmodium berghei* liver stage PVM resident protein Uis4	3%BSA in PBS	IFA	1:300

Secondary Antibodies	Source Organism	Target Organism	Solvent	Application	Fluorophore/Enzyme conjugate	Dilution (ratio)
DAG_A568	Donkey	Goat	3%BSA in PBS	IFA	Alexa568	1:500
DAG_A660	Donkey	Goat	3%BSA in PBS	IFA	Alexa660	1:500
DAR_A546	Donkey	Rabbit	3%BSA in PBS	IFA	Alexa546	1:500
DAR_A549	Donkey	Rabbit	3%BSA in PBS	IFA	Alexa549	1:500
DAR_Dylight549	Donkey	Rabbit	3%BSA in PBS	IFA	Dylight549	1:500
DAM_A488	Donkey	Mouse	3%BSA in PBS	IFA	Alexa488	1:500
GAR_A488	Goat	Rabbit	3%BSA in PBS	IFA	Alexa488	1:500
Hoechst	--		3%BSA in PBS	IFA	--	1:1000
Anti-Rab_HRP	Goat	Rabbit	3%BSA in PBS	WB	HRP	1:5000
Anti-Mou_HRP	Goat	Mouse	3%BSA in PBS	WB	HRP	1:5000

1.3.2. Primers

Primer Code	Primer Name	Sequence	Application	Target Organism	Target gene locus	Concentration (µM)
uma1288	PbVIT RTf	GTATGATACCTCTATTTTCTTATGTCC	Genotyping PCR, qPCR	*P.berghei*	PbVIT	50
uma1289	PbVIT RTr	GTGGTAAACTGGGACTTGAATAAAC	Genotyping PCR, qPCR	*P.berghei*	PbVIT	50
uma1292	PbDMT RTf	GTGAATAAAGACCTTAGTAATACAGCA	qPCR	*P.berghei*	PbDMT	50
uma1293	PbDMT RTr	TCATTATAACCATTGCCATCA	Genotyping PCR, qPCR	*P.berghei*	PbDMT	50
uma1340	PbDMT 5int	CACTTTGGCATATAACATTTTTATAG	Genotyping PCR	*P.berghei*	PbDMT 5'UTR	50
uma1341	PbDMT 3intR	CACATTCATTATTTTTATTGGTGC	Genotyping PCR	*P.berghei*	PbDMT 3'UTR	50
uma1342	PbVIT5int	GCATTAATTCATAACTCTGATGTG	Genotyping PCR	*P.berghei*	PbVIT 5'UTR	50
uma1343	PbVIT3intR	CATTATTATGTATTTAAAGGCATGG	Genotyping PCR	*P.berghei*	PbVIT 3'UTR	50
uma1803	DD for 1	ATGGGCCCATCAGTCTGATTGCGGCGTTAG	DD Cloning	pBMN DHFR(DD)-YFP	DD	50
uma1804	DD rev 1	TAGCGGCCGCGGTCATGCGTAG	DD Cloning	pBMN DHFR(DD)-YFP	DD	50
uma1812	PbVIT myc f	tagatatcCATAGTCACTATCATAATCTCGATAAG	Genotyping PCR	*P.berghei*	PbVIT-myc f	50
uma1813	PbVIT myc r	atggatccATCCCCTGAGTTTGTTTTAAGT	Genotyping PCR	*P.berghei*	PbVIT-myc r	50
uma1814	PbDMT myc f	tagatatcGCTATTATAGGTGTATTTGTG	Genotyping PCR	*P.berghei*	PbDMT-myc f	50
uma1815	PbDMT myc r	atggatccACTGTCTTTGTAATATGTTTTTG	Genotyping PCR	*P.berghei*	PbDMT-myc r	50
uma1959	HA-DDfor	atGGGCCCTATCCATATGATGTACCAGATTATGCAgcaATCAGTCTGATTGCGGCGTTAG	PbDMT_HA_DD cloning	*P.berghei*	PbDMT	50
uma2231	PbDMT iKOf	atGCCGGCATGCATCAAGACAAATCGATG	PbDMT_iko cloning	*P.berghei*	PbDMT iKOf	50
uma2232	PbDMT iKOr	taGCTAGCCTAAATTCTTTTCGGCATAATGC	PbDMT_iko cloning	*P.berghei*	PbDMT iKOr	50
uma2233	5'PbDMT iKOf	taGCTAGCGTATGGATATAATATAGAAAGAGTTAG	PbDMT 5' UTR Cloning	*P.berghei*	5'PbDMT iKOf	50
uma2234	5'PbDMT iKOr	atCCGCGGctttgtgattatatatttcttgttc	Genotyping PCR, PbDMT 5' UTR Cloning	*P.berghei*	5'PbDMT iKOr	50
uma2262	Tet_for	GAGAAAAGTGAAAGTCGAGCTC	Genotyping PCR	*P.berghei*	PbDMT	50
uma2263	Trad_rev	Gagttgatgactttgctcttgtc	Genotyping PCR	*P.berghei*	PbDMT	50
uma2264	PbDMT rev	CACCTATAATAGCTTGCAAATGTG	Genotyping PCR	*P.berghei*	PbDMT	50

1.4. Maps of Plasmids

a. **PbVIT_myc vector:** used for generating a C-terminal myc tag fusion protein of PbVIT through single cross-over homologous recombination at the native PbVIT genomic locus in *P.berghei*.

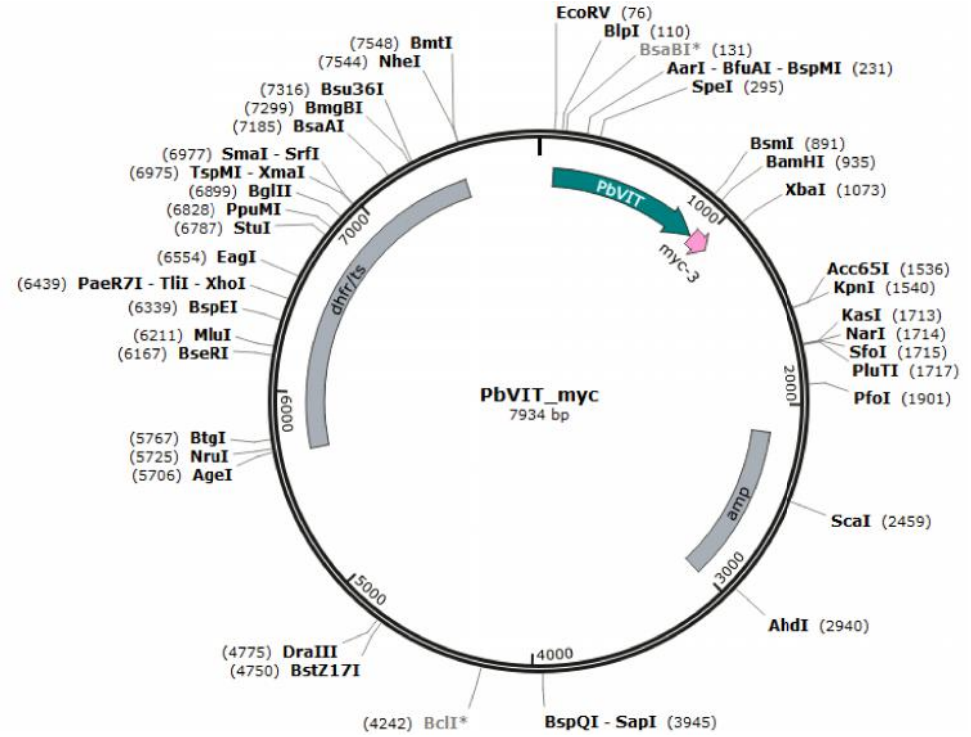

b. **PbDMT_myc:** used for generation of C-terminal myc tag fusion protein of PbDMT through single cross-over homologous recombination at the native PbDMT genomic locus

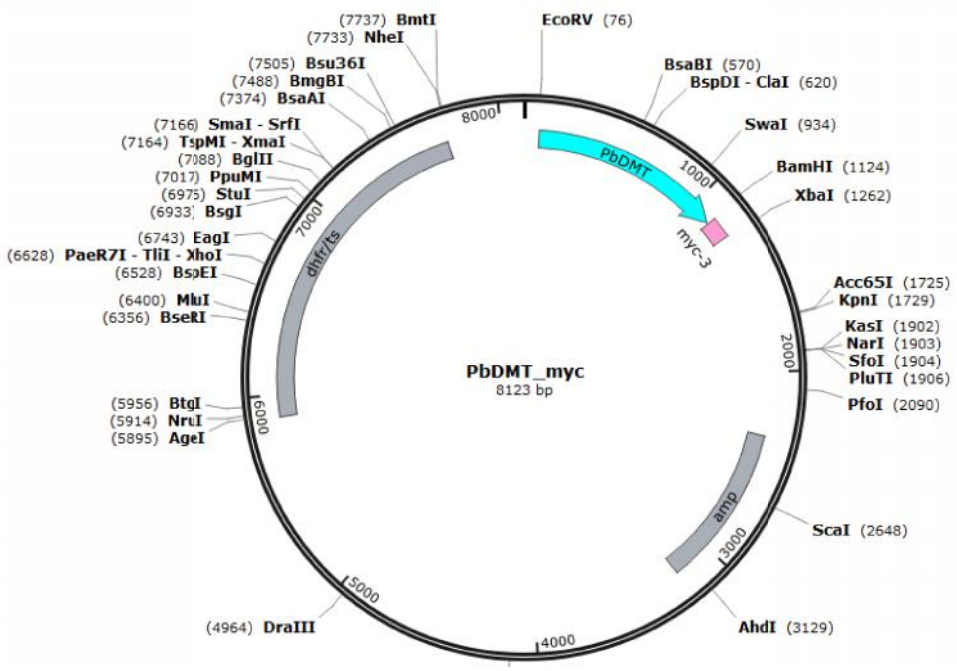

c. **PbDMT_DD:** employed to generate C-terminal Destabilization domain fusion of protein of PbDMT through single cross-over homologous recombination at the native PbDMT genomic locus; and produce a conditional knock down system for PbDMT in *P.berghei*.

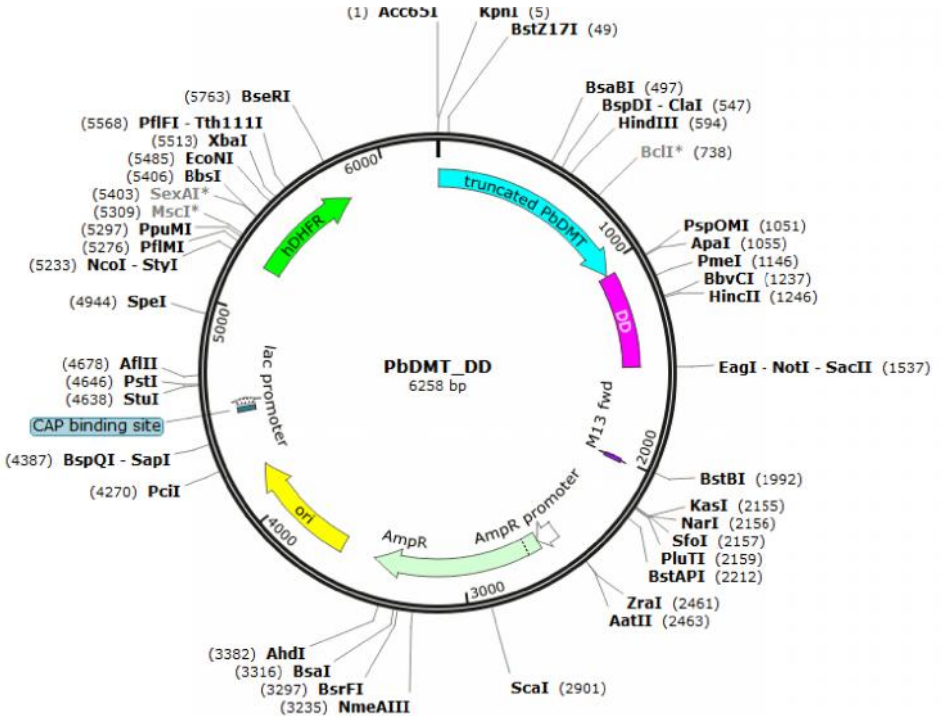

d. **PbDMT_HA_DD:** employed to generate a C-terminal HA tag and Destabilization domain containing fusion protein of PbDMT by single cross-over homologous recombination at the native PbDMT genomic locus; and produce a conditional knock down system for PbDMT in *P.berghei.*

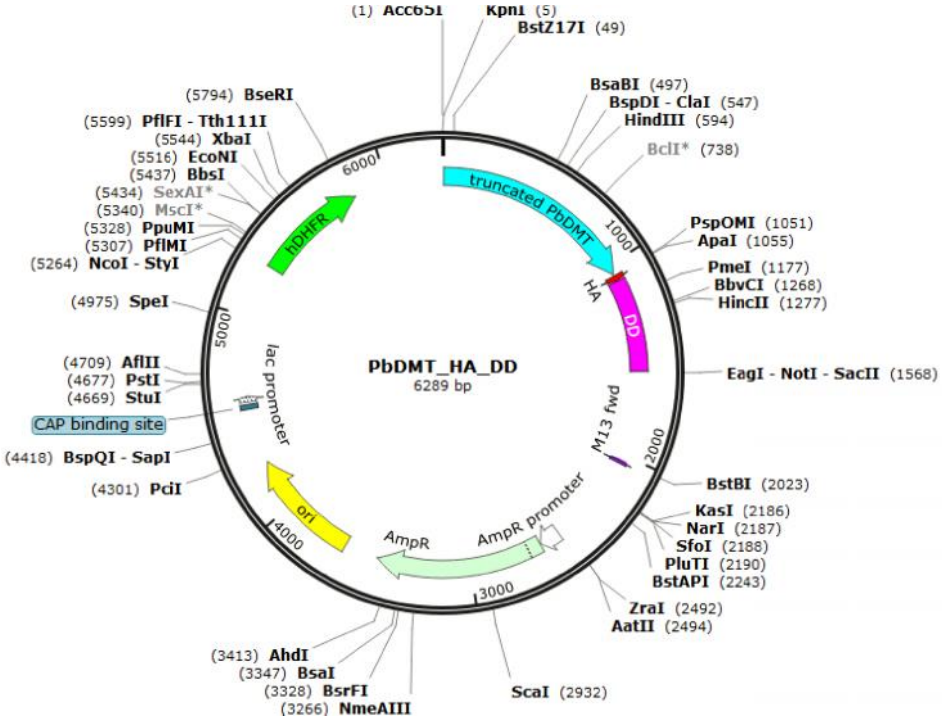

e. **PbDMT_iKo:** used to introduce a TRAD-TetO7 sequence in the 5'UTR region of the native PbDMT gene via double cross-over homologous recombination and produce an inducibly regulated promoter to conditionally knockdown PbDMT expression.

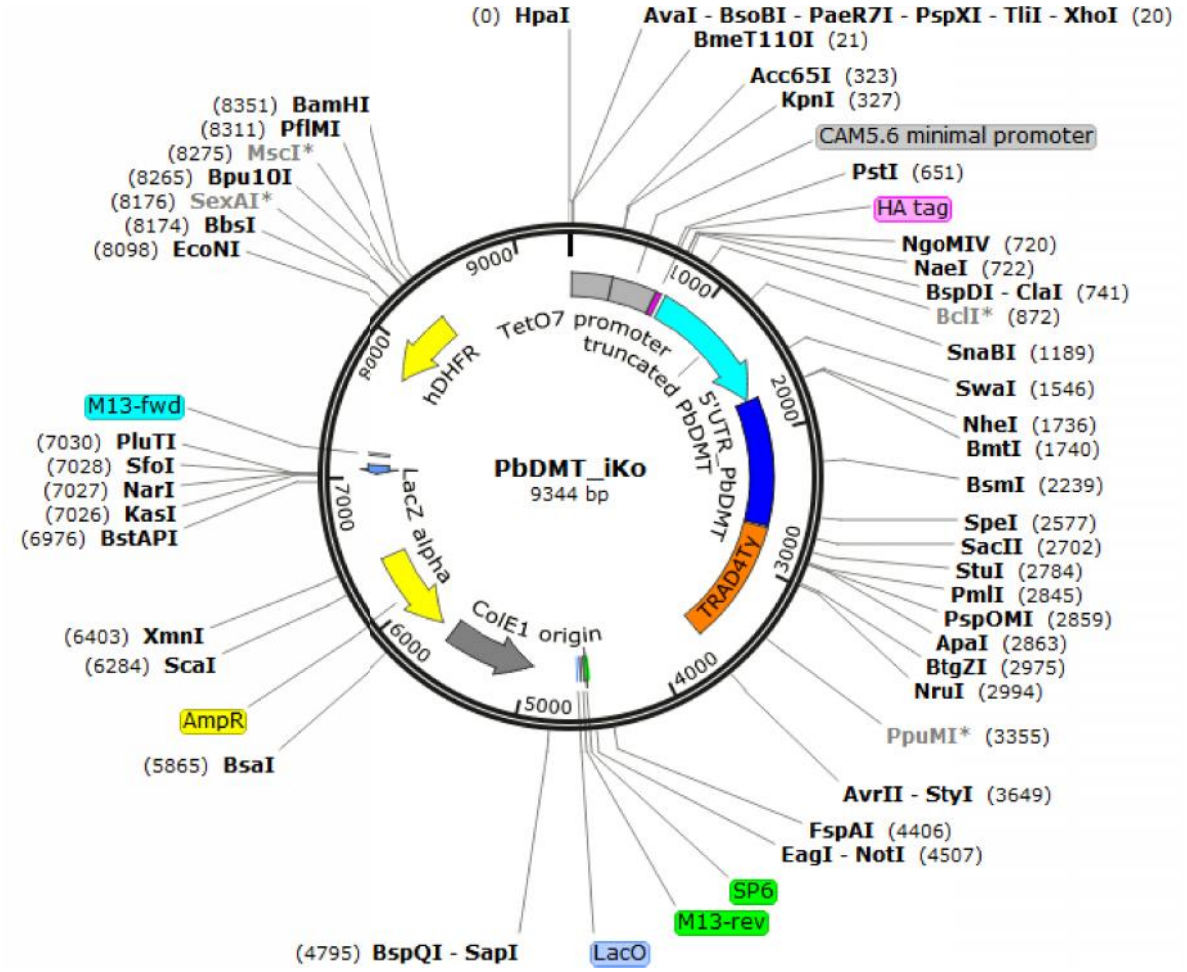

1.5. Constraint based alignment Tool (COBALT) Multiple sequence alignments

Vacuolar Iron transporter homologues

```
PbVIT      1   M   GKQKIID    ARKAYYE    GDIEKSKEIH---SHYHNLDKHAEH   HSLDKDHLKTIIFGSLDGIITIFAI  62
PyVIT      1   M   GKQKIID    ARKAYYE    GDIEKSKEIH---SHYHNLDKHAEH   HSLDKDHLKTIIFGSLDGIITIFAI  62
PchVIT     1   M   GKQKIID    ARKAYYE    GDIEKSKEVH---NHYHSLDKHAEN   HSLDKDHLKTIIFGSLDGIITIFAI  62
PkVIT      1   M   VSKKTLE    ARKAFYD    DDVEKSKEAH---DSYHSLDKHGEQ   HSLDKDNLKTIIFGSLDGIITIFAI  62
PvVIT      1   M   VSKKTLE    ARKAFYD    EDVEKSKEAH---DSYHSLDKHGEQ   HSLDRDNLKTIIFGSLDGIITIFAI  62
PfVIT      1   M   VSKKTIE    ARKAYYN    EDVVLSKEAH---DFYHNLDKHGEN   HNLDKDNLKTIIFGSLDGIITIFAI  62
PcyVIT     1   M   VSKKTIE    ARKAFYD    EDVEKSKEAH---DSYHSLDKHGEQ   HSLDRDNLKTIIFGSLDGIITIFAI  62
LbVIT      1   M   SESAALN[14]ARSAFRA     GDVEASRREH---MKPMHIESHNSS   AS---EYVKSVVFGGLDGIMTTFAI  73
TbVIT      1   M   SESEKID[12]ARKAFET     GDIEMSRMEH---QKHIYKEVHNPS   AS---DYVKSVVFGGLDGIITSFTV  71
AtVIT1     1   -   -------    -------[ 3]EEDKITRISI-epEKQTLLDHHTEK   HFTAGEIVRDIIIGVSDGLTVPFAL  52
Sc_CCC1    1   M[17]GSGGTSE[14]SNSSRHD[16]QDLENSPMSVgkdNRNGDNGSDNEK[6]QSVDPRVISDLIIGLSDGLTVPFAL 118

PbVIT      63  VSGCVGANITPAQVIIIGVGNLFANAISMGFSEYTSSTAQIDFM---LAERQREEWEIENCPTEEKQEMIDIYINKYKFD 139
PyVIT      63  VSGCVGANITPAQVIIIGVGNLFANAISMGFSEYTSSTAQIDFM---LAERQREEWEIENCPTEEKQEMIDIYINKYKFD 139
PchVIT     63  VSGCVGANITPAQVIIIGVGNLFANAISMGFSEYTSSTAQIDFM---AAERQREEWEIENCPTEEKQEMIDIYINKYKFD 139
PkVIT      63  VSGCVGAKITPAQVIIIGVGNLFANAISMGFSEYTSTTAQRDFM---LAEKKREEWEIENCPSEEKQEMIDIYMNKYKFD 139
PvVIT      63  VSGCVGAKITPAQVIIIGVGNLFANAISMGFSEYTSTTAQRDFM---LAEKKREEWEIENCPSEEKQEMIDIYMNKYKFD 139
PfVIT      63  VSGCVGAKITPTQVIIIGIGNLFANAISMGFSEYTSSTAQRDFM---LAEKKREEWEIENCPSEEKQEMIDIYMNKYKFD 139
PcyVIT     63  VSGCVGAKITPAQVIIIGVGNLFANAISMGFSEYTSTTAQRDFM---LAEKKREEWEIENCPSEEKQEMIDIYMNKYKFD 139
LbVIT      74  IAAAAGSGGNYATVLIFGFSNVIADGFAMGFGEYVSGEAERENA---VSERHREEWEVENSFDLEVDEMVQIYMAKGL-S 149
TbVIT      72  VSAAVGSNSSVASVLIFGFSNVIADGFAMGFGEYVSGEAERDNA---LSERRREEWEVENAFDMEVDEMVQIYEMKGL-S 147
AtVIT1     53  AAGLSGANASSSIVLTAGIAEVAAGAISMGLGGYLAAKSEEDHY---AREMKREQEEIVAVPETEAAEVAEI-LAQYGIE 128
Sc_CCC1    119 TAGLSSLG-DAKLVITGGFAELISGAISMGLGGYLGAKSESDYYhaeVKKEKRKFYDNSNLINREIEDILLEINPNFSDE 197

PbVIT      140 SKDAKNLVEITFRNKHFFLEHMMSEELGLILTNEDKSEAFKKGILMFLSFCFFGMIPLFSYVLYNLFFSAENYTSSFAVV 219
PyVIT      140 SKDARNLVEITFRNKHFFLEHMMSEELGLILTNEDKSEAFKKGILMFLSFCFFGMIPLFSYVLYNLFFSAENYTASFAVV 219
PchVIT     140 SKDAKNLVEITFRNKNFFLEHMMSEELGLILTNEDKTEAFKKGILMFLSFCFFGMIPLFSYVLYNLFFSAANYTASFAVV 219
PkVIT      140 SEDARNLVEITFRNKNFFLEHMMSEELGLIITHEDKNESLKKGIIMFLSFCVFGMIPLFSYVAYTFFFQYTDYNTSFVVV 219
PvVIT      140 SEDARNLVEITFRNKIFFLEHMMSEELGLIITHEDKNESLKKGIIMFLSFCVFGMIPLCSYVAYTFFFEYTDYNTSFFVV 219
PfVIT      140 SEDARNLVEITFRNKNFFLEHMMSEELGLIVTNEDKNECLKKGIIMFLSFAVFGIIPLSAYVAYTVFFGYTDYTTSFLVV 219
PcyVIT     140 SEDARNLVEITFRNKNFFLEHMMSEELGLIITHEDKNESLKKGFIMFLSFCIFGMIPLCSYVAYTFFFEYTDYNTSFFVV 219
LbVIT      150 FDDAQTIVGIISKDPKMFVDFMMVEELGLLVDLDDAYGPMKQGVVMFISFVLFGSIPLLAYLPGK----GQGTDLVFFVS 225
TbVIT      148 HEDATTIVNIISKDPKLFVDFMMTEELGIIIDTEDTHGPKKQGLVMFLSFMFFGAVPLLAYLPGK----GKGIDGVFALS 223
AtVIT1     129 PHEYSPVVNALRKNPQAWLDFMMRFELGL--EKPDPKRALQSAFTIAIAYVLGGFIPLLPYMLIP------HAMDAVVAS 200
Sc_CCC1    198 --TIVSFIKDLQRTPELMVDFIIRYGRGL--DEPAENRELISAVTIGGGYLLGGLVPLVPYFFVS------DVGTGLIYS 267

PbVIT      220 FISTLITLFILGLFKSQFTTQK   PIVCALSMVLNGSIAGMLPFLFGVLLKTNSGD      273
PyVIT      220 FISTLITLFILGLFKSQFTTQK   PIVCALSMVLNGSIAGMLPFLFGVLLKTNSGD      273
PchVIT     220 FISTLITLFILGLFKSQFTTQK   PIVCALSMVLNGSIAGMLPFLFGVLLKTNTAD      273
PkVIT      220 FVSTLITLFILGIFKSQFTNQK   PIECALYMVLNGSIAGMVPFLLGILLKNNISD      273
PvVIT      220 FVSTLITLFILGIFKSQFTNQK   PIQCALCMVFNGSIAGMVPFLLGILLKNKIAD      273
PfVIT      220 FISTLTTLFILGLFKSQFTNQK   PITCALYMVLNGMIAGMVPFLLGVVLKNNISE      273
PcyVIT     220 FVSTLITLFILGIFKSQFTNQK   PIHCALCMVFNGSIAGMVPFLLGILLKNNIAD      273
LbVIT      226 CFLTMASLVFLGSVKGYLVGVS   MGRSAVLMVLNGIISGIFSFLAGHLIQMALTT[10]  289
TbVIT      224 CFLATCALIVLGMLRGYLSGVS   MLRSAALMVFNGVVSGLFSFTVGSLVEHALR-[ 5]  281
AtVIT1     201 VVITLFALFIFGYAKGHFTGSK   PLRSAFETAFIGAIASAAAFCLAKVVQH----       250
Sc_CCC1    268 IIVMVVTLFWFGYVKTKLSMGS[6]KVTEGVEMVVVGGVAAGAAWFFVKLLG-----      322
```

Divalent Metal Transporter 1 homologues


AtNramp
ScSmf1
TgDMT 1 [427]LNGRETEAARsIAGPLCHAGEGRDthAENLRRLLTVAPEE-RVSSLVESDVEDQQ----ASRDVGHRASVSSDHD 497
EcDMT
PbDMT 1 MHQDKSMIRG-MNQSRNGGNDSCD--INNGRKHDNINRNS-YINNFHIENINNDQ-NGYKDYKSEEPYIYCSDR- 69
PvDMT 1 MHQDNSMRRA-INQSRNGGSDSCD--INNDREHDNINRNS-YINNFHIENINSDK-N-------EQSYIYCSDRA 63
PchDMT 1 MHQDTSMRIP-MNQSRKDGNDSCD--INNDLEHDN--RNS-YINNFHIENINNDK-NGYKGYKNEQSYIYRSEKT 68
PcyDMT 1 MSPAHEGNSNaSVASKKGSNNSREvnLNSGRNRTHQSGNShHIGNAQRRNVKENQaNVYSYRMNAKSKFDQEENE 75
PkDMT 1 MSPSGKSKSGaSVASREGSNQSREsnLYSSRNGAQESRNNeYGRKGQRRNGKENQaNVYSYRMNATKASWQEENE 75
PvDMT 1 MSPTHEGSSGaSVASKKGSNSSREvnLNSGRNRAHQGGNAhHGGNTQRRNGKENQaNVYSYRMNAKSKAGQEENE 75
PfDMT 1 MEKDFTERS--TKGQRKLANGVVE-nIES----------KLKNHLDNN-NVINKSVNYE--------- 45
AtNramp
ScSmf1
TgDMT 498 SFAARLLVPSPSPS[4]PGSPSLSSNSALGSLLLsCAQSSCNSSLCSd-DDAAPETSAASRPLWCSFFfapFSLPGLSSP 577
EcDMT
PbDMT 70 EVTDPILGNRKHTH[4]NSSELFSRTNYEYSNKNnVDMEMYNMSNNNfyNGNNNIHSNDIIDYINNNNhvnKDLSNTANN 150
PvDMT 64 QVTDSILGNRKYTH[4]NSTEMFSRTNYEYSNKNnVDIEMYNISNNNfyNGNNNGHSNDIIDYINNNN-vnKDLSNTSNN 143
PchDMT 69 DVTDPILGNRKHAY[4]NSSELIARTNYEYSTKTdMGIEMYNMGNNNfyNGNNNLHSSDIINYINNNN-vtKDLDNTENN 148
PcyDMT 76 AGEAAEAAVAPDVG --EVKQSKHDNAYDGKF-IKKDVCNMGKIN--NDKSNMNSNATSTNFKEE----SSMANVDMD 143
PkDMT 76 REYVTHRVAAVDGG --EVKESRHNNEYELNF-IGKDSCSFSKIN--NDNSNMNSNATSTNFKEEG---SSIANMDMD 144
PvDMT 76 AGEAAEAAVAVEAA[4]AAEVKQSKHDDAYDGKF-IKKDVCNLGKLN--NDKLNMNSNATSSNFKEE----SSVANADVD 149
PfDMT 46 -----------DVM CSNVKLSVHDDEYDIKN-IKKDVCNLSKLS--EERLSNN-----ISLKDNN---KVVKNPEID 100
AtNramp 1 ----------MENDVKENLEeEEDRLLPPPppSQSLPST 29
ScSmf1 1 ----------MVNVGPSHAAVAVDASEARKRNISeEVFELRDKKdsTVVIEGE 43
TgDMT 578 CFLlsSRYVSRCLLGFSTFSVSSRQTHARRSSP[13]RLCLLAICVALPLAVLLLFLNLLLlLAQLLMRGL--------- 657
EcDMT
PbDMT 151 TDT--NTYIKKLTSNQSTAYCDGNGYNESVNGS[2]---DINFRDAIKNNNNKSYKNNIN----------NNHVHDD 211
PvDMT 144 ADI--NTYIKKLTSNQSTAYCDGKGYNESANGS[2]---DINFRDVIKNNNNKNYKNN--------------NHVPDD 201
PchDMT 149 AEI--NTYIKKLTSNQSTAYCDGKGYNESAHGS[2]---DINFRDVIKSNNNKNYKNNIN----------NKHVPDE 209
PcyDMT 144 TEKvhSMYIKKLNSTQSTMNIEGNNDTYKEEEL[10]KMEDCSYNYKNKKMTKSKHKNNNNmLEDKMDDQL--ANGEDGD 227
PkDMT 145 PERarSMYIKKLQSTQSTMHMEGNTDIYKEE--[9]KMEDCMYSYKNKRMSKSKHKNNN--LDDTMDHQL--A-EEDGD 222
PvDMT 150 AEKvrSMYIKKLNSTQSTMNIEGNNDTYKEEEL[10]NMEDCTYNYKNKKMIKSKHKNNK--LEDKMDNQL--ANEEDGD 231
PfDMT 101 TKTarQQYKKRLNSTQSTMNIEGNINNEKDDII[20]KRNNNNNNNNNNNNNNNNNNNNNnNNNNNNNNN--SNNVDNR 194
AtNramp 30 DsesEAAFETNEKILIVDFESpDDPTTGDTPPPFSWRKLWL-FTGPGFLMSIAFLDPGNLEGDLQAGAI---------- 97
ScSmf1 44 A---PVRTFTSSSSNH--ERE-DTYVSKRQVMRDIFAK-YLKFIGPGLMVSVAYIDPGNYSTAVDAGAS---------- 105
TgDMT 658 ----------HLLLP----------PPLPPRFQWKK-FVAFLGPGWLVAMAYLDPGNLEGDLQAGSRRE-DPGVLPPG 713
EcDMT 1 --------MTNYRV---------ESSSGRAA-----RKMRLALMGPAFIAAIGYIDPGNFATNIQAGAS---------- 47
PbDMT 212 MlelGDRSFDSSFYMHNNVEE-TDNERSSKLSFMSKLKMYFNYFGPGWIVAIAYLDPGNICGNLNVGLIRSADFNNADSS 290
PvDMT 202 MlelGDRSFDSSFYIHNNVEE-IDTERSNRLSFMSKLKMYFNYFGPGWIVAIAYLDPGNICGNLNVGLIRSDDFINVNSS 280
PchDMT 210 MlelGDGSFDSSFYMHNNAEE-VDNEEQGALSFMNKLKIYFNYFGPGWIVAIAYLDPGNICGNLNVGLIRDNDFNSANGT 288
PcyDMT 228 K-----EMYNNSFYLSDNM-E-ELGNEEKNISFIKKIKMCFNYFGPGWIVAIAYLDPGNLCSNLNVGLIRSPVDNATNNL 300
PkDMT 223 K-----EMYNHSFYLSDNMEE-ELSTDGKNISFMKKIKMCFNYFGPGWIVAIAYLDPGNLCSNLNVGLIRSPGD--TNNL 294
PvDMT 232 K-----EMYNNSFYLSDNMDE-ELSNGGKNISFIKKIKMCFNYFGPGWIVAIAYLDPGNLCSNLNVGLIRSPDDNVNNNL 305
PfDMT 195 KrnkNEECYDESYCISDNL-D-EITSYRNKLSLYNKLRMCFNYFGPGWIVAIAYLDPGNLCSNLNVGLIRSPDP----TL 268

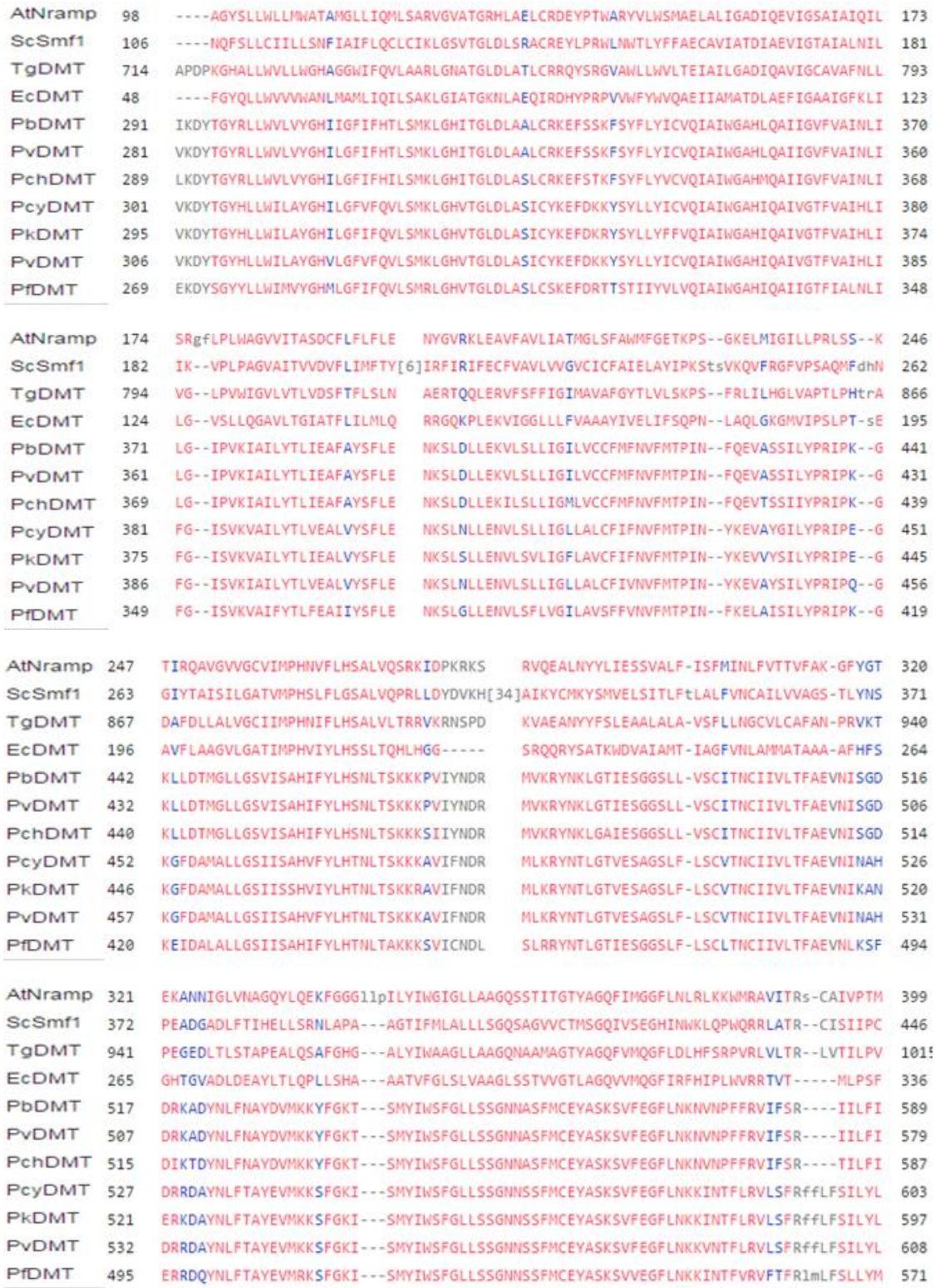
AtNramp 98 ----AGYSLLWLLMWATAMGLLIQMLSARVGVATGRHLAELCRDEYPTWARYVLWSMAELALIGADIQEVIGSAIAIQIL 173
ScSmf1 106 ----NQFSLLCIILLSNFIAIFLQCLCIKLGSVTGLDLSRACREYLPRWLNWTLYFFAECAVIATDIAEVIGTAIALNIL 181
TgDMT 714 APDPKGHALLWVLLWGHAGGWIFQVLAARLGNATGLDLATLCRRQYSRGVAWLLWVLTEIAILGADIQAVIGCAVAFNLL 793
EcDMT 48 ----FGYQLLWVVVWANLMAMLIQILSAKLGIATGKNLAEQIRDHYPRPVVWFYWVQAEIIAMATDLAEFIGAAIGFKLI 123
PbDMT 291 IKDYTGYRLLWVLVYGHIIGFIFHTLSMKLGHITGLDLAALCRKEFSSKFSYFLYICVQIAIWGAHLQAIIGVFVAINLI 370
PvDMT 281 VKDYTGYRLLWVLVYGHILGFIFHTLSMKLGHITGLDLAALCRKEFSSKFSYFLYICVQIAIWGAHLQAIIGVFVAINLI 360
PchDMT 289 LKDYTGYRLLWVLVYGHILGFIFHILSMKLGHITGLDLASLCRKEFSTKFSYFLYVCVQIAIWGAHMQAIIGVFVAINLI 368
PcyDMT 301 VKDYTGYHLLWILAYGHILGFVFQVLSMKLGHVTGLDLASICYKEFDKKYSYLLYICVQIAIWGAHIQAIVGTFVAIHLI 380
PkDMT 295 VKDYTGYHLLWILAYGHILGFIFQVLSMKLGHVTGLDLASICYKEFDKRYSYLLYFFVQIAIWGAHIQAIVGTFVAIHLI 374
PvDMT 306 VKDYTGYHLLWILAYGHVLGFVFQVLSMKLGHVTGLDLASICYKEFDKKYSYLLYICVQIAIWGAHIQAIVGTFVAIHLI 385
PfDMT 269 EKDYSGYYLLWIMVYGHMLGFIFQVLSMRLGHVTGLDLASLCSKEFDRTTSTIIYVLVQIAIWGAHIQAIIGTFIALNLI 348
AtNramp 174 SRgfLPLWAGVVITASDCFLFLFLE NYGVRKLEAVFAVLIATMGLSFAWMFGETKPS--GKELMIGILLPRLSS--K 246
ScSmf1 182 IK--VPLPAGVAITVVDVFLIMFTY[6]IRFIRIFECFVAVLVVGVCICFAIELAYIPKStsVKQVFRGFVPSAQMFdhN 262
TgDMT 794 VG--LPVWIGVLVTLVDSFTFLSLN AERTQQLERVFSFFIGIMAVAFGYTLVLSKPS--FRLILHGLVAPTLPHtrA 866
EcDMT 124 LG--VSLLQGAVLTGIATFLILMLQ RRGQKPLEKVIGGLLLFVAAAYIVELIFSQPN--LAQLGKGMVIPSLPT-sE 195
PbDMT 371 LG--IPVKIAILYTLIEAFAYSFLE NKSLDLLEKVLSLLIGILVCCFMFNVFMTPIN--FQEVASSILYPRIPK--G 441
PvDMT 361 LG--IPVKIAILYTLIEAFAYSFLE NKSLDLLEKVLSLLIGILVCCFMFNVFMTPIN--FQEVASSILYPRIPK--G 431
PchDMT 369 LG--IPVKIAILYTLIEAFAYSFLE NKSLDLLEKILSLLIGMLVCCFMFNVFMTPIN--FQEVTSSIIYPRIPK--G 439
PcyDMT 381 FG--ISVKVAILYTLVEALVYSFLE NKSLNLLENVLSLLIGLLALCFIFNVFMTPIN--YKEVAYGILYPRIPE--G 451
PkDMT 375 FG--ISVKVAILYTLIEALVYSFLE NKSLSLLENVLSVLIGFLAVCFIFNVFMTPIN--YKEVVYSILYPRIPE--G 445
PvDMT 386 FG--ISVKIAILYTLVEALVYSFLE NKSLNLLENVLSLLIGLLALCFIVNVFMTPIN--YKEVAYSILYPRIPQ--G 456
PfDMT 349 FG--ISVKVAIFYTLFEAIIYSFLE NKSLGLLENVLSFLVGILAVSFFVNVFMTPIN--FKELAISILYPRIPK--G 419
AtNramp 247 TIRQAVGVVGCVIMPHNVFLHSALVQSRKIDPKRKS RVQEALNYYLIESSVALF-ISFMINLFVTTVFAK-GFYGT 320
ScSmf1 263 GIYTAISILGATVMPHSLFLGSALVQPRLLDYDVKH[34]AIKYCMKYSMVELSITLFtLALFVNCAILVVAGS-TLYNS 371
TgDMT 867 DAFDLLALVGCIIMPHNIFLHSALVLTRRVKRNSPD KVAEANYYFSLEAALALA-VSFLLNGCVLCAFAN-PRVKT 940
EcDMT 196 AVFLAAGVLGATIMPHVIYLHSSLTQHLHGG----- SRQQRYSATKWDVAIAMT-IAGFVNLAMMATAAA-AFHFS 264
PbDMT 442 KLLDTMGLLGSVISAHIFYLHSNLTSKKKPVIYNDR MVKRYNKLGTIESGGSLL-VSCITNCIIVLTFAEVNISGD 516
PvDMT 432 KLLDTMGLLGSVISAHIFYLHSNLTSKKKPVIYNDR MVKRYNKLGTIESGGSLL-VSCITNCIIVLTFAEVNISGD 506
PchDMT 440 KLLDTMGLLGSVISAHIFYLHSNLTSKKKSIIYNDR MVKRYNKLGAIESGGSLL-VSCITNCIIVLTFAEVNISGD 514
PcyDMT 452 KGFDAMALLGSIISAHVFYLHTNLTSKKKAVIFNDR MLKRYNTLGTVESAGSLF-LSCVTNCIIVLTFAEVNINAH 526
PkDMT 446 KGFDAMALLGSIISSHVIYLHTNLTSKKRAVIFNDR MLKRYNTLGTVESAGSLF-LSCVTNCIIVLTFAEVNIKAN 520
PvDMT 457 KGFDAMALLGSIISAHVFYLHTNLTSKKKAVIFNDR MLKRYNTLGTVESAGSLF-LSCVTNCIIVLTFAEVNINAH 531
PfDMT 420 KEIDALALLGSIISAHIFYLHTNLTAKKKSVICNDL SLRRYNTLGTIESGGSLF-LSCLTNCIIVLTFAEVNLKSF 494
AtNramp 321 EKANNIGLVNAGQYLQEKFGGGllpILYIWGIGLLAAGQSSTITGTYAGQFIMGGFLNLRLKKWMRAVITRs-CAIVPTM 399
ScSmf1 372 PEADGADLFTIHELLSRNLAPA---AGTIFMLALLLSGQSAGVVCTMSGQIVSEGHINWKLQPWQRRLATR--CISIIPC 446
TgDMT 941 PEGEDLTLSTAPEALQSAFGHG---ALYIWAAGLLAAGQNAAMAGTYAGQFVMQGFLDLHFSRPVRLVLTR--LVTILPV 1015
EcDMT 265 GHTGVADLDEAYLTLQPLLSHA---AATVFGLSLVAAGLSSTVVGTLAGQVVMQGFIRFHIPLWVRRTVT-----MLPSF 336
PbDMT 517 DRKADYNLFNAYDVMKKYFGKT---SMYIWSFGLLSSGNNASFMCEYASKSVFEGFLNKNVNPFFRVIFSR----IILFI 589
PvDMT 507 DRKADYNLFNAYDVMKKYFGKT---SMYIWSFGLLSSGNNASFMCEYASKSVFEGFLNKNVNPFFRVIFSR----IILFI 579
PchDMT 515 DIKTDYNLFNAYDVMKKYFGKT---SMYIWSFGLLSSGNNASFMCEYASKSVFEGFLNKNVNPFFRVIFSR----TILFI 587
PcyDMT 527 DRRDAYNLFTAYEVMKKSFGKI---SMYIWSFGLLSSGNNSSFMCEYASKSVFEGFLNKKINTFLRVLSFRffLFSILYL 603
PkDMT 521 ERKDAYNLFTAYEVMKKSFGKI---SMYIWSFGLLSSGNNSSFMCEYASKSVFEGFLNKKINTFLRVLSFRffLFSILYL 597
PvDMT 532 DRRDAYNLFTAYEVMKKSFGKI---SMYIWSFGLLSSGNNSSFMCEYASKSVFEGFLNKKVNTFLRVLSFRffLFSILYL 608
PfDMT 495 ERRDQYNLFTAYEVMRKSFGKI---SMYIWSFGLLSSGNNSSFMCEYASKSVVEGFLNKKINTFVRVFTFRlmLFSLLYM 571

Abbreviations:

AtNramp - *Arabisopsis thaliana* Nramp

ScSmf1 – *Saccharomayces cerevisiae* Smf1 (Nramp homologue)

TgDMT – *Toxoplasma gondii* DMT 1 homologue

EcDMT – *Escherichia coli* DMT

PbDMT – *Plasmodium berghei* DMT 1 homologue

PyDMT - *Plasmodium yoelii* DMT 1 homologue

PchDMT - *Plasmodium chabaudi* DMT 1 homologue

PcyDMT - *Plasmodium cynomolgi* DMT 1 homologue

PvDMT - *Plasmodium vivax* DMT 1 homologue

PkDMT - *Plasmodium knowlesi* DMT 1 homologue

PfDMT - *Plasmodium falciparum* DMT 1 homologue